North Luzon and the Philippine Sea Plate motion model: Insights following paleomagnetic, structural, and age-dating investigations

Karlo L. Queano,[1,2] Jason R. Ali,[1] John Milsom,[1,3] Jonathan C. Aitchison,[1] and Manuel Pubellier[4]

[1]   Results of one of the most comprehensive paleomagnetic and supporting geological programs ever carried out in offshore SE Asia on North Luzon, northern Philippines, are reported. Six new results, based on 66 sites, are reported from a total collection of 243 individual sites. Declinations in the data subset are sometimes scattered, likely reflecting combinations of major plate and local rotations in both clockwise and counterclockwise directions, and thus have a somewhat limited value for tectonic modeling. The inclination data are, however, much more valuable and can be best explained if North Luzon traveled as part of the Philippine Sea Plate for most of its history, a scenario which is compatible with the known geology of the eastern Philippines and broader region. In the proposed model, for all of its Eocene-Pliocene history, North Luzon is placed on the western edge of the Philippine Sea Plate, effectively always just to the west of the site where the Benham Plateau formed ~40 Ma. The paleomagnetic data indicate a substantial northward migration of the area since the start of the Neogene, with an earlier interval stretching back to at least the mid-Early Cretaceous when this part of the plate occupied equatorial latitudes. Post-15 Ma motion of the plate has involved the indentation of the Palawan microcontinental block into the western side of the Philippine Archipelago. Deformations induced by this process offer the most likely explanation for the scattered declinations observed in North Luzon and areas a short distance to the south.

1.   Introduction

[2]   The ~4.7 × 10⁶ km² Philippine Sea Plate (PSP) has played a key role in the tectonic evolution of SE Asia and the western Pacific. Its importance for regional tectonic modeling becomes obvious when one considers that it has formed the eastern boundary to the collage of much smaller plates-blocks and tectonic systems which have occupied SE Asia for a large portion of the Cenozoic [e.g., *Rangin et al.*, 1990; *Hall*, 2002; *Pubellier et al.*, 2003a, 2003b]. Luzon island in the northern Philippines sits just to the west of the present-day Philippine Sea Plate, the two being separated by the East Luzon Trough. The trough represents a short sector of the much longer (~2400 km) double subduction zone which runs between Halmahera (S) and Taiwan (N) and which accommodates convergence (currently varying along

strike from ~5 cm/yr in the north to 10 cm/yr in the south) between Eurasia and the West Philippine Basin [e.g., *Seno et al.*, 1993].

[3]   Various workers have modeled the Luzon-Philippine Sea Plate link in quite different ways. This freedom is very likely a result of the limited information base that is available for the northern Philippines. In comparing different proposals, as a reference point we use the Benham Plateau (~16.5°N, 125.0°E), an oceanic plateau that formed ~40 Ma on the western side West Philippine Basin just south of the "Central Basin Fault." Today the plateau sits immediately to the east of the East Luzon Trough (Figure 1).

[4]   *Rangin et al.* [1990] placed Luzon at 43 Ma in a position relative to the Benham Plateau very similar to that it occupies today, plotting this part of the then actively spreading West Philippine Basin just south of the equator. The PSP as a whole subsequently had to undergo a 40°CW rotation for the plateau to reach its current position. *Lee and Lawver* [1995], on the other hand, although proposing similar relative positions for the plateau and North Luzon, had them occupying almost their present-day latitudinal positions and orientations throughout much of the Cenozoic.

[5]   The 45 Ma reconstruction of *Hall et al.* [1995a, 1995b] and *Hall* [2002] was very different, with northern

---

[1]Department of Earth Sciences, University of Hong Kong, Hong Kong, China.
[2]Now at Mines and Geosciences Bureau, Quezon City, Philippines.
[3]Also at Gladestry Associates, Gladestry, UK.
[4]Laboratoire de Géologie, Ecole Normale Supérieure URA 1316 du CNRS UMR 8538, Paris, France.

Eurasian Plate

Pacific Plate

Izu Bonin Trench

Nankai Trough

Shikoku Basin

Amami Plateau

Ogasawara Plateau

Ryuku Trench

Daito Ridge

Oki Daito Ridge

Urdaneta Plateau

Philippine Sea Plate

West Mariana Ridge

Mariana Trough

Mariana Arc

Mariana Trench

Manila Trench

LUZON

West Philippine Basin

Palau Kyushu Ridge

Parece Vela Basin

Benham Plateau

Philippine Fault

Philippine Trench

Sulu Sea

Yap Trench

Palau Trench

East Morotai Plateau

Caroline Plate

Celebes Sea

Molucca Sea

New Guinea Trench

West Melanesian Trench

Sorong Fault

Bismarck Sea

Banda Sea

	Cretaceous		Pal	Eocene			Oligo		Miocene			Plio	
				E	M	L	E	L	E	M	L		
In MYA	130 120		60	50		40	30		20		10		0

West Philippine Basin
Shikoku Basin
Parece-Vela Basin
Mariana Trough
South China (S.C) Sea
Sulu Sea Basin
Celebes Sea Basin
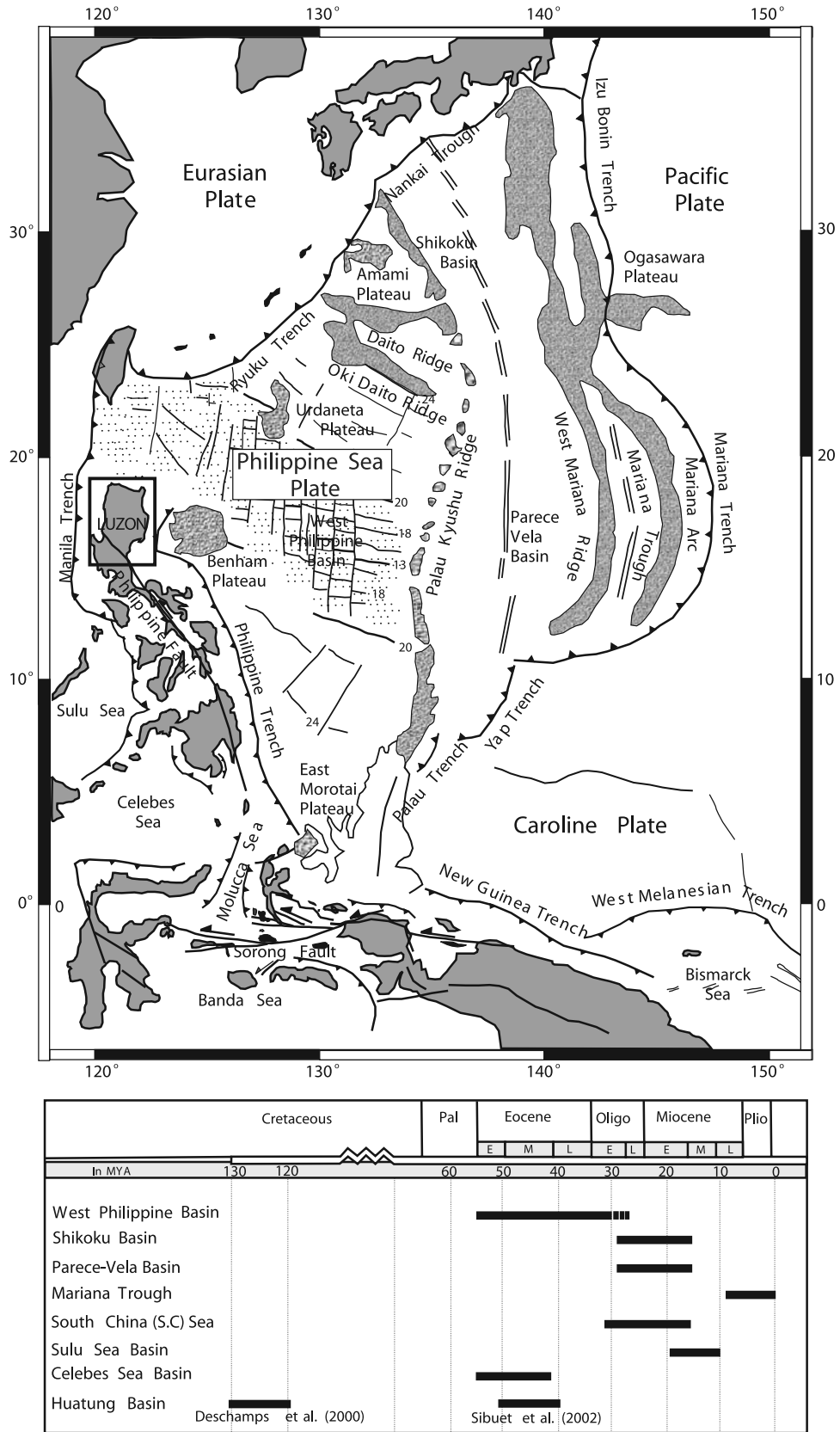Huatung Basin

Deschamps et al. (2000)

Sibuet et al. (2002)

Figure 1

and central Luzon situated some 1000 km ENE of Sabah (northern Borneo) in the northern part of the West Philippine Basin but with the Benham Plateau emplaced at 40 Ma near to, but south of, the spreading axis. By the time spreading had ceased (~33 Ma), the plateau was about 1500 km away from North Luzon and the two were then shown as traveling along parallel trajectories until the Luzon Trough formed at around the Mio-Pliocene boundary. Only then did the Benham Plateau start moving toward North Luzon. *Deschamps and Lallemand* [2002] generally followed the *Hall et al.* [1995a, 1995b] Philippine Sea Plate kinematic model, but placed North Luzon in the southern part of the West Philippine Basin at 45 Ma, separated from Borneo by a major N-S fault that was later to become the Manila Trench.

2. Tectonic Setting

[6] The central part of North Luzon lies ~800 km SE of the main Asian landmass in southern China, trapped at the margins of the Eurasian and the Philippine Sea plates. Relative to Eurasia, the Philippine Sea Plate moves WNW, rates varying from about 10 mm/yr at the southern tip to about 5 mm/yr near Taiwan, the Euler pole being located near to Japan [*Seno et al.*, 1993]. The NW-SE oblique convergence between these plates is currently being absorbed by two oppositely dipping subduction zones: the Manila Trench to the west and the East Luzon Trough-Philippine Trench to the east (Figure 2). These subduction zones extend southward by approximately 1500 km, delineating a 400-km-wide deformation zone that *Gervasio* [1966] named the Philippine Mobile Belt (PMB). The Manila Trench connects with the Negros-Sulu-Cotobato trench system along which the marginal basins (i.e., South China Sea, Sulu Sea and the Celebes Sea) on the eastern edge of the Eurasian Plate are being subducted [*Rangin and Pubellier*, 1990; *Ringenbach et al.*, 1993]. These subduction zones continue on as collision zones in Taiwan, Mindoro, Panay and Mindanao islands where continental fragments of Eurasian affinity (parts of the Palawan microcontinental block) have been transferred to the PMB [*Lewis and Hayes*, 1984; *Rangin*, 1989; *Pubellier et al.*, 1991; *Quebral et al.*, 1996] (Figure 2). *Wolfe* [1981] and *Lewis and Hayes* [1984] proposed that subduction along the Manila Trench started ~15 Ma. However, *Malettere* [1989] noted that the island arc volcanism presumably related to the activity along the Manila Trench in western Luzon commenced sometime earlier.

[7] The East Luzon Trough is a young feature, defined by a shallow Benioff zone and lacking an associated volcanic arc [*Hamburger et al.*, 1983; *Bautista et al.*, 2001]. This is connected with the Philippine Trench by an ENE trending transcurrent fault zone. On the basis of the rate of conver-

gence (8 cm/yr), the depth of the Wadati-Benioff zone (<200 km), the age of volcanic rocks and the lack of any well-developed accretionary prism, this plate boundary is widely believed to have initiated 3–5 Ma [*Karig*, 1975; *Cardwell et al.*, 1980; *Hamburger et al.*, 1983; *Ozawa et al.*, 2004]. This implies that prior to the Pliocene, parts of the Philippine archipelago, including northern Luzon, formed part of the Philippine Sea plate.

[8] Intense deformation affects the PMB, with the sinistral Philippine Fault transecting the archipelago from Luzon to eastern Mindanao for more than 1200 km [*Aurelio et al.*, 1991]. The fault system accommodates a lateral component of the oblique convergence between the Philippine Sea Plate and Eurasian Plate, with the other component being absorbed by subduction along the Philippine Trench, under a shear partitioning mechanism [*Fitch*, 1972; *Barrier et al.*, 1991; *Aurelio*, 2000]. This mechanism implies synchronous formation of the trench and fault.

[9] A summary of ages and tectonic events around the Philippine Mobile Belt is shown in Figures 1 and 2.

3. Geology of Northern Luzon

[10] Regional geological studies on North Luzon date back more than a century, with the work of *Becker* [1899] (as cited by *Billedo* [1994]), *Corby et al.* [1951], *Durkee and Pederson* [1961], *Christian* [1964]; *Caagusan* [1977], *Japan International Cooperation Agency–Metal Mining Agency of Japan* (*JICA-MMAJ*) [1977], *Japan International Cooperation Agency–Metal Mining Agency of Japan–Mines and Geosciences Bureau* (*JICA-MMAJ-MGB*) [1990], *Billedo* [1994] and *Florendo* [1994] providing much of the key information. On the basis of physiographic and morphostructural features, the region can be divided into four major zones: (1) Cagayan Valley Basin; (2) northern Sierra Madre–Caraballo Range (including Palaui Island); (3) southern Sierra Madre and; (4) Central Cordillera (including the Ilocos foothills) (Figure 3). Figures 4 and 5 provide a summary of the stratigraphy and magmatic events of North Luzon.

3.1. Cagayan Valley Basin

[11] The Cagayan Valley Basin separates the Central Cordillera and Sierra Madre mountain ranges. It is bounded in the north by the ENE-WSW Sicalao Ridge, also referred to as Sicalao-Cassigayan High [*Durkee and Pederson*, 1961] or Cassigayan Ridge [*Florendo*, 1994], and in the south by the Caraballo Range. The basin is highly asymmetric, with the sedimentary section thickening to the west [*Christian*, 1964; *Caagusan*, 1977], a configuration thought to have resulted from the volcanism and uplift of the Central Cordillera between the Miocene and Pleistocene [*Christian*, 1964]. The basin fill comprises volcanic-epiclastic and

---

Figure 1. Regional map of the Southeast Asian region (data source after *Hall et al.* [1995b]). Also shown is the opening duration of some marginal basins in SE Asia. References are as follows: West Philippine Basin [*Deschamps and Lallemand*, 2002]; Shikoku Basin [*Okino et al.*, 1994; *Sdrolias et al.*, 2004]; Parece-Vela Basin [*Okino et al.*, 1994; *Sdrolias et al.*, 2004]; Mariana Trough [*Jolivet et al.*, 1989]; South China Sea Basin [*Briais et al.*, 1993; *Li et al.*, 2005]; Sulu Sea Basin [*Jolivet et al.*, 1989; *Rangin and Silver*, 1991]; Celebes Sea Basin [*Weissel*, 1980; *Silver and Rangin*, 1991]; Huatung Basin [*Deschamps et al.*, 2000; *Sibuet et al.*, 2002].
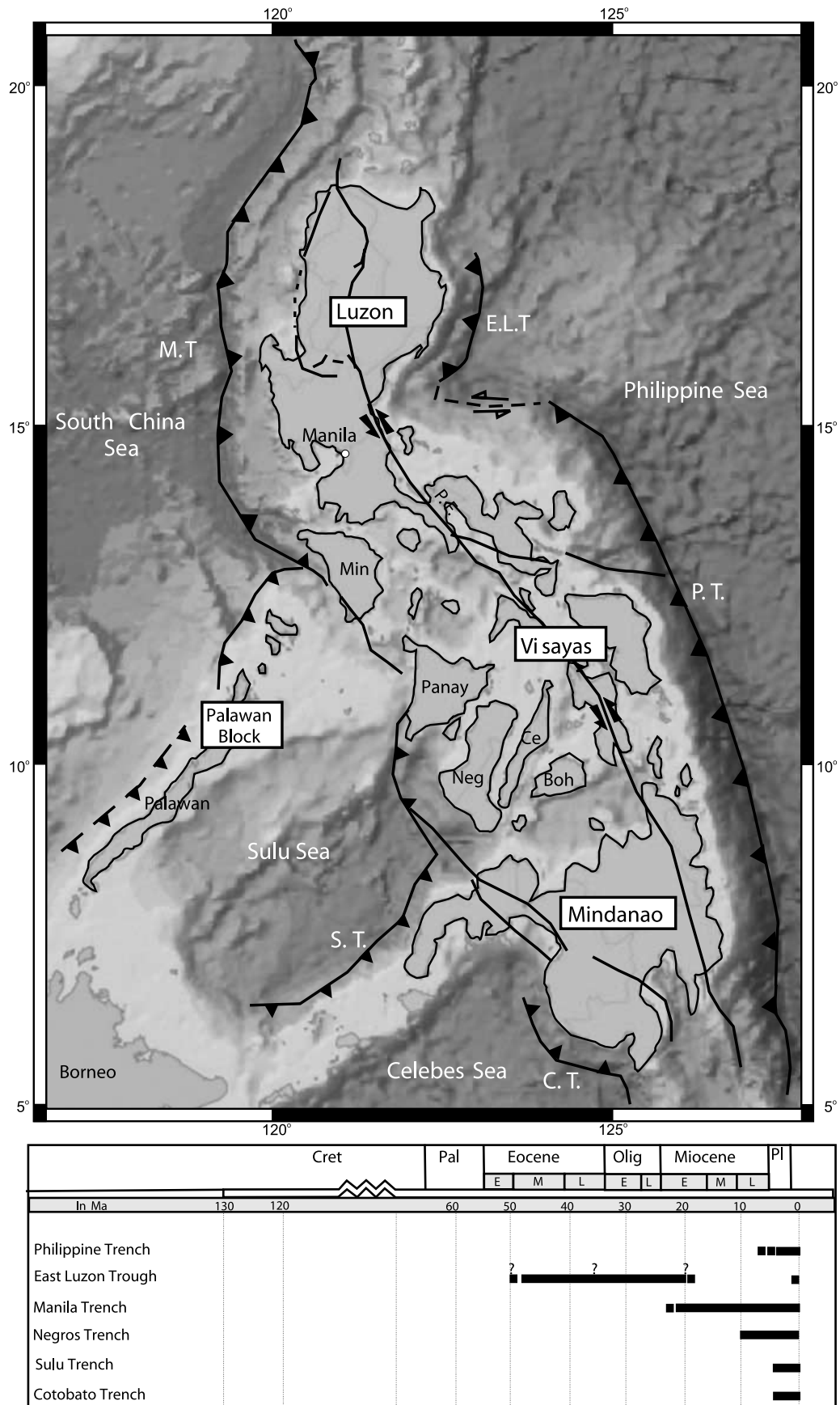
Figure 2

clastic sedimentary units, attaining a cumulative thickness of ~7 km [*Caagusan*, 1977]. Seismic studies and correlation with outcrops from adjacent mountain ranges indicate that the lower part of the sedimentary sequence is of at least Oligocene age, and is largely composed of deep marine sediments and extrusive igneous rocks [*Durkee and Pederson*, 1961; *Caagusan*, 1981; *Florendo*, 1994]. The age of the basement possibly extends back to the Eocene based on geological information from the NE Sierra Madre [e.g., *Billedo*, 1994, Mines and Geosciences Bureau, Geology and mineral resources of the Philippines, vol. 1, revised edition, unpublished, 2002; this work] (see below). Marine conditions prevailed in the basin until the early Pliocene, with the deposition of carbonates and clastic rocks (mainly turbidites) [*Caagusan*, 1981]. In the NW Sierra Madre, these Eocene to early Pliocene units are represented by middle to upper Eocene Caraballo Formation, uppermost Oligocene to lower Miocene Lubuagan Formation, middle Miocene Callao Formation and upper Miocene to upper lower Pliocene Cabagan Formation.

3.2. Northern Sierra Madre–Caraballo Range

[12] The northern Sierra Madre (NSM) parallels the east coast of North Luzon, extending more than 300 km from Santa Ana, Cagayan Province, in the north to Dingalan, Aurora Province, in the south. South of Aurora, the NSM converges with the northwest-southeast trending Caraballo Range (CR). Comprehensive geologic studies on the NSM-CR were conducted by *JICA-MMAJ* [1975, 1977], *JICA-MMAJ-MGB* [1990], *Aurelio and Billedo* [1987], *Ringenbach* [1992], and *Billedo* [1994]. On the basis of these studies, the region can be divided into two morphostructural units: (1) western NSM consisting largely of folded Cenozoic epiclastic and volcanic rocks (middle to upper Eocene Caraballo Formation, uppermost Oligocene to lower Miocene Lubuagan Formation and upper Miocene to upper lower Pliocene Cabagan Formation), limestones (middle Miocene Callao Formation) and mafic/felsic intrusive bodies and (2) eastern NSM (also referred to as the "Coastal Strip" by *Billedo* [1994]) predominantly composed of the pre-Cenozoic ophiolite belt (the Casiguran Ophiolite) (Figures 3 and 4). Radiometric age dating of igneous bodies suggest at least four magmatic events occurred in the region [*Ringenbach*, 1992; *Billedo*, 1994]: (1) an Eocene magmatic phase spanning 45–43/39 Ma (Coastal Batholith); (2) a late early Oligocene to early Miocene magmatic episode 33–22 Ma (Dupax and northern Sierra Madre batholiths); (3) a late Oligocene to earliest Miocene high-K calc-alkaline magmatic event 25–22 (Cordon Syenite Complex); and (4) a late early to early middle Miocene magmatic event at around 17 Ma (Palali Formation).

[13] On the basis of the similarity of ages, *Ringenbach* [1992] interpreted the Caraballo Formation as being the

volcanic equivalent to the Coastal Batholith. He further considered the plutonic bodies intruding the Caraballo Formation in the southern NSM and along the Baler-Casiguran coast as belonging to the Coastal Batholith. Meanwhile, *Billedo* [1994] suggested that the Dupax and northern Sierra Madre batholiths were the plutonic equivalents of a volcanic arc represented by the lower Oligocene Dibuluan River Formation. *Ringenbach* [1992] classified the plutonic bodies in the NSM (west of the Palanan-Dinapique coast) as also belonging to the Dupax-NSM Batholith. It must be emphasized, however, that mapping these units as separate entities in the study area is extremely difficult due to the similarities in the lithofacies of the two plutonic bodies. *Billedo* [1994, p. 122] acknowledged this noting that the "Eocene and Oligocene magmatic arcs were developed essentially on the same volcanic axis." Therefore for this study the plutonic bodies are herein mapped as one body.

[14] Together with the Cordon Syenite, the Palali Formation represents the last major magmatic phase in the Caraballo-NSM-Cagayan Valley areas. *Albrecht and Knittel* [1990] suggested that these formations were "comagmatic" based on similarities in geochemistry (mainly alkaline/shoshonitic), and argued that the younger age (~17 Ma) obtained by *Knittel* [1983] for the Palali Formation was due to argon loss. *Knittel and Cundari* [1990] related these alkalic bodies to an extensional event (intra-arc rifting) in northern Luzon that resulted to the formation of the Cagayan Valley Basin in the late Oligocene to early Miocene. The similarity in the early Cenozoic stratigraphies of the Central Cordillera and northern Sierra Madre bounding the basin is the principal evidence.

[15] It is noteworthy that recent magmatic activity occurred in the northern portion of NSM, at Mount Cagua, one of the recently active volcanoes forming part of the Babuyan segment [*Defant et al.*, 1989] or Bashi segment [*Yang et al.*, 1996]. The magmatic activity in the Bashi segment is attributed to the subduction of the South China Sea at the northern Manila Trench.

[16] The Casiguran Ophiolite, a dismembered ophiolite sequence of ultramafic rocks, gabbros and pillow basalts, is found along the eastern coast the NSM [*Florendo*, 1994; *Billedo*, 1994]. *Billedo* [1994] also introduced the Dibut-Bay Metaophiolite from the coast south of Baler as being the metamorphosed equivalent of the Casiguran Ophiolite. The Dibut Bay metaophiolite includes highly tectonized ultramafic rocks, foliated layered gabbros and amphibolites [*Billedo*, 1994]. Cherts amongst pillow basalts of the Casiguran Ophiolite contain Lower Cretaceous (upper Barremian–lower Aptian to Albian) radiolarian assemblage [*Queano*, 2006]. Together with other Mesozoic ophiolite outcrops in Luzon and neighboring regions, this ophiolite provides evidence for the existence of an oceanic basement

Figure 2. Geodynamic setting of the Philippine archipelago. Also shown is the timing of subduction events around the Philippine Mobile Belt. References are as follows: Philippine Trench [*Aurelio et al.*, 1991; *Barrier et al.*, 1991; *Ozawa et al.*, 2004], East Luzon Trough [*Lewis and Hayes*, 1983; *Cardwell et al.*, 1980; *Wolfe*, 1981; *Malettere*, 1989]; Manila Trench [*Cardwell et al.*, 1980; *Malettere*, 1989; *Bellon and Yumul*, 2000]; Negros Trench [*Cardwell et al.*, 1980; *Rangin et al.*, 1999; *Sajona et al.*, 1993]; Sulu Trench [*JICA-MMAJ-MGB*, 1990; *Rangin et al.*, 1999]; Cotobato Trench [*JICA-MMAJ-MGB*, 1990; *Rangin et al.*, 1999].
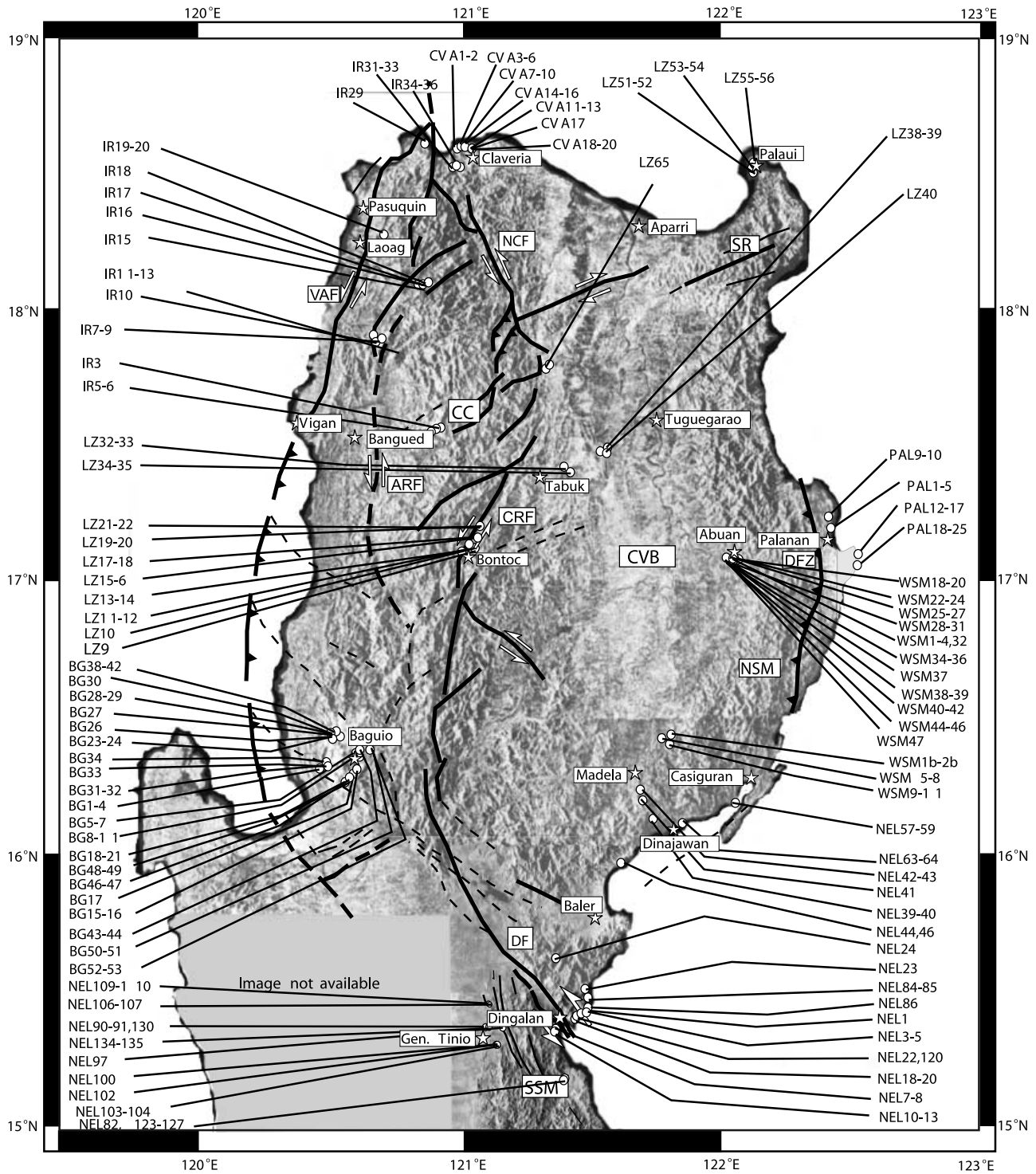
Figure 3. Radar image of northern Luzon showing the different morphostructural/structural features [see *Louvenbruck*, 2003] of northern Luzon. Also shown is the location of paleomagnetic sites. CC, Central Cordillera; CVB, Cagayan Valley Basin; NSM, northern Sierra Madre; SSM, Southern Sierra Madre.
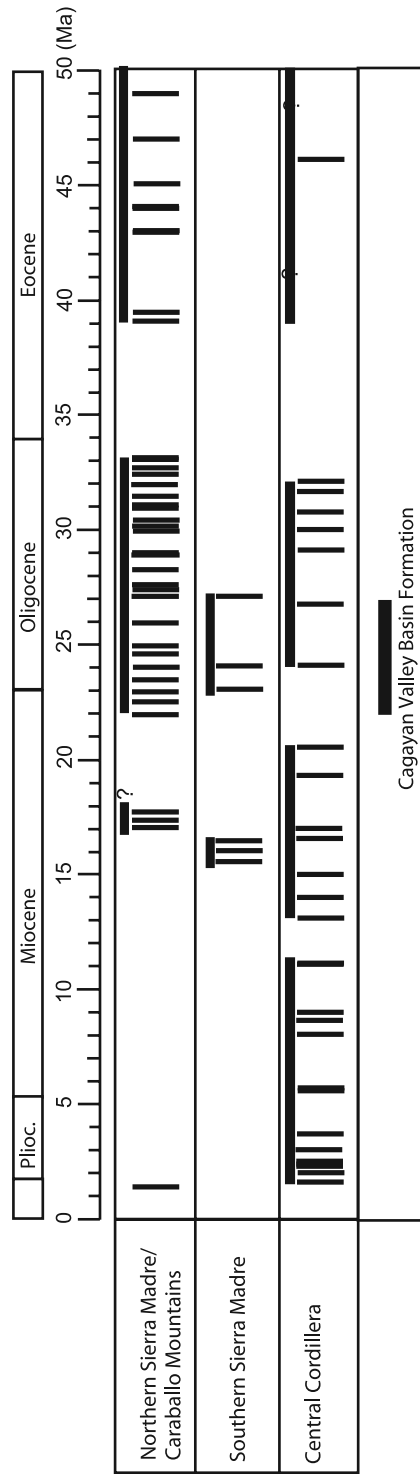
upon which Luzon and areas within the Philippine archipelago were likely built.

3.3. Southern Sierra Madre

[17] The southern Sierra Madre (SSM) is a N-S trending mountain range extending over 200 km on the eastern side of Luzon. It is separated from the NSM by the active Philippine Fault. To the west, it is onlapped by the sediments of the Central Valley Basin [*Ringenbach*, 1992]. The stratigraphy of the SSM has been studied previously by *Corby et al.* [1951], *Revilla and Malaca* [1987], *Haeck* [1987], and *Ringenbach* [1992]. Despite these investigations, the age of the ophiolitic basement rocks and the

Figure 4. Compiled stratigraphy of northern Luzon. U.P.-NIGS Geology 170, 1993 (University of the Philippines, National Institute of Geological Sciences Geology 170 Class, Geology of Baguio City and vicinity, unpublished reports, 1993) (ICS, International Commission on Stratigraphy, International stratigraphic chart, 2004, available at http://www.stratigraphy.org/chus.pdf).

Figure 5. Magmatic activity in northern Luzon. Vertical bars refer to the ages of igneous bodies compiled from previous works. The major magmatic phases as interpreted by previous workers [e.g., *Ringenbach*, 1992; *Billedo*, 1994; *Deschamps and Lallemand*, 2002] are represented by horizontal bars.
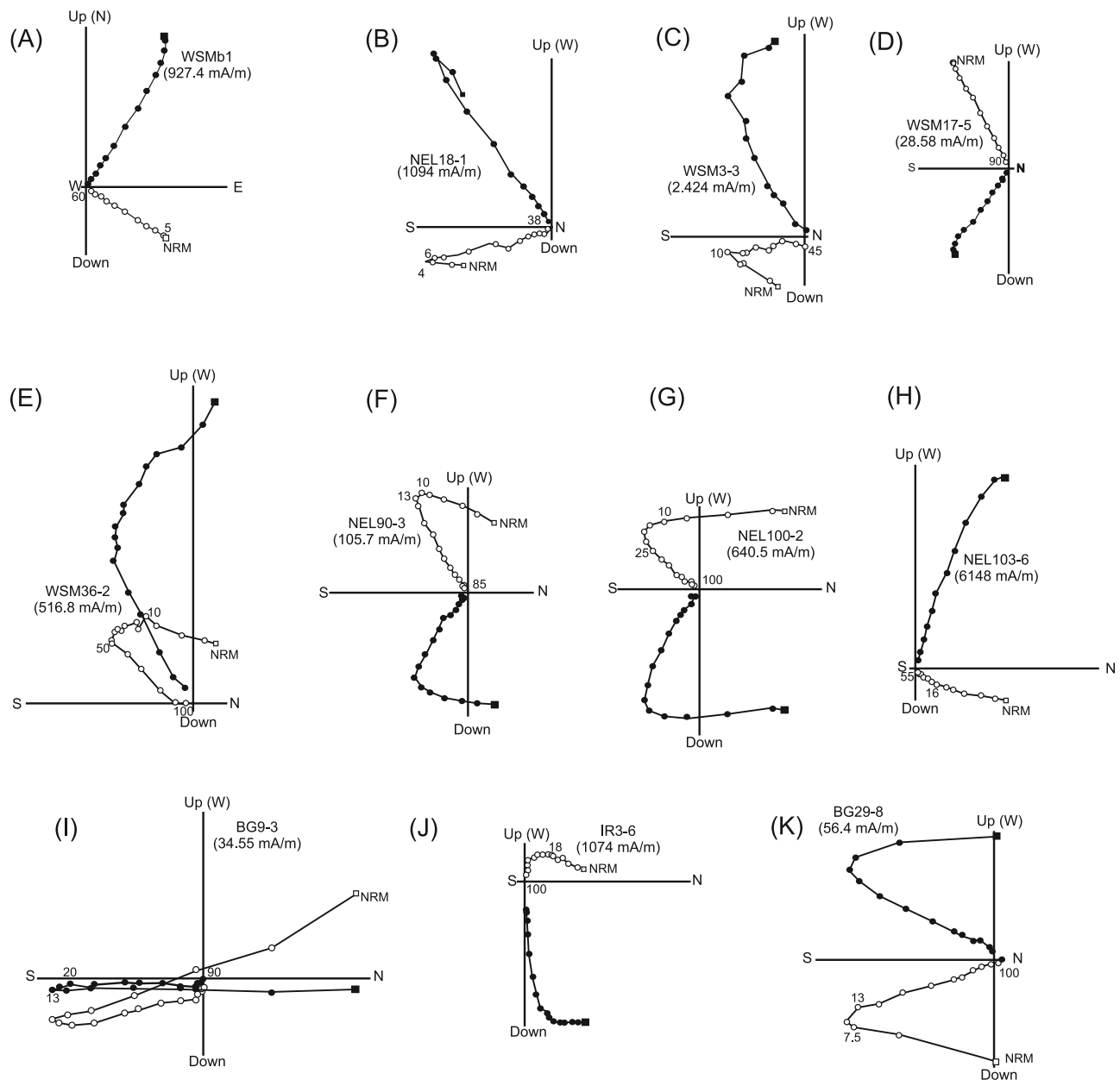
Figure 6. Vector end-point plots [*Zijderveld*, 1967] showing examples of demagnetization data in tilt-corrected coordinates for the units of northern Luzon. Plots refer to representative specimens obtained from the (a) Lubuagan Formation; (b) Caraballo Formation (Dingalan coastal section); (c–e) Caraballo Formation (Abuan River section); (f–h) Madlum Formation; (i) Plio-Pleistocene rock unit (Central Cordillera); (j) intrusive unit (Central Cordillera); (k) Klondyke Formation.

correlation of number of stratigraphic units remain unresolved. The numerous strike-slip faults cutting the range add to the complexity. Essentially, the region has a basement of ophiolitic rocks (Cretaceous? Angat Ophiolite) overlain by arc volcanic and epiclastic rocks (Eocene Maybangain Formation, lower Miocene to lower middle Miocene Madlum Formation). As with the NSM, the SSM is a site where Eo-Oligocene arc magmatism took place, which is marked by quartz diorite-granodiorite.

[18] It is worth noting that outcrops of the Maybangin Formation in the northern SSM (Dingalan area) closely resemble the Caraballo Formation epiclastic units observed

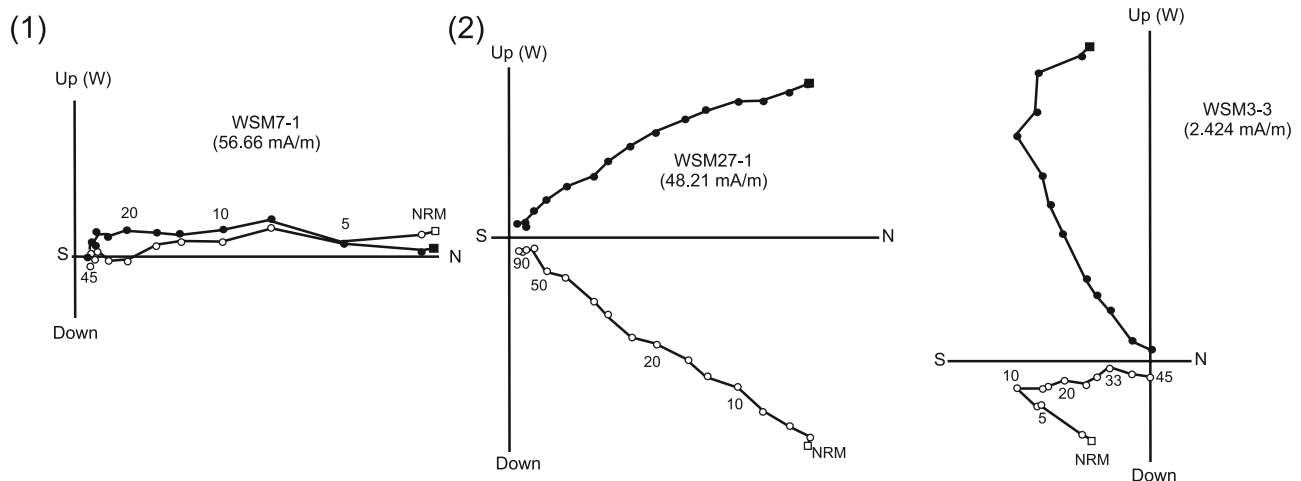just north of this area, and the two formations may be correlative.

3.4. Central Cordillera

[19] The Central Cordillera, with peaks up to 3000 m, is a 300-km-long north-south trending mountain range separating the Ilocos foothills in the west and the Cagayan Basin in the east. Understanding of the geology of Central Cordillera is based principally on the studies and exploration work conducted in the southern (Baguio City) and central (Cervantes-Lepanto) portions of the range [e.g., *Balce et al.*, 1980; *Tamesis et al.*, 1982; *United Nations Development Program* (*UNDP*), 1987; *Malettere*, 1989; *Pena*, 1992], the
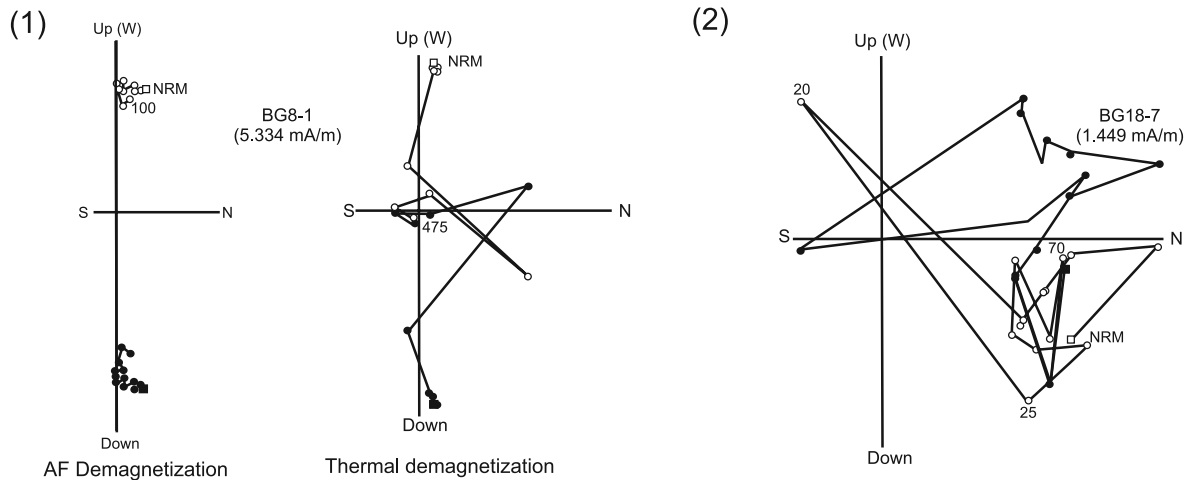
Figure 7. Vector end-point diagrams [*Zijderveld*, 1967] showing examples of demagnetization data in tilt-corrected coordinates for sites excluded for tectonic modeling. (a) Erratic demagnetization behavior being exhibited by a specimen from the (1) Zigzag (following thermal demagnetization) and (2) Klondyke formations. (b) Overprinting by secondary magnetization noted in specimens from the Lubuagan (1) and Caraballo formations (note direction of the ChRM of WSM27-1 similar to that of the LCC of WSM3-3).

latter being one of the most prolific gold-producing mining districts in the Philippines. Previous geological data [*Bellon and Yumul*, 2000] from these areas indicate that the Central Cordillera corresponds to a magmatic arc which resulted from early Miocene-Recent subduction along the Manila Trench. This arc was built upon a Cretaceous?-Eocene? ophiolitic complex (Pugo Formation-Lepanto Metavolcanics-Chico River pillow basalts) and Eocene to lower Miocene epiclastic and sedimentary rocks (e.g., Bangui Formation, Zigzag Formation, Lubuagan Formation) and intrusive bodies. The earliest pulse of plutonic activity in the region occurred in the late Eocene to Oligocene [*Florendo*, 1994]. *Wolfe* [1981] referred to the Oligocene (average age

of 27 Ma using K-Ar) plutons in the region as the Central Batholith. A high-level gabbro unit reported by *Encarnacion et al.* [1993] was also dated as late Oligocene (26.8 ± 0.5 Ma) using the U-Pb method. Meanwhile, *Malettere* [1989] reported early Oligocene K-Ar ages for gabbro (~29 Ma) and granodiorite (~30 Ma) samples from Bontoc. These Oligocene bodies may correlate with the Oligocene to early Miocene Dupax and northern Sierra Madre batholiths in eastern Luzon.

4. Paleomagnetism of Northern Luzon

[20] Rocks were sampled at 243 paleomagnetic sites in North Luzon (Figure 3). Six to eight, 2.54-cm-diameter core

Table 1a. Paleomagnetic Results From Northern Sierra Madre

Locality[a]	Sample	Lithologic Unit	NRM, mA/m	LCC Np/Nc	In Situ Dec	In Situ Inc	Tilt-corrected Dec	Tilt-corrected Inc	α95/AS	k	ChRM Np/Nc	In Situ Dec	In Situ Inc	Tilt-Corrected Dec	Tilt-Corrected Inc	α95/AS	k
Uppermost Oligocene to lower Miocene Lubuagan Formation																	
Abbag Ferry Station, Isabela	WSMb1	Siltstone	572–695	—	—	—	—	—	—	—	6/6	43.4	30.8	42.8	−2.1	3.1	479.0
	WSMb2	Siltstone	763–1085	—	—	—	—	—	—	—	7/7	35.5	52.3	36.7	19.4	3.7	332.9
Locality mean											2/2	40.1	41.6	39.8	8.7	22.3	
Abbag, Isabela	WSM9	Fine sandstone	514–762	6/7	4.5	13.4	4.3	−17.7	11.3	36.4	6/7	13.3	4.3	16.3	−16.5	4.5	224.43
	WSM10	Fine sandstone	503–629	4/6	351.2	15.0	348.5	−5.1	11.0	69.9	4/6	15.0	15.0	12.9	−6.0	7.2	162.0
	WSM11	Fine sandstone	486–632	5/7	356.8	21.3	354.5	−6.6	3.5	479.4	5/7	20.1	12.5	18.5	−6.1	6.1	157.1
Locality mean				3/3	357.5	16.6	355.6	−9.9	1.6	60.8	3/3	16.1	10.6	15.9	−9.5	10.1	148.6
Santo Nino River, Madela	WSM14	Fine sandstone	82–254	2/7	98.2	18.1	359.4	41.0	38.5		5/7	220.8	−29.5	212.5	−28.1	5.6	190.2
ChRM mean[b]																	
		Fisher									6	26.8	24.5	26.5	2.7	17.9	15
											6					17.9	15
		M & R									6	NA	26	NA	2.9	18.4	11.2
											6					18.3	11.3
Eocene Caraballo Formation: Coast North of Dingalan, Eastern NSM																	
Coast north of Dingalan	NEL18	Pillow basalt	1094–3688	—	—	—	—	—	—	—	4/5	246.1	−22.0	243.3	6.7	9.2	100.6
	NEL19	Pillow basalt	1506–22860	—	—	—	—	—	—	—	5/5	261.6	−32.3	251.7	−8.2	9.5	66.4
	NEL20	Pillow basalt	2500–11670	—	—	—	—	—	—	—	3/6	250.7	−3.5	254.9	22.2	20.6	11.6
Locality mean (NEL18 and 19)											**2/3**	**253.5**	**−27.4**	**247.5**	**−0.8**	**17.1**	**15.4**
Site 70 to 100 m stratigraphically higher than NEL18 to 20 sites	NEL22	Pillow basalt	114–313	—	—	—	—	—	—	—	6/6	301.8	−3.3	298.9	−4.2	17.7	15.4
Coast north of Dingalan	NEL120	Pillow basalts	2415–4222	—	—	—	—	—	—	—	4/6	226.5	−2.8	226.7	7.3	14.4	41.6
ChRM mean[c]		Fisher									3	243.8	−19.6			35.1	13.4
		M & R									3		−20.0	240.6	2.0	23.9	27.8
											3					38.2	14.7
											3				2.0	22.0	42.7
Eocene Caraballo Formation: Extrusives and Volcaniclastics																	
Abuan River; western NSM Section																	
Locality 1	WSM1	Lava flow	10–43	4/4	322.9	44.6	312.1	15.6	50.4	4.3	3/4	244.5	33.9	252.2	6.2	22.8	30.3
	WSM2	Lava flow	2–13	—	—	—	—	—	—	—	6/7	205.7	32.9	227.7	21.3	6.8	98.7
	WSM3	Tuffaceous siltstone	2.4–2.8	3/6	316.7	50.9	305.9	19.9	27.9	20.5	4/6	230.1	25.6	237.5	4.1	6.7	190.4
	WSM4	Tuffaceous siltstone	2.6–3.9	4/7	313.5	34.0	308.3	3.2	34.4	8.1	6/7	226.2	28.5	235.6	8.0	7.4	108.7
	WSM32	Tuffaceous siltstone	0.9–1.6	5/6	325.8	64.0	305.3	34.0	16.8	21.8	6/6	204.2	28.4	218.7	18.4	13.9	24.1
Locality mean											5/5	222.1	30.7	234.6	11.8	13.8	31.9
Locality 2	WSM30	Tuffaceous siltstone	43–67	—	—	—	—	—	—	—	6/6	192.8	40.3	217.4	42.4	3.8	309.0
	WSM31	Tuffaceous siltstone	4–6	3/6	329.4	49.3	320.1	25.9	22.6	30.9	4/4	225.7	5.8	226.3	−2.4	13.1	50.4
Locality mean																	
Locality 3	WSM17	Lava flow	28–45	—	—	—	—	—	—	—	6/7	181.0	−60.3	139.1	−56.6	6.3	114.6
	WSM19	Lava flow	29–48	—	—	—	—	—	—	—	5/6	192.3	−56.2	152.1	−57.9	2.7	826.0
	WSM20	Lava flow	25–33	—	—	—	—	—	—	—	5/6	196.3	−52.5	160.2	−57.2	5.7	181.6
Locality mean																	
Locality 4	WSM22	Pillow basalt	54–297	3/6	12.4	−11.9	7.6	6.0	33.7	14.5	6/6	53.6	−35.4	55.9	−2.0	4.8	198.0
	WSM24	Pillow basalt	182–266	4/7	355.7	36.3	328.3	39.6	23.6	16.1	6/7	44.0	−20.8	45.1	10.9	8.0	71.6
Locality mean																	

Table 1a. (continued)

Locality[a]	Sample	Lithologic Unit	NRM, mA/m	LCC Np/Nc	In Situ Dec	In Situ Inc	Tilt-corrected Dec	Tilt-corrected Inc	α95/AS	k	ChRM Np/Nc	In Situ Dec	In Situ Inc	Tilt-Corrected Dec	Tilt-Corrected Inc	α95/AS	k
Locality 5	WSM25	Tuffaceous siltstone	210-393	—	—	—	—	—	—	—	5/6	350.8	24.6	333.4	28.3	3.5	477.5
	WSM27	Lava flow	25-80	—	—	—	—	—	—	—	6/6	347.8	33.2	324.6	33.4	7.7	77.3
Locality mean																	
Locality 6	WSM34	Pillow basalt	508-1320	5/6	2.7	27.4	353.1	19.0	15.1	26.7	6/6	25.7	0.7	24.7	4.8	6.3	112.6
	WSM35	Pillow basalt	203-578	4/6	0.2	27.1	350.8	19.5	9.5	94.3	4/7	293.3	−22.1	295.9	−44.8	14.6	40.3
Locality mean																	
Locality 7	WSM37	Lava flow	2-23	3/4	343.8	31.5	332.6	14.2	51.3	6.8	4/4	322.9	42.8	312.7	13.8	30.6	10.0
Locality 8	WSM38	Tuffaceous siltstone	1.9-3.5	2/6	327.7	61.7	300.9	35.5	15.1	—	3/6	235.8	44.7	246.3	15.2	10.9	129.0
Locality 9	WSM40	Pillow basalt	79-332	—	—	—	—	—	—	—	5/6	347.9	35.1	336.8	23.1	9.5	65.3
Locality 10	WSM45	Lava flow	256-625	3/6	32.1	20.3	19.0	14.6	38.3	11.5	4/6	304.4	46.8	304.2	6.8	9.5	95.5
Eocene Caraballo Formation: Intrusives																	
Abuan River; western NSM Section																	
Locality 1	WSM18	Basaltic dike	4-10	4/6	215.2	47.2	226.7	27.0	11.5	65.3	5/6	222.4	21.9	225.3	1.2	8.5	82.9
Locality 2	WSM23	Basaltic dike	55-105	—	—	—	—	—	—	—	4/6	350.5	31.5	328	33.5	9.2	101.4
Locality 3	WSM36	Basaltic dike	517-1263	3/6	351.4	45.8	334.9	33.4	87.5	2.9	5/6	244.4	−8.1	239.7	−25.1	5.2	220.1
Locality 4	WSM39	Basaltic dike	13-16	—	—	—	—	—	—	—	5/5	232.8	43.3	243.6	14.7	4.7	268.5
Locality 5	WSM44	Basaltic dike	111-311	7/7	357.8	26.2	213.0	−13.8	5.9	107.3	3/7	285.3	22.2	286.1	−15.7	20.7	36.6
ChRM mean[d]	Fisher										13/13	222.1	25.1	229.7	6.5	11.1	15.0
											13/13					10.6	16.3
	M & R										13/13	NA	26.9	NA	7.0	10.2	12.1
																10.2	12.0

[a]See Table 2 for locality descriptions.
[b]Individual site means combined.
[c]For α95 < 15°; NEL18, 19, and 120.
[d]Sites α95 < 15°; siltstone WSM3, 4, 30,31,32,38; lava flow WSM2, 22, 24, 34; dikes 18, 36, 39.

samples were obtained at each site using a portable gasoline powered rock drill and oriented using a Brunton compass mounted in a Pomeroy orientation table. In the majority of cases, stepwise magnetic "cleaning" and remanence measurement was carried out using a Molspin alternating field tumbling demagnetizer (100 mT peak field) in tandem with the JR5A spinner magnetometer. In cases were AF treatment was ineffective, thermal demagnetization was carried out using a Magnetic Measurement MMTD18 Thermal demagnetizer. Demagnetization data were analyzed using vector end-point diagrams and equal area stereographic projections (Figures 6 and 7).

[21] Isothermal remanent magnetization (IRM) experiments were carried out on a representative sample for each site to provide basic information on the magnetic carriers. An ASC IM-10 Impulse Magnetizer (1.1 T peak field) was used to generate the IRM in samples that had previously been AF demagnetized. The IRM ratio (IRM at 0.3 T/IRM at 1.1 T; see *Ali* [1989], as cited by *Ali and Hall* [1995] and *Ali et al.* [2001]) was used to help determine the principal remanence carriers. As a general guide, IRM ratios above 0.9 indicate magnetite as the dominant carrier, whereas values below 0.9 indicate that the remanence is attributed to other minerals. The *Lowrie* [1990] test was conducted on representative samples to provide a more in-depth analysis of the magnetic properties of the samples, especially with those having two or more magnetization carriers.

[22] As an aid to the interpretation of the remanent magnetization, the NRM/IRM demagnetization technique developed by *Fuller et al.* [1988] and *Cisowski et al.* [1990] was applied to a representative sample from each site. This technique involves comparing the decay of the sample's NRM with that of its IRM at equivalent AF demagnetization steps. On the basis of empirical observations, fine-magnetite bearing igneous samples that have acquired primary thermoremanent magnetization tend to display NRM/IRM ratios greater than 10^{-2}. However, for rocks with NRM/IRM ratios less than 10^{-3}, it is generally considered that the remanence is a secondary chemical signal. The *Fuller et al.* [1988] test can also be applied for sedimentary rocks carrying detrital magnetite, although in this case it is anticipated that the primary depositional signal is less efficiently recorded than a secondary overprint. From experimental observations, the ratio for sediments carrying a primary NRM is often in the order of 10^{-3}.

[23] It is worth noting that a number of sites excluded for tectonic modeling have specimens carrying large secondary overprints (Figure 7). NRM/IRM demagnetization experiments show the clear influence of this overprint on the specimens' remanence (see section 4.1). Results from the other sites were also excluded due to the erratic demagnetization behavior being displayed by the specimens or the poor clustering of characteristic remanent magnetization (ChRM) directions ($\alpha_{95} > 15°$) (Figure 7). Sites (e.g., WSM28, PAL11) that have only two specimens useful for paleomagnetic analyses were also rejected.

[24] Six out of 13 formations/intrusive suites sampled on northern Luzon yielded reliable data (from 66 sites) (Tables 1a, 1b, 1c, and 2). These include (1) the Oligo-Miocene Lubuagan Formation and the Eocene Caraballo Formation in the northern Sierra Madre, (2) the upper lower to lower middle Miocene Madlum Formation in the south-

ern Sierra Madre, and (3) the Plio-Pleistocene rock units, the middle? to late? Miocene intrusive units and the middle to upper Miocene Klondyke Formation. Reliable results (from five sites) were also obtained from the Cretaceous?-Eocene? Chico River basalts exposed near Bontoc (K. L. Queano et al., manuscript in preparation, 2007). Results from the other rock units were excluded from tectonic interpretations mainly due to three main reasons (the data and basic interpretation are discussed in some detail by *Queano* [2006]): (1) poor clustering of the combined site directions (e.g., Lower Cretaceous Casiguran ophiolite and Oligocene? to early? Miocene dikes, northern Sierra Madre; Eocene Maybangain Formation, southern Sierra Madre; Oligo-Miocene pillow basalts, Palaui Island), (2) erratic demagnetization behavior displayed by specimens such as those from the upper Oligocene to lower Miocene Zigzag Formation, making it impossible to identify their characteristic remanent magnetization (Figure 7) (the sites from this formation have 40–80% of their initial NRM remaining after AF demagnetization to 100 mT), and (3) weak magnetization of specimens such as those from the upper Eocene Bangui Formation. Remanence of specimens (especially those from pillow basalts) from this formation is dominated by high-coercivity hematite. Subsequent thermal demagnetization of the specimens from these sites only yielded erratic demagnetization behavior or widely scattered paleomagnetic directions.

4.1. Paleomagnetic Results: Northern Sierra Madre
4.1.1. Oligo-Miocene Lubuagan Formation

[25] Block samples (WSMb1 and WSMb2) and drill core specimens were collected from twelve sites in three localities in fine-grained sandstones and siltstones of the upper-most Oligocene to lower Miocene Lubuagan Formation, western northern Sierra Madre (Figure 3 and Table 1a). Six sites were excluded from tectonic interpretations based on the initial AF demagnetization results of pilot samples (three per site). The rejected sites mostly carry secondary overprints mainly in the form of large viscous magnetizations. AF demagnetization of specimens from sites WSMb1and WSMb2 (from the same locality) essentially revealed a single component of magnetization (Figure 6a). Demagnetization was usually completed at 60 mT. In contrast, sites WSM9, WSM10 and WSM11 (from the same locality) have two components of remanence: a low-coercivity component (LCC) viscous remanence remanence removed at ~10 mT and a higher stability ChRM isolated above 10–15 mT (Table 1a).

[26] IRM experiments on representative specimens show IRM ratios of 0.98, suggesting magnetite as the principal remanence carrier. This result is supported by thermal demagnetization of a representative specimen from site WSMb1 which shows complete demagnetization at ~600°C. The plot of the soft coercivity fraction also shows a marked discontinuity at 350°C and at 475°C, which could be ascribed to some form of titanomagnetite.

[27] The presence of both normal and reverse polarity sites suggests that the magnetization is primary (Figure 8). This is supported by NRM/IRM demagnetization experiments which show most representative specimens plotting some distance above 10^{-3} (Figure 9). The remanence of

Table 1b. Paleomagnetic Results From the Southern Sierra Madre for Upper Lower to Lower Middle Miocene Madlum Formation

Locality	Sample	Lithologic Unit	NRM, mA/m	LCC Np/Nc	In Situ Dec	In Situ Inc	Tilt-corrected Dec	Tilt-corrected Inc	α95/AS	k	ChRM Np/Nc	In Situ Dec	In Situ Inc	Tilt-Corrected Dec	Tilt-Corrected Inc	α95/AS	k
Rio Chico River, General Tinio	NEL90	Siltstone	123–142	6/6	4.2	7.5	1.4	21.4	7.2	86.6	6/6	132.2	−43.9	115.1	−42.5	5.6	143.6
	NEL91	Siltstone	113–137	7/7	9.9	18.1	5.4	33.7	13.3	21.5	5/7	102.2	1.4	103.7	9.0	3.9	377.6
	NEL130	Siltstone	80–162	7/7	0	8.3	356.6	23.3	5.6	146.3	6/7	127.6	−16.1	121.9	−15.1	6.7	99.6
Locality mean				3/3	4.6	11.3	1.0	26.2	11.7	111.2	3/3	119.4	−19.9	113.4	−16.3	43.8	9.0
Rio Chico River, General Tinio, Nueva Ecija	NEL134	Siltstone	58–174	6/6	2.9	19.4	3.2	−17.2	11.0	38.3	6/6	104.7	−14.9	115.2	−19.7	8.0	71.1
Sumacbao River, General Tinio	NEL100	Andesite flow	116–148	6/6	2.3	12.5	358.5	−3.7	5.7	138.4	6/6	132.3	−72.5	116.6	−25.6	3.0	505.6
	NEL101	Agglomerate	1448–3191	5/5	20.1	3.3	17.3	13.1	21.5	13.6	5/5	114.3	−66.9	111.2	−19.0	9.4	67.5
Locality mean				2/2	11.3	8	7.8	4.8	25.1	—	2/2	122.1	−69.9	113.8	−22.3	8.3	—
Sumacbao River, General Tinio	NEL103	Basaltic dike	287–293	—	—	—	—	—	—	—	5/5	287.5	8.5	290.2	12.1	4.9	249.8
	NEL104	Basaltic dike	1821–13210	—	—	—	—	—	—	—	6/6	283.6	8.3	286.3	13.1	8.1	69.0
Locality mean				—	—	—	—	—	—	—	2/2	285.5	8.4	288.3	12.6	3.9	—
Dona Josefa	NEL109	Basaltic dike	1467–1939	—	—	—	—	—	—	—	5/5	174.6	−54.6	152.0	−28.7	4.3	323.5
	NEL110	Basaltic dike	214–218	—	—	—	—	—	—	—	6/6	217.2	−7.2	211.6	−10.6	3.6	352.5
Locality mean											2/2	201.7	−32.6	183.7	−22.4	58.4	8.0
ChRM mean[a]	Fisher										4/4	291.0	27.6	292.6	17.7	34.6	251.9
											4/4					5.8	251.9
	M & R										4/4	NA	34.1	NA	17.8	48.0	4.2
											4/4					6.7	185.5

[a]Combined locality means; NEL 109 and 110 excluded; reverse polarity sites inverted to normal.

Table 1c. Paleomagnetic Results From the Central Cordillera

Locality	Sample	Lithologic Unit	NRM, mA/m	LCC Np/Nc	In Situ Dec	In Situ Inc	Tilt-Corrected Dec	Tilt-Corrected Inc	α95/AS	k	ChRM Np/Nc	In Situ Dec	In Situ Inc	Tilt-Corrected Dec	Tilt-Corrected Inc	α95/AS	k
Plio-Pleistocene Rock Units																	
Bontoc Road 1	LZ9	Lava flow	442-2427								6/6	3.9	23.6	3.9	23.6	8.6	61.0
Bontoc Road 2[a]	LZ10	Lava flow	2938-11200								7/7	354.3	31.6	354.3	31.6	1.7	1215.0
Tabuk	LZ39	Mudstone (Ilagan Fm)	13-31								5/6	10.6	32.3	338.7	63.1	18.5	25.5
Bued River, Kennon Road	BG9	Fine andesite dike	14-187	3/7	350.0	-19.4	350.0	-19.4	14.5	73.2	7/7	183.9	-26.9	183.9	-26.9	4.6	172.4
Mount Sto Tomas	BG44	Lamprophyric dike	1121-1796								6/7	358.0	22.2	358.0	22.2	3.5	365.0
Philex Road 1	BG52	Fine andesite dike	128-435	4/5	351.8	-2.7	348.9	-16.5	50.7	4.3	5/5	310.2	42.2	333.2	36.2	11.9	42.4
Philex Road 2	BG53	Fine andesite dike	79-346	5/5	7.3	30.5	44.5	4.0	8.8	3.9	5/5	288.4	47.1	319.6	36.9	7.3	158.9
ChRM mean[b]											6/7	344.2	35.4			23.6	9.0
		Fisher									6/7	NA	33.2	349.9	30.6	10.8	31.3
		M & R									6/7	NA		NA	29.9	6.4	82.6
Middle? to Late? Miocene Intrusive Units																	
Mount Agapang	IR 3	Andesite dike	418-2150	6/6	2.3	18.3	2.3	18.3	8.0	71.0	6/6	82.4	-18.3	82.4	-18.3	5.3	161.8
Barangay Nalbuan, Abra	IR 5 & 6	Diorite (IR5) Andesite xen. (IR6)	268-291	8/9	358.8	13.2	358.8	13.2	9.5	34.6	6/9	279.5	30.9	279.5	30.9	5.7	96.4
Nueva Era, Ilocos Norte	IR 10	Andesite dike	408-1800	—	—	—	—	—	—	—	5/6	207.8	-26.0	207.8	-26.0	4.9	246.1
Nagbasa River, Ilocos Norte	IR 11	Andesite dike	356-714	6/6	359.7	21.1	2.0	3.9	4.8	192.9	5/6	82.6	3.2	84.3	-9.3	7.8	96.2
	IR 13	Andesite dike	578-1243	7/8	355.5	23.3	357.0	1.9	50.9	2.4	8/8	115.8	-8.2	118.5	-9.9	3.6	243.3
Mean											2/2	101.4	-10.0	99.1	-2.6	33.7	106.0
Solsona, Ilocos 1	IR 15	Diorite	613-4076	5/7	17.0	-59.7	17.0	-59.7	22.6	12.4	5/7	221.3	20.5	221.3	20.5	7.5	19.6
Solsona, Ilocos 2	IR 16	Andesite dike	654-953	4/5	354.7	21.4	354.7	21.4	15.4	36.4	3/5	278.5	35.6	278.5	35.6	21.3	25.4
	IR 17	Andesite dike	381-1613	5/6	349.8	19.4	349.8	19.4	24.2	10.9	3/6	258.5	20.7	258.5	20.7	25.4	23.4
Mean (Directions of specimens combined)				—	—	—	—	—	—	—	6/11	272.6	33.4	272.6	33.4	14.1	
Claveria coast	CVA15	Andesite dike	705-843	—	—	—	—	—	—	—	3/7	103.0	-16.4	103.0	-16.4	8.1	232.0
ChRM mean[c]	Fisher										7/7	269.4	21.3			18.9	11.2
	M & R										7/7	NA	20.3	NA		8.8	37.3
Middle to Upper Miocene Klondyke Formation																	
Asin Road 1	BG26	fine sandstone	100-915	—	—	—	—	—	—	—	6/6	350.1	23.7	338.3	34.8	15.2	20.3
Asin Road 2	BG29	fine sandstone	55-103	4/6	355.3	59.7	326.5	0.3	45.3	—	4/6	194.3	13.3	219.8	21.9	9.4	67.8
Marcos Highway 1	BG31	fine sandstone	76-139	3/5	33.5	-12.3	28.7	-14.6	35.3	13.2	5/5	97.8	-4.6	96.3	-23.7	21.8	33.0
Marcos Highway 2	BG33	fine sandstone	318-454	5/7	328.5	24.4	334.6	33.2	36.8	5.3	6/7	70.3	-12.2	67.9	-24.3	5.2	220.7
Marcos Highway 3	BG34	fine sandstone	162-311	—	—	—	—	—	—	—	3/7	356.0	34.4	334.3	15.6	22.9	30.0

Table 1c. (continued)

Locality	Sample	Lithologic Unit	NRM, mA/m	LCC Np/Nc	In Situ Dec	In Situ Inc	Tilt-Corrected Dec	Tilt-Corrected Inc	α_{95}/AS	k	ChRM Np/Nc	In Situ Dec	In Situ Inc	Tilt-Corrected Dec	Tilt-Corrected Inc	α_{95}/AS	k
Nagtalisan River, Asin 1	BG39	fine sandstone	80–108	—	—	—	—	—	—	—	5/7	357.0	14.4	352	12.2	6.2	81.7
Nagtalisan River, Asin 2	BG40	mudstone	30–139	3/6	242.4	47.7	255.2	32.3	64.8	4.7	5/6	40.9	0.2	39.7	8.5	6.3	216.9
	BG42	fine sandstone	21–60	—	—	—	—	—	—	—	7/7	353.2	14.0	350.0	7.6	6.3	92.9
Bued River, Kennon Road	BG48	siltstone	12–16	—	—	—	—	—	—	—	4/7	350.6	7.8	340	20.2	8.8	110.9
	BG49	siltstone	16–30	—	—	—	—	—	—	—	5/6	356.8	6.5	345.9	23.3	6.7	132.6
Locality mean											2/2	353.7	7.2	342.9	21.8	6.3	
ChRM mean (sites α_{95}<15°)	M & R										8/8	NA	11.7	NA	23.7	5.8	69.1
Sites 26, 29, 33 (inverted to normal polarity), 39, 40, 42, 48, 49											8/8					8.9	46.6

[a]Approximately 2 km NNE of LZ9; volcanics almost flat-lying.
[b]Sites α_{95} < 15°: LZ9, 10, BG9, 44, 52, 53.
[c]Sites CVA15, IR3, 5/6, 11 (in TC), 13 (in TC), 15 and 16/17; CVA 15 and IR3, 11 and 13 inverted to normal polarity.

WSM14 is less efficiently recorded, with NRM/IRM starting below 10^{-3}. At higher demagnetization steps, the plot swings to above this value as the contribution of the low-coercivity grains is separated from higher coercivity phases. The in situ mean direction for the six sites (WSM14 inverted to normal polarity) is D = 26.8°, I = 24.5°, α_{95} = 17.9°, k = 15.0; the tilt-corrected mean direction is D = 26.5°, I = 2.7°, α_{95} = 17.9°, k = 15.0. Applying the inclination-only statistics of *McFadden and Reid* [1982] gives almost similar results (in situ: I = 26.0°, α_{95} = 18.4°, k = 11.2; tilt-corrected: I = 2.9°, α_{95} = 18.3°, k = 11.3). The inclination suggests a near equatorial latitude (1.4° ± 9.2°).

4.1.2. Eocene Caraballo Formation
4.1.2.1. Dingalan Area

[28] Five drill core sites were collected from pillow basalts of the middle to upper Eocene Caraballo Formation along a coastal section approximately 2 km north of the Dingalan town. Three sites (NEL18 to 20) were sampled on the southern portion of the embayment (Figure 3). The remaining sites (NEL22 and NEL120; stratigraphically higher by ~70 to 100 m), were drilled about 1 km away on the northern side of the bay. The attitude of the pillows varies quite significantly (from a 12° dip to the north, to a 40° dip to the NE), and several prominent listric normal faults cut the outcrop. Sedimentary rocks conformably overlying the volcanic rocks provided useful structural control.

[29] Demagnetization revealed a simple magnetization history. Typically, a viscous remanence is removed at ~5 mT and a higher stability magnetization is isolated above ~7.5 mT. In tilt-corrected coordinates, the declinations are west directed, with inclinations generally varying from shallow positive (NEL18 and NEL120) to shallow negative (NEL19 and NEL22) (Figures 6b and 10). IRM analysis of representative specimens showed IRM ratios of 0.99 indicating magnetite as the dominant remanence carrier. The different orthogonal components of the composite IRM demagnetize completely by 580°C, suggesting that magnetite is present in a wide range of coercivities (Figure 11). A part of the soft fraction also shows a slight drop at 350°C, which may be ascribed to a form of titanomagnetite.

[30] Sites NEL18, NEL19 and NEL120 have site-mean directions with relatively good clustering (α_{95} < 15°). Combining these site-mean directions gives an in situ direction of D = 243.8°, I = −19.6°, α_{95} = 35.1°; k = 13.4 and a tilt-corrected direction of D = 240.6°, I = 2.0°, α_{95} = 23.9°, k = 27.8. Sites NEL20 (α_{95} = 20.6°, k = 11.6) and NEL22 (α_{95} = 17.7°, k = 15.6) have relatively scattered directions, and based on *Van der Voo* [1990], these directions should probably be excluded from any tectonic interpretation. It is interesting to note, however, that site NEL22, which sits well away from the main cluster both in in situ and in tilt-corrected coordinates, has a mean inclination that appears to be consistent with the shallow inclination (in tilt-corrected coordinates) exhibited by most sites. This could suggest that the spread in the declination data from this area reflects localized rotations possibly related to the movement(s) of the faults within section.

[31] The tilt-corrected site mean direction gives better clustering statistics than that of the in situ direction (Tables 1a–1c). This suggests that the remanence predates

Table 2. Descriptions of Localities Used in Table 1

Locality	Latitude	Longitude	Strike	Dip
Northern Sierra Madre				
Abbag Ferry Station, Isabela	16°15.589′N	121°39.914′E	309°	33° → NE
Abbag, Isabela	16°15.382′N	121°39.307′E	233°	33° → NW
Santo Nino River, Madela	16°17.667′N	121°41.264′E	222°	16° → NW
Coast north of Dingalan	15°22.666′N	121°25.896′E	300°	40° → NNE
Coast north of Dingalan	15°22.666′N	121°25.896′E	285°	12° → N
Abuan River; western NSM				
Locality 1	17°12.00′N	122°25.233′E	195°	34° → WNW
Locality 2	17°04.398′N	122°01.781′E	208°	26° → WNW
Locality 3	17°04.799′N	122°02.952′E	168°	25° → WSW
Locality 4	17°04.437′N	122°01.983′ E	158°	34° → SW
Locality 5	17°04.427′N	122°01.960′ E	158°	34° → SW
Locality 6	17°04.693′N	122°01.169′E	195°	23° → WNW
Locality 7	17°04.489′N	122°01.554′E	197°	34° → WNW
Locality 8	17°04.505′N	122°01.379′E	182°	34° → W
Locality 9	17°04.619′N	122°01.290′E	195°	23° → WNW
Locality 10	17°04.489′N	122°01.55′E	215°	40° → NW
Abuan River; western NSM				
Locality 1	17°04.799′N	122°02.952′E	168°[a]	25° → WSW (adjacent clastic unit)[a]
Locality 2	17°04.437′N	122°01.983′E	156°[a]	34° → WSW (adjacent clastic unit)[a]
Locality 3	17°04.693′N	122°01.169′E	195°[a]	23° → WNW (adjacent sed)[a]
Locality 4	17°04.505′N	122°01.379′E	182°[a]	34° → W (adjacent bed)[a]
Locality 5	17°04.489′N	122°01.55′E	215°	40° → NW (adjacent sed)
Southern Sierra Madre				
Rio Chico River, General Tinio	15°21.495′N	121°06.914′E	128°	18° → SW
Rio Chico River, General Tinio, Nueva Ecija	15°20.850′N	121°07.707′ E	299°	33° → NE
Sumacbao River, General Tinio 1	15°18.077′N	121°08.341′E	199°	48° → WNW
Sumacbao River, General Tinio 2	15°18.087′N	121°09.016′E	303°	75° → NE
Dona Josefa	15°26.021′ N	121°08.451′E	209°	55° → NW
Central Cordillera				
Bontoc Road[b]	17°06.284′N	121°00.042′E		
Tabuk	17°28.524′N	121°33.238′ E	130°	40° → SW
Bued River, Kennon Road	16°21.930′N	120°36.000′E	256°	subvertical
Mount Sto Tomas	16°21.050′N	120°33.267′E	304°	subvertical
Philex Road 1	16°17.133′N	120°38.750′E	312°	62 → SW
Philex Road 2	16°17.350′N	120°38.750′E	290°	55° → SW
Mount Agapang	17°33.80′N	120°54.833′E	040°	vertical
Barangay Nalbuan, Abra	17°33.100′N	120°53.267′E		
Nueva Era, Ilocos Norte	17°53.50′N	120°41.033′E	005°	vertical
Nagbasa River, Ilocos Norte	17°53.233′N	120°40.850′E	303°	70° → NE
Solsona, Ilocos 1	18°05.550′N	120°51.967′E		
Solsona, Ilocos 2	18°05.717′N	120°51.967′E	163°	subvertical (85°)
Claveria coast	18°36.212′N	121°01.067′E	220°	vertical
Asin Road 1	16°26.067′N	120°31.583′ E	139°	25° → SW
Asin Road 2	16°26.267′N	120°30.150′E	213°	70° → NW
Marcos Highway 1	16°20.483′N	120°20.667′E	024°	20° → ESE
Marcos Highway 2	16°21.100′N	120°29.817′E	010°	14° → ESE
Marcos Highway 3	16°23.317′N	120°31.817′E	188°	47° → W
Nagtalisan River, Asin 1	16°26.483′N	120°29.183′E	181°	21° → W
Nagtalisan River, Asin 2	16°26.150′N	120°28.950′E	193°	18° → WNW
Bued River, Kennon Road	16°14.667′N	120°31.900′E	149°	42° → SW

[a]For TC.
[b]Volcanics almost flat-lying.

deformation. NRM/IRM demagnetization experiments further show that NEL18, NEL19 and NEL20 have values $\geq 10^{-2}$, suggesting that the remanence of the sites is probably primary (Figure 11). Sites NEL18 and NEL20 have values that sit midway between a clear primary thermoremanent magnetization (TRM) and a secondary chemical remanent magnetization (CRM). Initial demagne-

tization field values clearly show the influence of viscous remanent magnetization (VRM) on the specimens' remanence. Using the statistics of *McFadden and Reid* [1982], the mean inclination in in situ coordinates for sites with $\alpha_{95} < 15°$ is $-20°$ ($\alpha_{95} = 38.2°$, $k = 14.7$); tilt-corrected mean

Lubuagan Formation, NSM
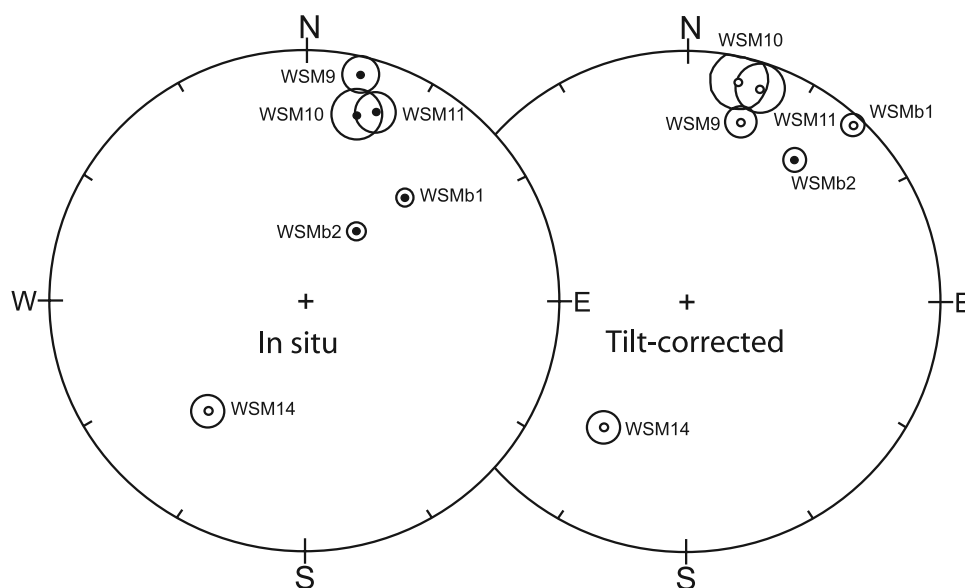
Figure 8. Summary of ChRM directional data from Lubuagan Formation sites in tilt-corrected coordinates. Solid/open symbols are downward/upward directed.

inclination is 2.0° (α_{95} = 23.9°; k = 42.7). The latter result equates to a formation latitude of 1.0°N ± 11.5°.

4.1.2.2. Abuan River

[32] Excellent exposures of the Caraballo Formation are present along the Abuan River, along the western flank of the northern Sierra Madre. The succession comprises at least a kilometer-thick sequence of west dipping (~30°) beds of volcanic breccia, basaltic flows and epiclastic deposits. Twenty-nine drill core sites were collected from 12 localities along a ~3.5 km stretch of the Abuan River. Seven of the sites were from tuffaceous siltstone beds, 16 were from the lava flows, and 6 were from basaltic dikes intruding the lavas and the epiclastic deposits.

4.1.2.3. Tuffaceous Siltstone

[33] NRM intensities of tuffaceous siltstone specimens are low for sites WSM3, 4, 32, 31 and 38, with intensities usually 2–10 mA/m. Demagnetization of specimens from these sites essentially revealed two components of magnetization: a low-coercivity component (LCC) removed at 5–0 mT and a higher stability ChRM usually isolated above 15 mT (Figure 6e and Table 1a). A possible intermediate coercivity component (ICC), commonly isolated between 7.5 to 16 mT, is also noted in some specimens collected from sites WSM3 and WSM4. In contrast, sites WSM25 and WSM30 have higher mean NRM intensities ranging from 200–400 mA/m and 40–70 mA/m, respectively. AF demagnetization of specimens from these sites revealed a single component of magnetization.

[34] Representative specimens from all seven sites have low-coercivity IRMs and with IRM ratio of greater than 0.9 which could suggest magnetite as the principal remanence carrier. However, thermal demagnetization of IRM of a representative specimen from site WSM31 indicates distinct unblocking temperatures of the low- and medium-coercivity fractions at 625–650°C. Representative specimen from site

WSM38 also shows an abrupt drop of the low- and medium-coercivity fraction at 600–650°C. These observations, along with the low-IRM saturation fields of the specimens, could imply the presence of a secondary mineral, possibly maghemite. Thermal demagnetization of the saturation magnetization of a representative specimen from sites WSM31 and 38 show several unblocking temperatures between 200° and 500°C of the low-coercivity component, indicative of high-titanium magnetites/maghemites. Remanence contribution from the high-coercivity component is almost negligible for specimen from WSM31. In contrast, the high-coercivity component (HCC) component of WSM38 has a substantial contribution to the specimen's remanence. Along with the intermediate component, the HCC of WSM38 demagnetizes completely at 700°C, possibly indicating the presence of hematite.

[35] Although poorly clustered ($\alpha_{95} > 15°$), the tilt-corrected mean direction of the LCC in all of the sites seems to point to a NW declination and a moderately steep, mostly positive inclination. When the directions of the specimens (only those with MAD < 10°) from sites WSM3, 4, 32, 31 and 38 are combined, the grouping gives a tilt-corrected LCC mean declination of 306.7° and inclination of 22.3° ($\alpha_{95} < 15°$; k = 12.2). This direction is likely not of recent origin but rather, was acquired prior or during the tilting of the strata.

[36] Directions of the ChRM group well at the sample mean level, with 4 sites (WSM3, 4, 30, 25) having confidence circles $\alpha_{95} < 10°$ (Figure 12). The clustering of the other remaining sites (WSM31, 32, 38) is also relatively good, passing *Van der Voo*'s [1990] reliability criteria of $\alpha_{95<} 15°$. NRM/IRM demagnetization experiments on representative specimens from sites WSM3, 4, 31 and 34 show values above 10^{-3} (Figure 13). Representative specimen from site WSM30 yielded NRM/IRM ratio values that start
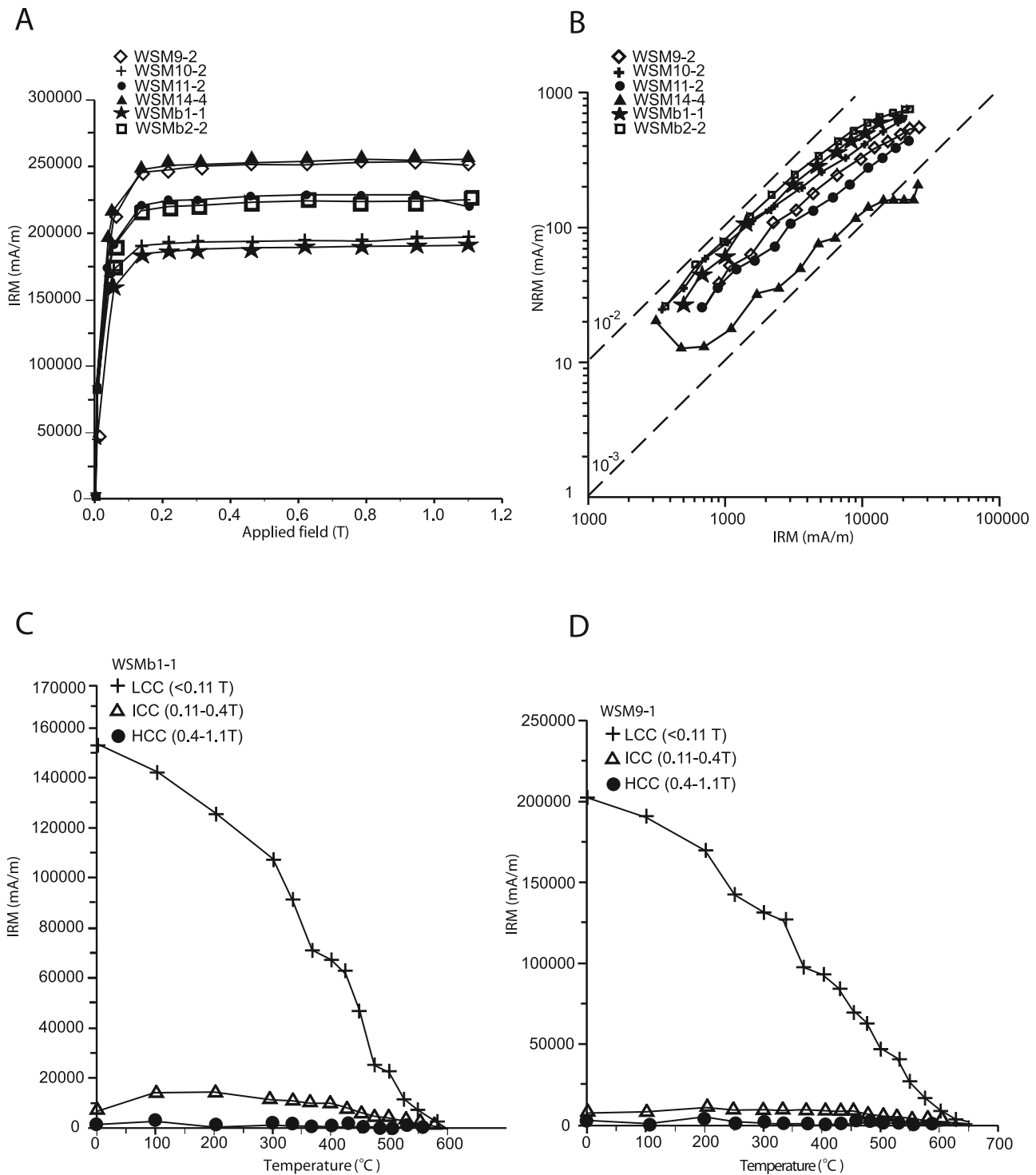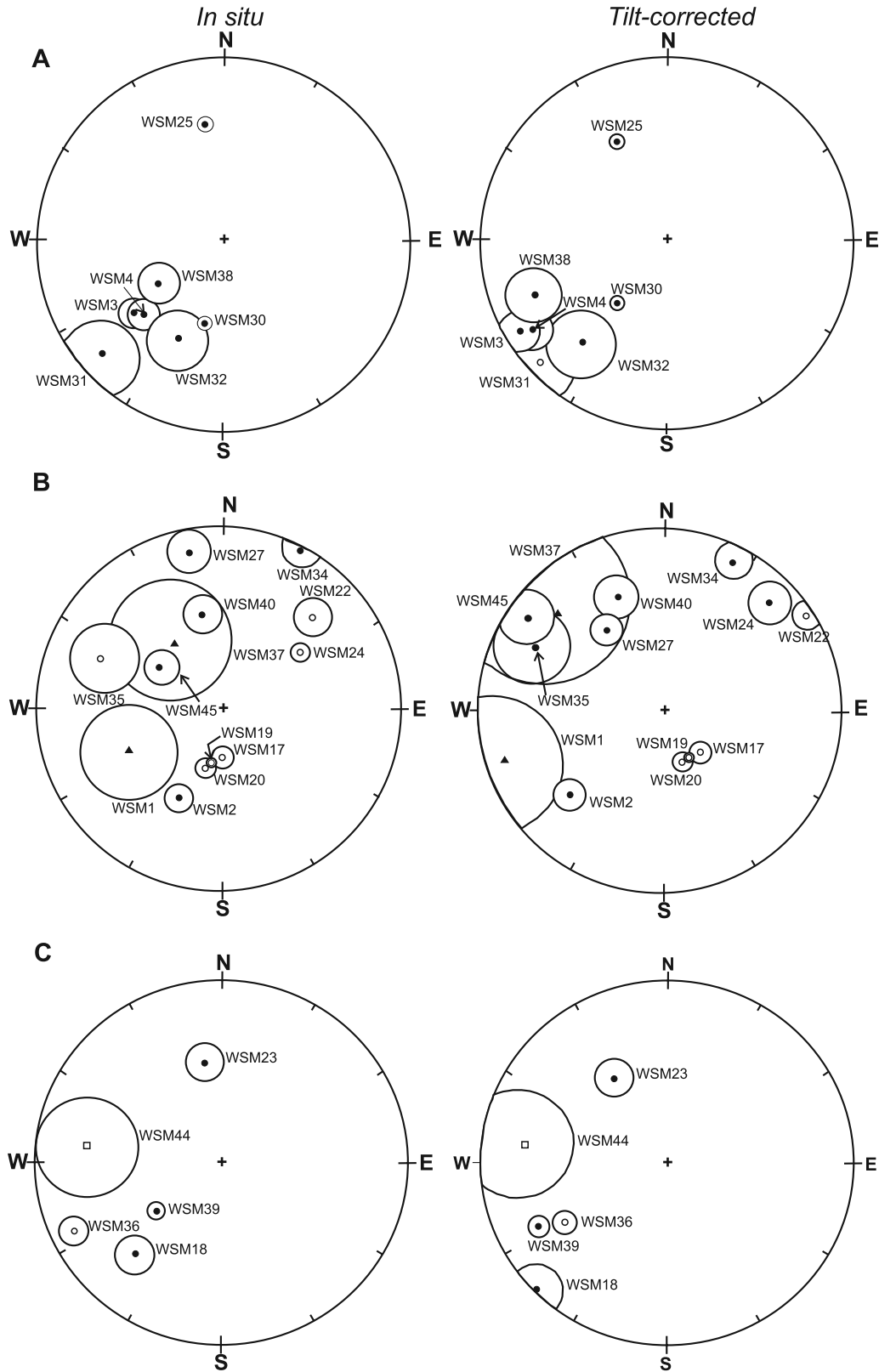
Figure 9. (a) IRM acquisition, (b) NRM/IRM demagnetization and (c–d) thermal demagnetization curves for representative specimens from Lubuagan Formation sites.

below 10^{-3}, but by the last few demagnetization steps, they are above this value. In contrast, WSM38 has values that start above 10^{-3}, but by middle magnetization they are slightly below this value. WSM 25 has values consistently below 10^{-3}, likely due to the strong secondary overprint on the specimen's ChRM. The locality-mean direction for the six siltstone sites with reliable ChRMs (WSM3, 4, 30, 31,

32, 38) is in situ D = 219.5°, I = 29.8°, α_{95} = 16.5°, k = 17.5; the tilt-corrected direction is D = 230.9°, I = 14.4°, α_{95} = 16.0°, k = 18.4.

4.1.2.4. Lava Flows

[37] Thirteen of the 16 lava flows sites have directions that could be evaluated for paleomagnetic-tectonic modeling. The sites (WSM28, 41 and 42) that were rejected either
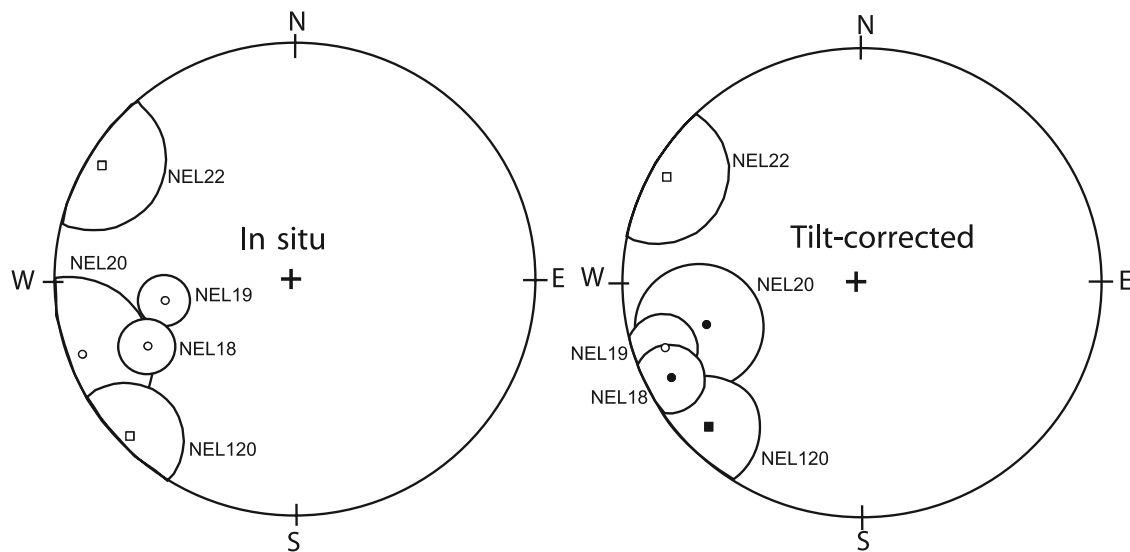
Figure 10. Summary of ChRM directional data from Caraballo Formation sites along the coast north of Dingalan in in situ and tilt-corrected coordinates. Symbols are as in Figure 8.

have only two specimens useful for paleomagnetic analysis or have specimens exhibiting different/erratic demagnetization behavior. Sites WSM17, 19, 20, and 27 yielded single components of magnetization whereas a substantial number of specimens from sites WSM1, 24, 34, 35, 37 and 45 yielded two components. LCC directions for sites WSM1, 37, 45 are randomly orientated ($\alpha_{95} > 15°$), which probably records a laboratory storage field. In contrast, those in sites WSM24, 34 and 35 are fairly well clustered, with orientation in in situ coordinates roughly parallel to that of the present field (i.e., a VRM). Specimens from WSM22, which is situated adjacent a dike (WSM23) have three components of magnetization, with the ICC isolated between 7.5 and 16 mT.

[38] Except for WSM1, representative specimens from 13 sites have low-coercivity IRMs and with IRM ratios typically 0.99 which suggests magnetite as being the principal remanence carrier (Figure 14). However, thermal demagnetization of IRM of representative specimens shows distinct unblocking temperatures of the coercivity fractions at $625-700°C$ (Figure 14). The low-IRM saturation fields and the characteristic unblocking temperature of the specimens suggest maghemite as the likely principal magnetic carrier, similar to the tuffaceous sediments. The demagnetization curves of the LCC (WSM 2, 17, 22, 34) as well as the ICC (WSM 34) fractions show several unblocking temperatures between $200°$ and $500°C$. This noisy behavior may be attributed to the presence of titanomagnetites and/or iron sulfides in the rocks. Notably, at site WSM2, several specks of pyrite are present in the rock. The presence of sulfides is also suggested more clearly by the thermal demagnetization curves for site WSM31. The curves show distinct unblocking temperature of the different coercivity fractions at around $300-350°C$ (with the HCC fraction completely demagnetized at this temperature), suggesting

that iron sulfide, probably pyrrhotite, is present in the rock at various coercivities. The remanence contribution from the HCC fraction of most specimens is minimal. For site WSM2, the HCC component decays at $700°C$, possibly indicating the presence of hematite formed either due to the breakdown of maghemite or iron sulfides during demagnetization.

[39] NRM/IRM demagnetization experiments on representative specimens show values of above 10^{-2} for WSM17, 19 and 20 (taken from the same locality) suggesting that the remanence of these sites is probably primary (Figure 14). However, the inclinations ($\sim 57.0°$) of these lava sites appear to be too steep for Eocene rocks presently situated at $\sim 17°N$, and it is possible that the effects of secular variation may have not been fully averaged. Sites WSM1, 27, 37 and 40 have NRM/IRM values that consistently plot near or below 10^{-3} indicating a strong overprint on their remanence. To note, WSM 27, 37 and 40 have declinations which roughly parallel that of the LCC of the siltstones. WSM2, 34, 35, have values that sit midway between a clear primary (10^{-2}) and a clear secondary (10^{-3}). The remanence of WSM35 is likely secondary whereas WSM2 and 34 are probably primary based on comparisons with directions from the other sites. In contrast, WSM 22 and 24 have values that start below 10^{-2} but at a higher demagnetization steps, the plots swing to above this value as the contribution of the low-coercivity grains is separated from higher coercivity phases. Along with WSM 34, these sites show direction apparently antipodal to the sites (including siltstone) with SW declinations. The mean direction for the four lava flow sites (WSM 2, 22, 24, 34; the last three sites reverted to SW) with reliable ChRMs (i.e., $\alpha_{95} < 15°$) is: $D = 216.6°$, $I = 22.8°$, $\alpha_{95} = 24.1°$, $k = 15.4$; the tilt-corrected direction is $D = 223.3°$, $I = 1.9°$, $\alpha_{95} = 22.3°$, $k = 17.9$. This mean direction roughly parallels that of the siltstone sites. Combining all mean directions
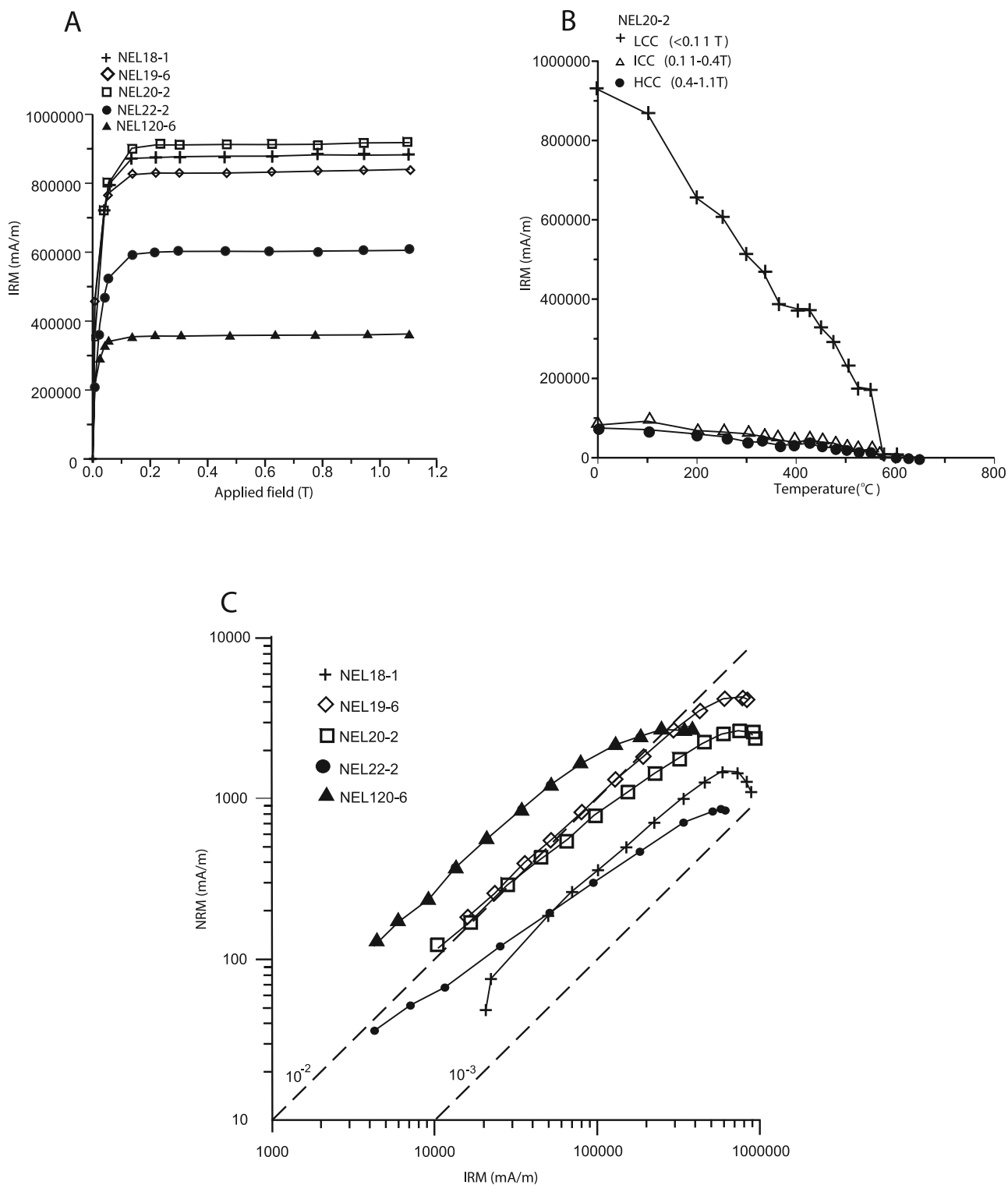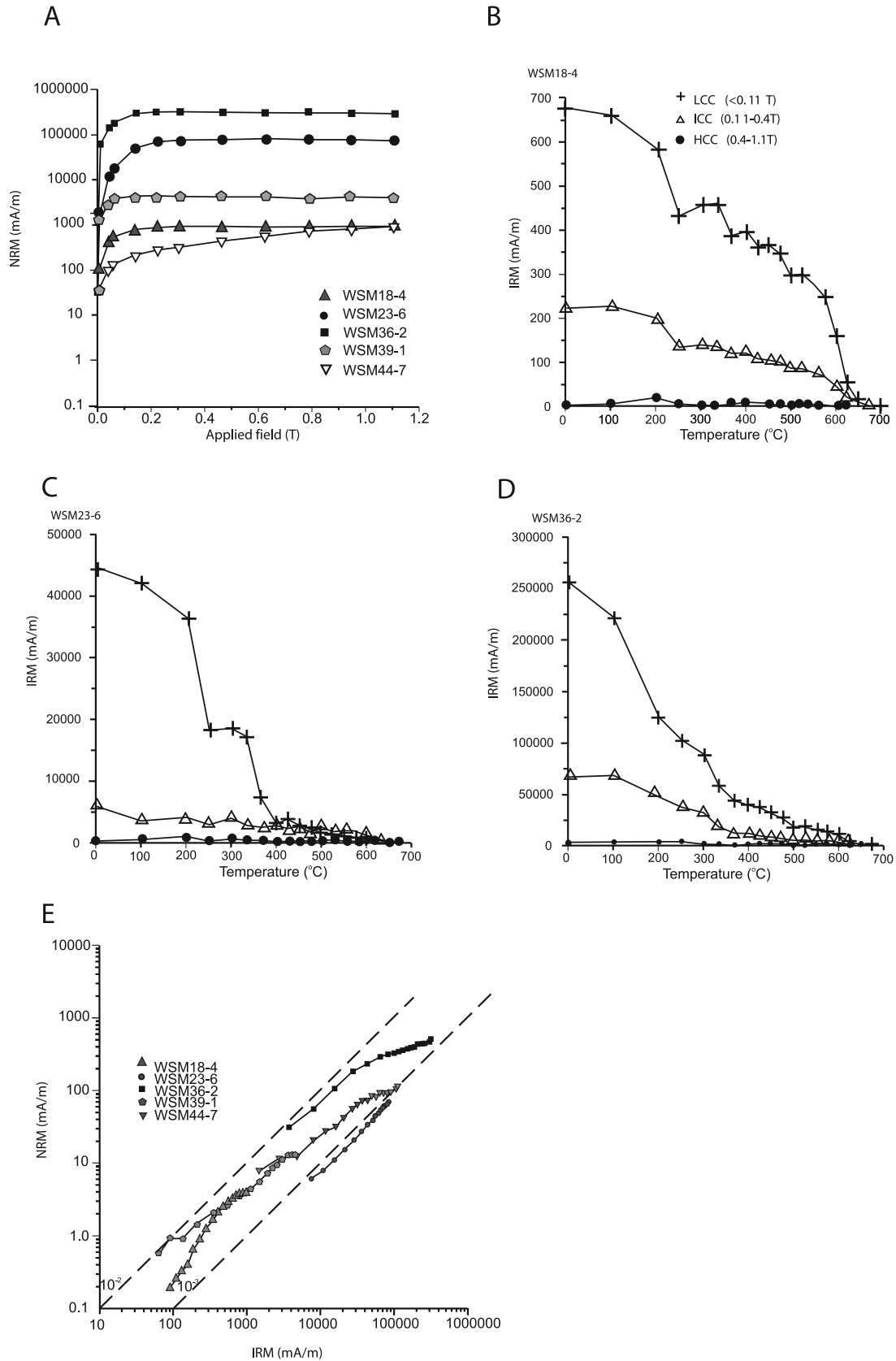
Figure 11. (a) IRM acquisition, (b) thermal demagnetization and (c) NRM/IRM demagnetization curves for representative specimens from the Caraballo Formation exposed along the coast north of Dingalan.

for the lava flow and siltstone sites with reliable ChRMs (N = 10) give an in situ mean direction of D = 218.4°, I = 26.9°, α_{95} = 11.7°, k = 18.0; the tilt-corrected direction is D = 227.8°, I = 9.4°, α_{95} = 11.9°, k = 17.5.

[40] As the principal remanence carrier of the sites is thought to be maghemite, the magnetization of the sites is probably a chemical remanence (CRM). The crucial issue that needs to be addressed is whether this CRM is acquired parallel to the primary magnetization. In this study, all specimens have been adequately demagnetized, allowing the separation of the LCC from the ChRM, the direction of which appears to be consistent in all the sites (with

Figure 12. Summary of ChRM directional data from Caraballo Formation sites along the Abuan River in in situ and tilt-corrected coordinates. (a) Tuffaceous siltstone; (b) Lava flows; (c) Basaltic dikes. Symbols are as in Figure 8.
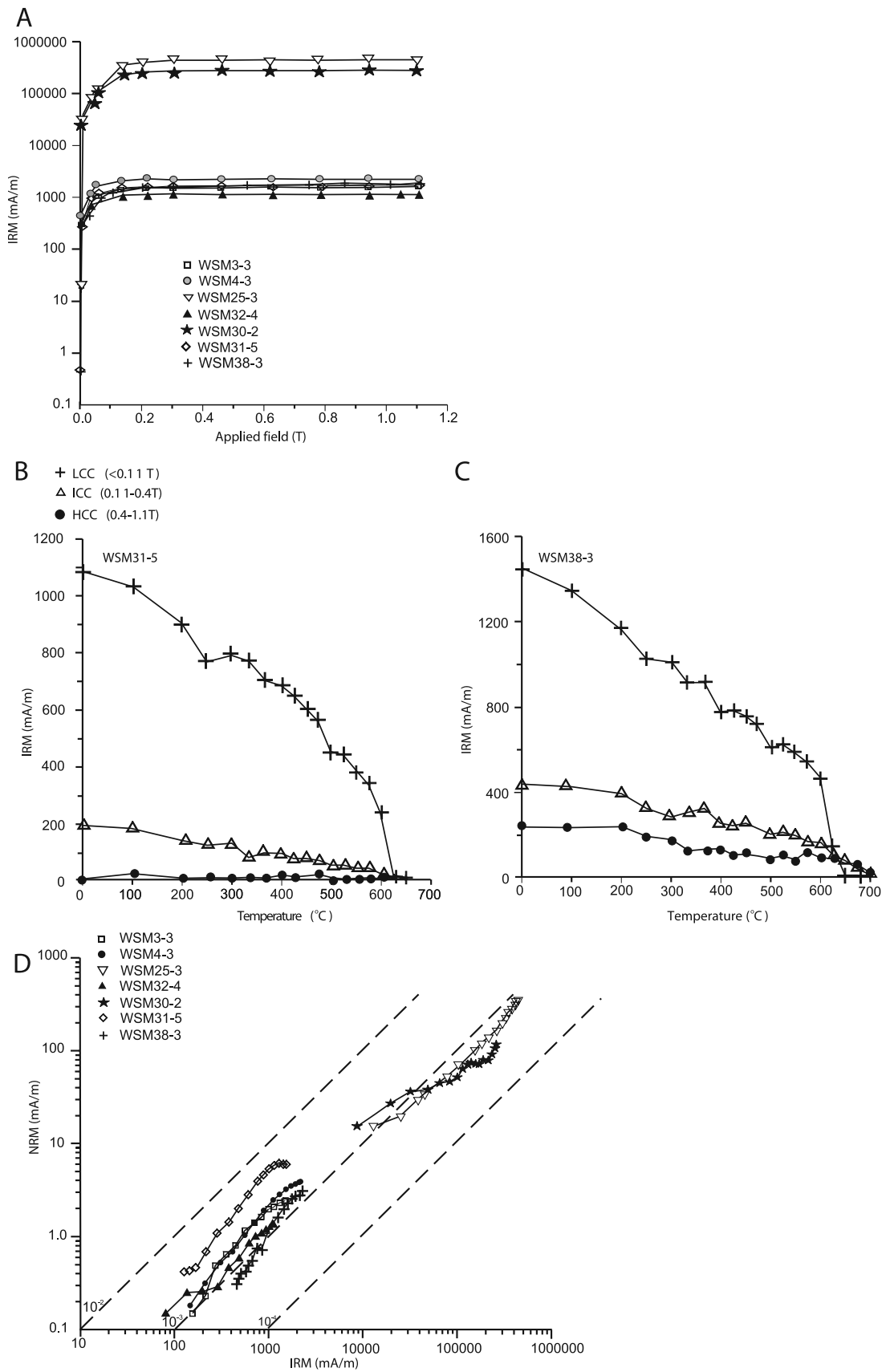
Figure 13. (a) IRM acquisition, (b-c) thermal demagnetization and (d) NRM/IRM demagnetization curves for representative specimens from siltstone sites (Caraballo Formation) along the Abuan River.
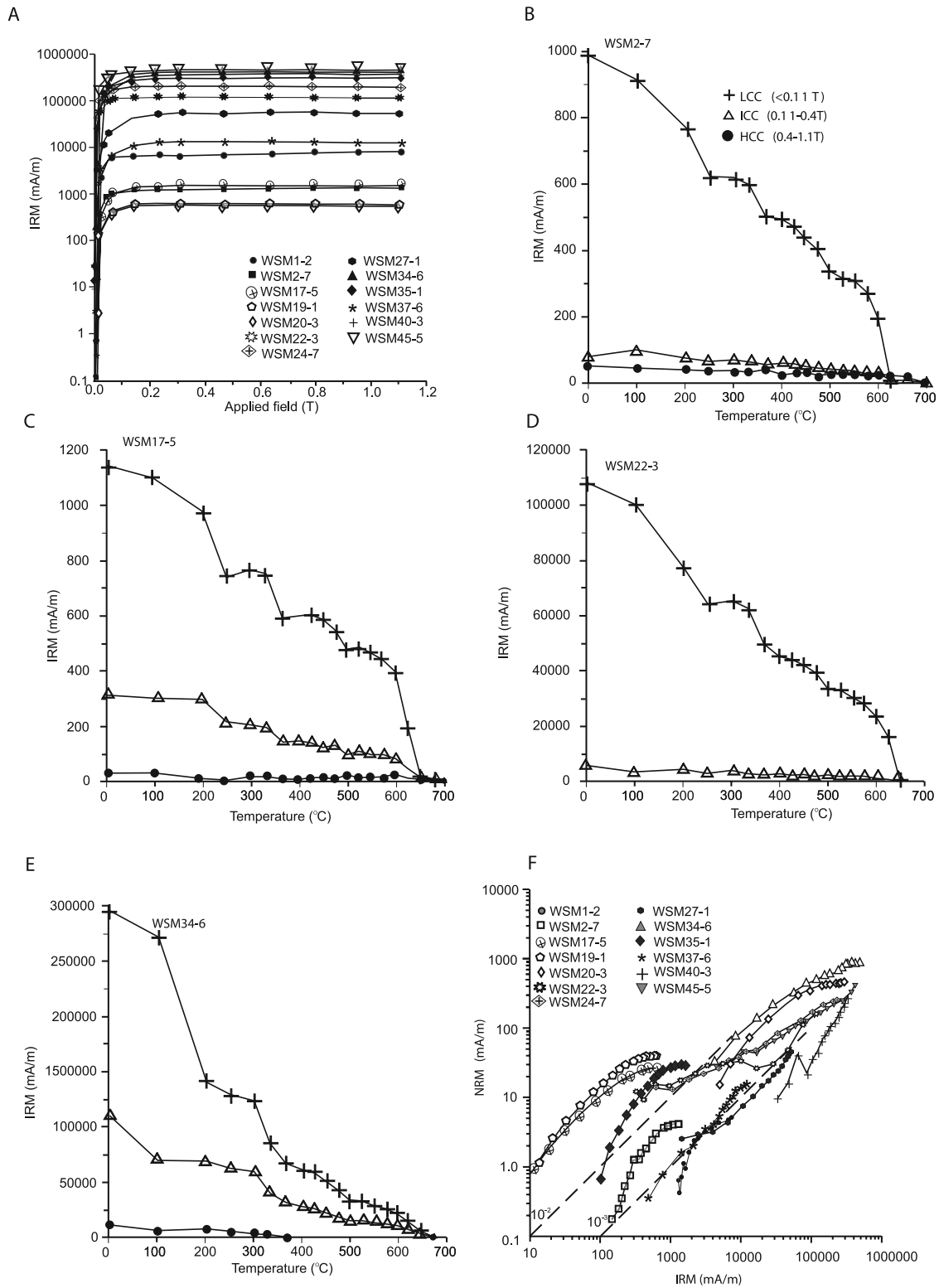
Figure 14. (a) IRM acquisition, (b–e) thermal demagnetization, and (f) NRM/IRM demagnetization curves for representative specimens from lava flow sites (Caraballo Formation) exposed along the Abuan River.

Figure 15. (a) IRM acquisition, (b–d) thermal demagnetization and (e) NRM/IRM demagnetization curves for representative dike specimens along the Abuan River.
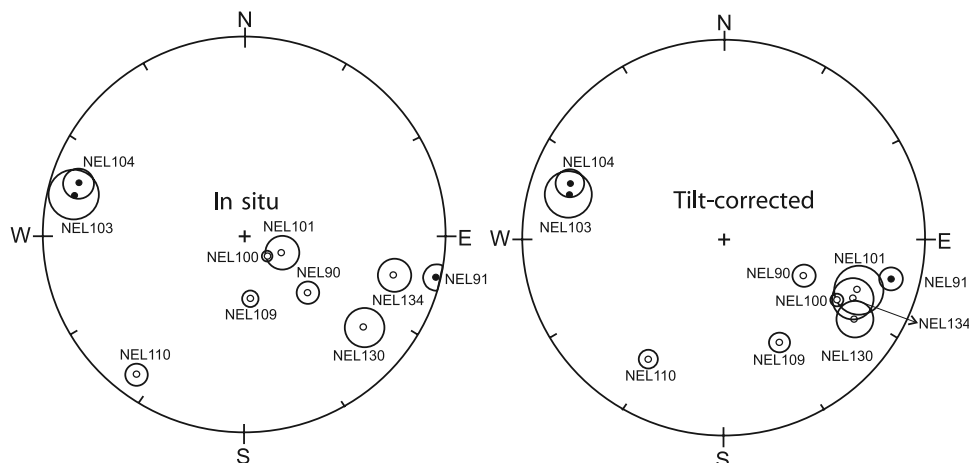
Figure 16. Summary of ChRM directional data from Madlum Formation sites in in situ and tilt-corrected coordinates. Symbols are as in Figure 8.

$\alpha_{95<}$ 15°). The presence of both normal and reverse polarity sites have also been noted. These observations provide support for a primary ChRM. It has also been demonstrated by most experimental studies that chemical magnetization due to maghemitization of magnetite or titanomagnetite is recorded in the same direction as the original direction of magnetization [*Dunlop and Ozdemir*, 1997]. As such, maghemization could still allow the preservation of the primary magnetization, although the process is marked by the attendant decrease in the intensity of the rocks [*McElhinny and McFadden*, 2000; R. F. Butler, Paleomagnetism: Magnetic domains to geologic terranes, electronic edition, 1998, available at http://www.geo.arizona.edu/Paleomag/book/], as demonstrated by many specimens collected along the Abuan River.

4.1.2.5. Basaltic Dikes

[41] A number of subvertical basaltic dikes (typically $1-3$ m wide) intrude the volcanic-sedimentary sequence. Four (WSM18, 23, 36 and 39) out of six sites yielded reliable paleomagnetic data (Table 1a and Figure 12). Demagnetization of specimens from sites WSM23 and 39 revealed a single component of magnetization. In contrast, AF demagnetization of the dike specimens from sites WSM18, 36 and 44 revealed two components of magnetization: a low-coercivity component, usually removed at $\sim$15 mT, and a higher stability ChRM. The LCC in WSM44 is likely a VRM whereas the LCCs of WSM18 and WSM44 are components acquired probably before or during tectonic tilting.

[42] Thermal demagnetization of the IRMs of representative specimens from three dikes (WSM18, 23 and 36) consistently shows complete demagnetization of the soft and medium-coercivity fractions at $\sim$650°C (Figure 15). Along with the low-IRM saturation of the dikes, this behavior suggests maghemite as the probable remanence carrier. The demagnetization curve of the low-coercivity fraction for sites WSM18, 23 and 36 shows a remarkable reduction between $200-250$°C, probably indicating the presence of some form of titanomagnetite. The presence

of this mineral, and possibly iron sulfides, could explain for the noisy behavior of the LCC curves (especially WSM 18) at higher demagnetization temperatures. Remanence contribution from the hard fraction of the specimens is minimal. WSM44 has a smooth IRM acquisition curve that does not reach saturation even in 1.1 T. This suggests a major remanence contribution from a high-coercivity mineral, possibly hematite or pyrrhotite.

[43] NRM/IRM demagnetization experiments show most representative dike specimens (WSM18, 36, 39, and 44) plotting between 10^{-2} and 10^{-3} (Figure 15). The remanence of WSM23 is less efficiently recorded, with NRM/IRM ratio of less than 10^{-3}. This suggests that the remanence of WSM23 is secondary whereas for the other sites, it is probably primary. However, WSM44 is excluded from tectonic interpretation due to the poor clustering of directions. On the basis of the three sites (WSM18, 36, and 39), the in situ ChRM mean direction for the dikes is D = 233.5°, I = 19.4°, α_{95} = 45°, k = 8.6.

[44] Interestingly, the paleomagnetic direction of the shallow intrusives is similar to the reliable ChRMs associated with the siltstone and lava flow units. This could imply that the rocks are almost coeval (hence the intrusion precedes the tilting of the succession), possessing similar "primary" ChRM directions. It is also noteworthy that the intrusive rocks also possess similar petrographic and, to a certain extent geochemical attributes as the lava flows. Alternatively, the rocks could have been formed at different geologic times but were simultaneously overprinted by secondary magnetization. The latter, however, is unlikely; the presence of both normal and reverse polarity sites from dikes as well siltstone and lava suggests that the remanence is likely primary.

[45] Using the tilt correction applied for the siltstone and lava units gives a better clustering of the HCC mean direction (D = 236.0°, I = -3.0°, α_{95} = 35.3°, k = 13.2). Combining the individual mean HCC directions from 13 sites (siltstone, lava and dike units) with reliable HCC gives an in situ direction of D = 222.1°, I = 25.4°, α_{95} = 11.2°,
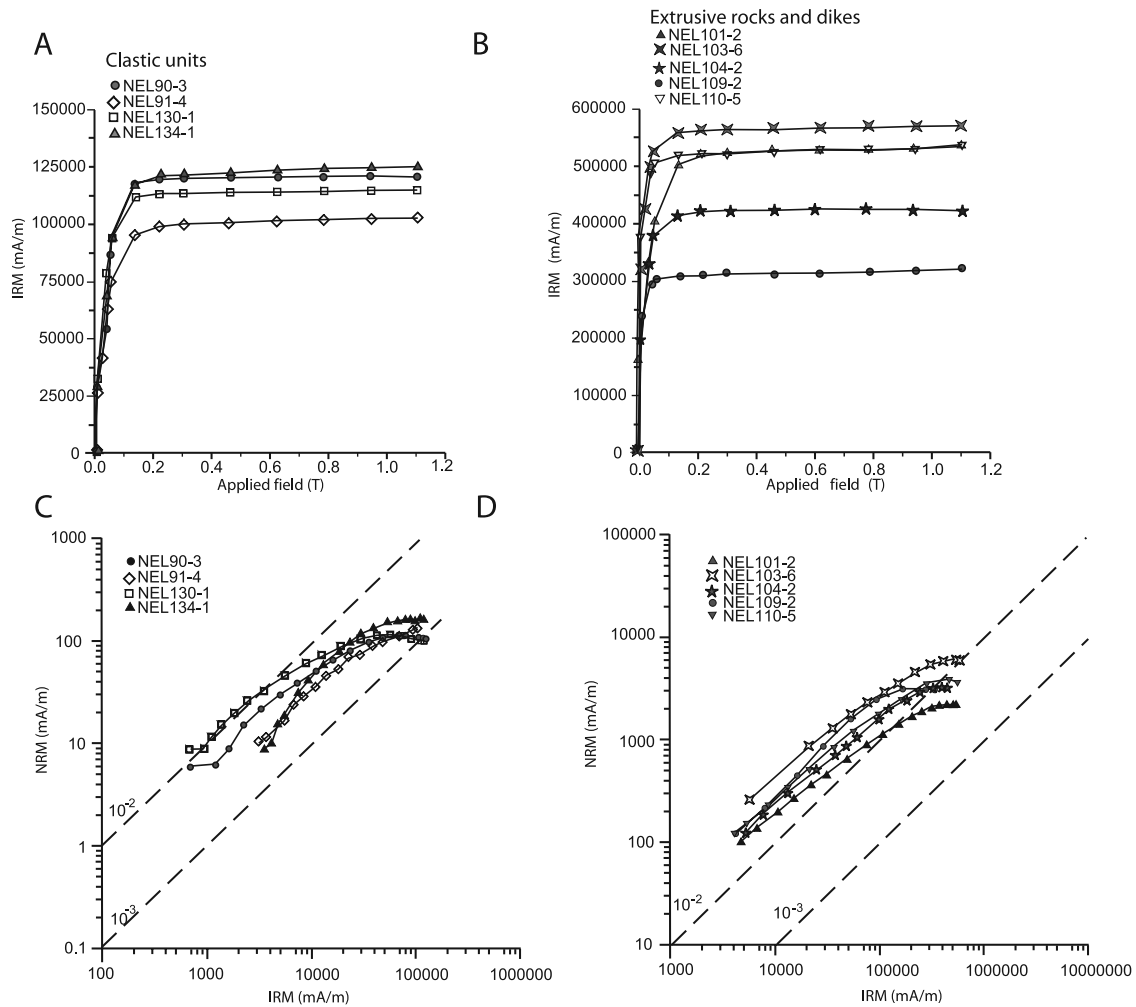
Figure 17. (a–b) IRM acquisition and (c–d) NRM/IRM demagnetization curves for representative specimens from Madlum Formation sites.

$k = 14.7$ and a tilt-corrected direction of D = 229.7°, I = 6.5°, $\alpha_{95} = 10.6°$, $k = 16.3$. The inclination data imply remanence acquisition (hence formation) at 3.3°N ±3.3° (assuming a normal polarity remanence; or south assuming a reverse polarity remanence).

4.2. Paleomagnetic Results: Southern Sierra Madre

4.2.1. Upper Lower to Lower Middle Miocene Madlum Formation

[46] Numerous outcrops of the Madlum Formation are observed along Rio Chico and Sumacbao rivers near General Tinio Municipality, western south Sierra Madre (Figure 3). Eleven drill sites were sampled from the clastic (mostly sandstones with siltstone interbeds) and extrusive units (agglomerates and lava flows) of the formation. Six additional drill sites were collected from basaltic dikes that intrude the agglomerates. These dikes are compositionally similar to the extrusive units and appear to be effectively coeval with the extrusives.

4.2.1.1. Clastic Units

[47] Nine drill sites were sampled from over 500 m of discontinuous outcrop of sandstone-siltstone interbeds of the Madlum Formation along the Rio Chico. The beds are

folded about axes approximately aligned NW-SE, with dips of 18–33°. Four drill sites (NEL90, 91, 130 and 134) representing two outcrops (~400 m apart) yielded useful paleomagnetic data (Table 1b and Figure 16). The remaining sites were rejected as pilot specimens (three per site) exhibit erratic demagnetization behavior or have ChRMs masked by massive VRMs.

[48] AF demagnetization isolates two component remanence: a LCC (likely a VRM) usually removed at 7.5–10 mT and a higher stability component, which is usually first isolated at 20–24 mT. IRM and thermal demagnetization experiments show that the remanence is mainly carried by magnetite (Figures 17 and 18). Combining the individual site means give an ChRM in situ direction of D = 115.5°, I = −18.7° ($\alpha_{95} = 27.7°$, $k = 12.0$) and a tilt-corrected direction of D = 113.8°, I = −17.2° ($\alpha_{95} = 26.1°$, $k = 13.4$). When the outcrop mean of sites NEL90, 91 and 130 (representing one limb of fold) is combined with that of NEL134 (opposite limb of fold), the in situ mean direction is D = 111.9°, I = −17.4° (angular separation, AS, being 14.9°) and the tilt-corrected direction is D = 114.3°, I = −18.0° (AS = 3.8°). This result, coupled with the presence of normal and reverse polarity sites in one outcrop, is highly
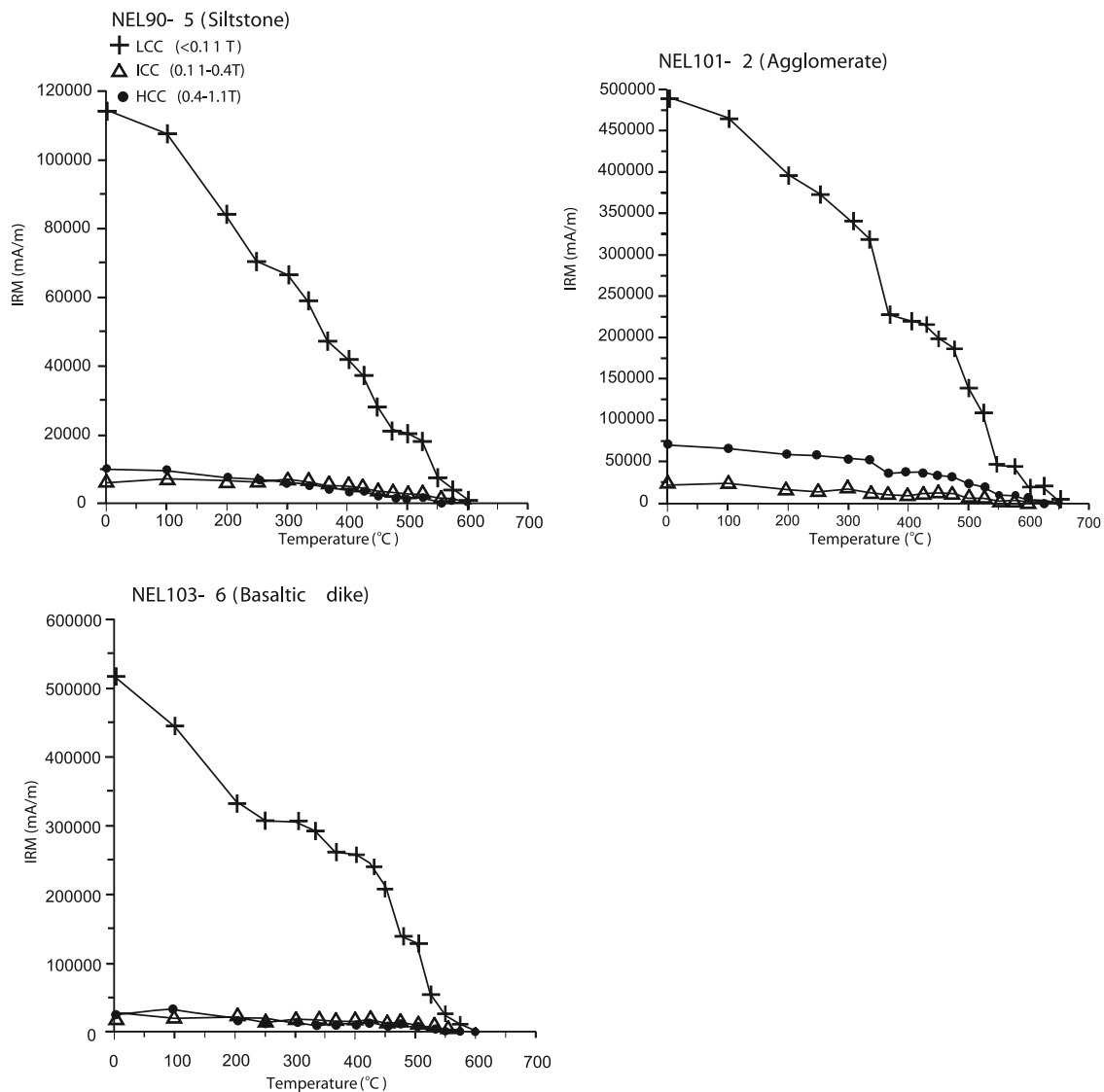
Figure 18. Thermal demagnetization curves for representative specimens from Madlum Formation sites.

suggestive of a prefolding, primary magnetization. NRM/IRM demagnetization experiments provide further support for a primary remanence, with representative specimens having NRM/IRM ratio between 10^{-2} and 10^{-3}.

4.2.1.2. Extrusive Units

[49] Two drill sites from a single outcrop were collected from Sumacbao River, a few kilometers south of the Chico River. The rocks consist of agglomerates containing cobble to boulder sized andesitic to basaltic clasts set in a grayish to reddish fine-grained groundmass. Cores were drilled in six clasts and comprise the specimens for site NEL101. Another site (NEL 100) was sampled in a 2-m-thick lava flow unit within the agglomerates. The flow and medium to coarse sandstones overlying the agglomerates along the Sumacbao River provided structural control for the outcrop.

[50] IRM experiment on a representative specimen from site NEL101 shows IRM ratio values of 0.98, suggesting magnetite as the principal remanence carrier (Figure 16). Results of the thermal demagnetization also suggest the presence of magnetite based on the discontinuity of the coercivity curves at $550-600°C$ (Figure 18). However, the result also shows the possible presence of maghemite, based on the decay of the low- and medium-coercivity fractions at around $650°C$. The low- and medium-coercivity curves also show a drop at $350°C$, probably indicating the presence of titanomagnetite.

[51] NRM/IRM experiment on a representative specimen from NEL101 shows NRM ratio above 10^{-2}, suggesting a primary remanence for the site (Figure 17). Combining the site mean directions of the extrusives give an in situ direction of D = 122.1°, I = −69.9° (AS = 3.9°) and a tilt-corrected direction of D = 113.8°, I = −22.3° (AS = 8.3). These directions closely resemble the outcrop mean directions of the clastic units. Combining the mean from the three outcrops (two outcrops from clastic), yielded an in situ direction of D = 113.5°, I = −34.6° (α_{95} = 51.2°, k = 6.9) and tilt-corrected direction of D = 114.1°, I = −19.4° (α_{95} = 4.4°, k = 769.0). Clearly, the significantly
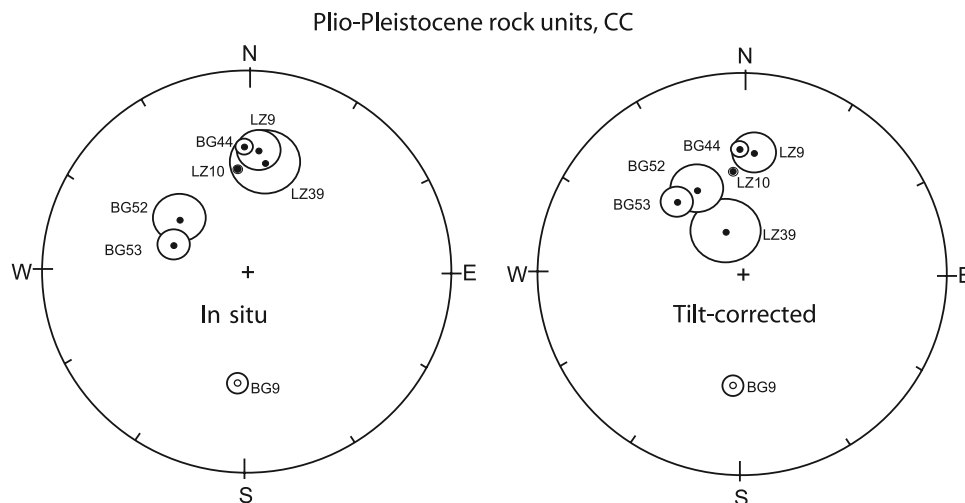
Figure 19. Summary of ChRM directional data from the Plio-Pleistocene rock units in in situ and tilt-corrected coordinates. Symbols are as in Figure 8.

improved directional clustering suggests that the magnetization predates tilting.

4.2.2. Dikes

[52] Four drill sites (NEL103, 104 109 and 110) from basaltic dikes intruding the agglomerates observed in three localities yielded useful paleomagnetic data. The two sites that were rejected had unstable magnetizations (NEL106) or have ChRM parallel to the present field (NEL107). AF demagnetization essentially yielded one component of magnetization. The magnetism of the dike specimens is carried by magnetite, identified by the low-IRM saturation and thermal decay of the coercivity fractions at 550–600°C. NRM/IRM demagnetization experiments on representative dike specimens show values plotting way above 10^{-2}, suggesting that the remanence of the sites are likely primary (Figure 17). The tilt-corrected (assuming a vertical dike orientation) outcrop mean direction (D = 288.3°, I = 12.6°, AS = 3.9°) of sites NEL 103 and 104 is antipodal to that of the combined outcrop means of the clastic and extrusive rocks. Inverting the outcrop mean directions of the clastic and extrusive units to normal polarity and combining them with that of the dike give an in situ direction of D = 291.0°, I = 27.6° (α_{95} = 34.6°, k = 8.0) and tilt-corrected direction of D = 292.6°, I = 17.7° (α_{95} = 5.8°, k = 251.9). The mean ChRM directions of sites NEL109 and 110 sit away from the main site clustering. As these sites are situated nearer the main trace of the Philippine Fault, it is probable that the units have undergone local rotation.

[53] In summary, it appears that the results from the Madlum Formation (including those from the dikes) consistently point to the ChRM as being primary. This is supported by the presence of reverse and normal polarity sites, the significant improvement in the clustering of the directions upon application of tilt correction and the results of the NRM/IRM experiments. Assuming a normal polarity magnetization, the inclination result from combined outcrop mean directions of the clastic rocks, extrusive units and dikes (NEL103 and 104) translates to a formation latitude of 9.0°N ± 3.1°.

4.3. Paleomagnetic Results: Central Cordillera

4.3.1. Plio-Pleistocene Rock Units

[54] Nine sites were sampled from Pliocene to Pleistocene rocks in the Central Cordillera. Two of these (LZ9 and 10) are from columnar basalt flows unconformably overlying the Cretaceous? to Eocene? Chico River pillow basalts in northern Bontoc region (Figure 3). Recent radiometric dating (K-Ar) of the former rocks gave an age of 1.38 ± 0.18 Ma (M. Pubellier, unpublished data). The remaining sites where from a series of subvertical andesite dikes outcropping at three localities in Baguio City. Ages of these dikes were based on stratigraphic relationship with other formations (e.g., upper middle to upper Miocene Klondyke Formation) as well as on radiometric ages reported by previous workers [e.g., *Bellon and Yumul*, 2000]. Only four sites from Baguio City yielded useful paleomagnetic data; the rest of the specimens mostly exhibited erratic demagnetization behavior (Table 1c and Figure 19). In addition, three drill sites were collected from Ilagan Formation mudstones in the western Cagayan Valley Basin (near Tabuk). Results from these sites, however, had to be rejected due to poor clustering of paleomagnetic directions (α_{95} > 15.0°).

[55] Representative specimens have low-coercivity IRMs and with IRM ratio of greater than 0.9 suggesting magnetite as the likely principal remanence carrier (Figure 20). The remanence of the specimens is considered primary, given the results of the NRM/IRM demagnetization experiments which show ratio values above 10^{-2} (Figure 20). The mean ChRM direction of site BG44 roughly parallels that of sites LZ9 and 10 in Bontoc (mean D = 359°, I = 27.7°, AS = 11.7°), while that of site BG9 is roughly antipodal to that of the latter sites. The directions of magnetization suggest no significant rotation for the region during the Plio-Pleistocene time. However, plots of sites BG52 and 53 deviate away from the major trend, with ChRM direction roughly directed NNE. Such deviation, however, could be reflective of local rotation brought about by the presence of several faults and joints cutting the intrusives in the area (i.e., Philex Road). Assuming a paleovertical position for the dike outcrops and using *McFadden and Reid* [1982]
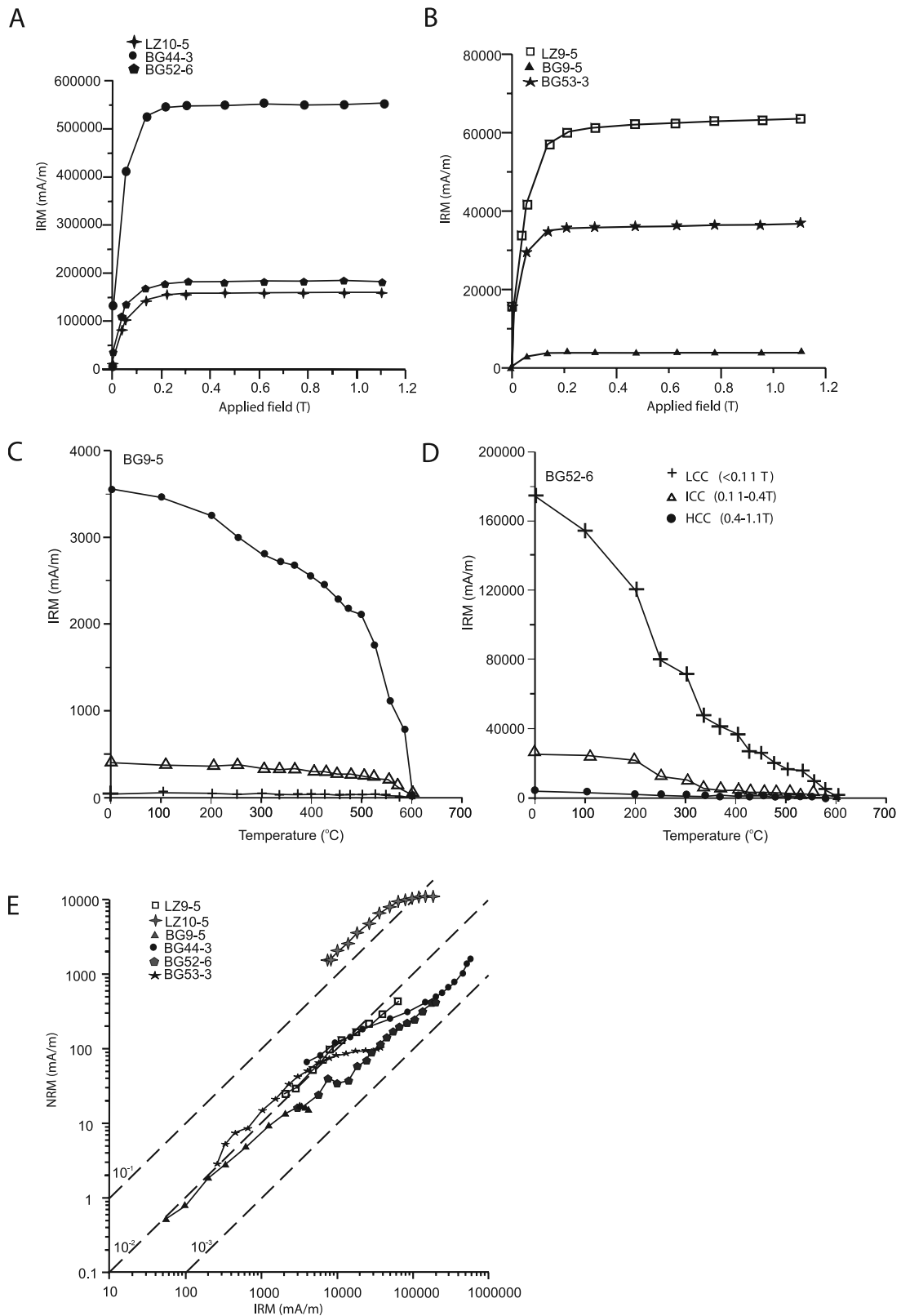
Figure 20. (a–b) IRM acquisition, (c–d) thermal demagnetization and (e) NRM/IRM demagnetization curves for representative specimens from the Plio-Pleistocene rock units.
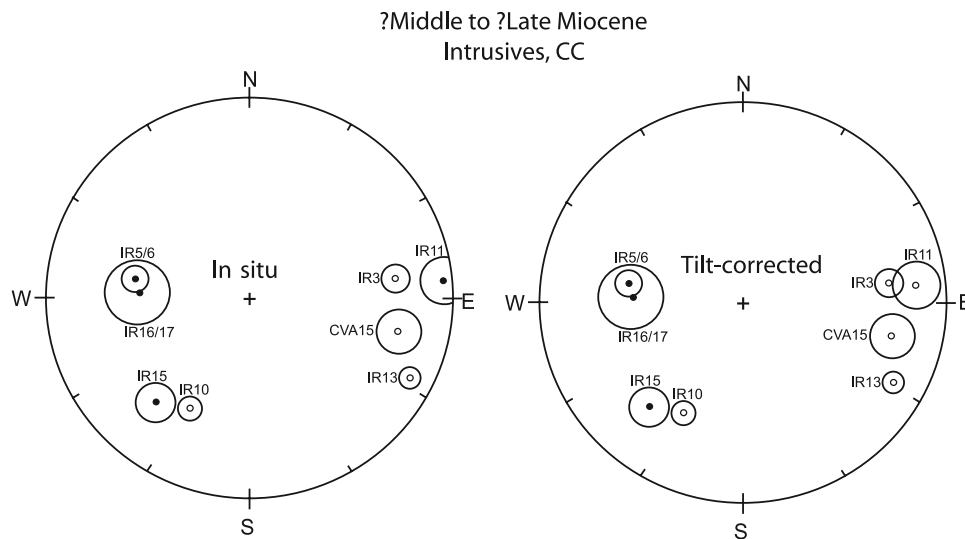
Figure 21. Summary of ChRM directional data from the intrusives of northern Central Cordillera in in situ and tilt-corrected coordinates. Symbols are as in Figure 8.

inclination only statistics give a mean inclination of 31.0° (α_{95} = 11.5°, k = 63.4). Combining the individual mean HCC directions from all sites give a tilt-corrected mean inclination of 29.9° (α_{95} = 6.4°, k = 82.5). This translates to a paleolatitude of 16.0°N ± 4.0°.

4.3.2. Middle to Late? Miocene Intrusive Units

4.3.2.1. Northwestern Central Cordillera (Abra-Ilocos)

[56] Six drill sites were sampled from andesite dikes in Abra and Ilocos provinces, northwestern Central Cordillera (Figure 3 and Table 1c). The dikes are subvertical (70–80°) and 1.0–1.5 m wide. One site was drilled on a diorite body containing andesite xenoliths exposed near Baay, Abra province. Another site was collected from a diorite batholith outcropping near Solsona. Ages of these dikes were based on stratigraphic relationship with other rock units (e.g., Bangui Formation) as well as on radiometric ages reported by previous workers [e.g., *Malettere*, 1989].

[57] IRM experiments indicate that the remanence of the specimens is carried mainly by magnetite. Thermal demagnetization of specimens from sites IR5 and 11 also suggests magnetite as the principal remanence carrier as indicated by the unblocking of the coercivity components at 550–600°C. The plot of specimen from site IR11 also shows a conspicuous drop of the coercivity components at 250°C, possibly indicative of some of form of titanomagnetite.

[58] AF demagnetization results show most specimens carrying a significant LCC (likely a VRM) usually removed by 16 mT (Figure 6j). Specimens from sites IR3 and IR11 also carry an intermediate component isolated between 13 and 50 mT. The ChRM direction for each specimen was determined using the principal component analysis method. However, for specimens displaying relatively noisy demagnetization behavior (i.e., those from IR5, 15, 16 and 17), the statistics of *Fisher* [1953] was applied instead. The mean ChRM direction of sites IR16 and 17 is poorly determined, with α_{95} > 15°. However, as site IR17 appears to be an extension of the dike drilled at site IR16, the mean direction of the two sites is combined using the data from the individual specimens, yielding D = 272.6°, I = 33.4°, α_{95} = 14.1°, k = 23.4. Also, it is worth noting that the

outcrop from site IR10 contains slickensides indicative of a left-lateral movement. The presence of fault in this locality puts a high degree of uncertainty as to how to position the dike to its original orientation. As such, the result from this site is tentatively excluded from paleomagnetic interpretation. Assuming a paleovertical position for the dike outcrops and combining the ChRM mean direction from sites IR3, 5, 11, 13, 15 and 16/17 (3, 11 and 13 inverted to normal polarity) give a direction of D = 266.9°, I = 22.0°, α_{95} = 22.4°, k = 9.9. Using *McFadden and Reid* [1982] inclination only statistics give an inclination of 20.9° (α_{95} = 10.8°, k = 31.8).

#### 4.3.2.2. Northern Central Cordillera (Claveria)

[59] A number of intrusives cut the Bangui Formation along the Claveria coast and the Pasaleng-Claveria road (Figure 3 and Table 1c). Only one site (CVA 15) from an andesitic dike yielded useful paleomagnetic data; the other sites either have different/erratic demagnetization behavior or have ChRM overprinted by secondary, usually viscous magnetization (Table 1c and Figure 21). The magnetism of the dike is likely carried by magnetite, identified by low-IRM saturation fields unblocking temperatures of ∼575°C.

[60] NRM/IRM demagnetization experiment on a representative specimen from CVA15 suggests that the ChRM component is likely primary (Figure 22). The specimen starts with NRM/IRM ratio of 10^{-3} but ends with values above 10^{-2}, after the low-coercivity component is removed. Site CVA15 has two components of magnetization: an LCC (viscous) component usually removed at 33 mT and a higher stability ChRM isolated at higher demagnetization fields. It has in situ ChRM direction of D = 103.0°, I = −16.4°, α_{95} = 8.1°, k = 231.9. This direction parallels those of the dikes noted in northwestern Central Cordillera. Combining the ChRM direction of site CVA15 with those from the latter region (i.e., sites IR3, 5, 11, 13, 15 and 16/17; CVA15 and IR3, 11 and 13 inverted to normal polarity) gives a mean direction of D = 269.4°, I = 21.3°, α_{95} = 18.9°, k = 11.2. Using *McFadden and Reid* [1982] inclination only statistics gives a mean inclination of 20.3°
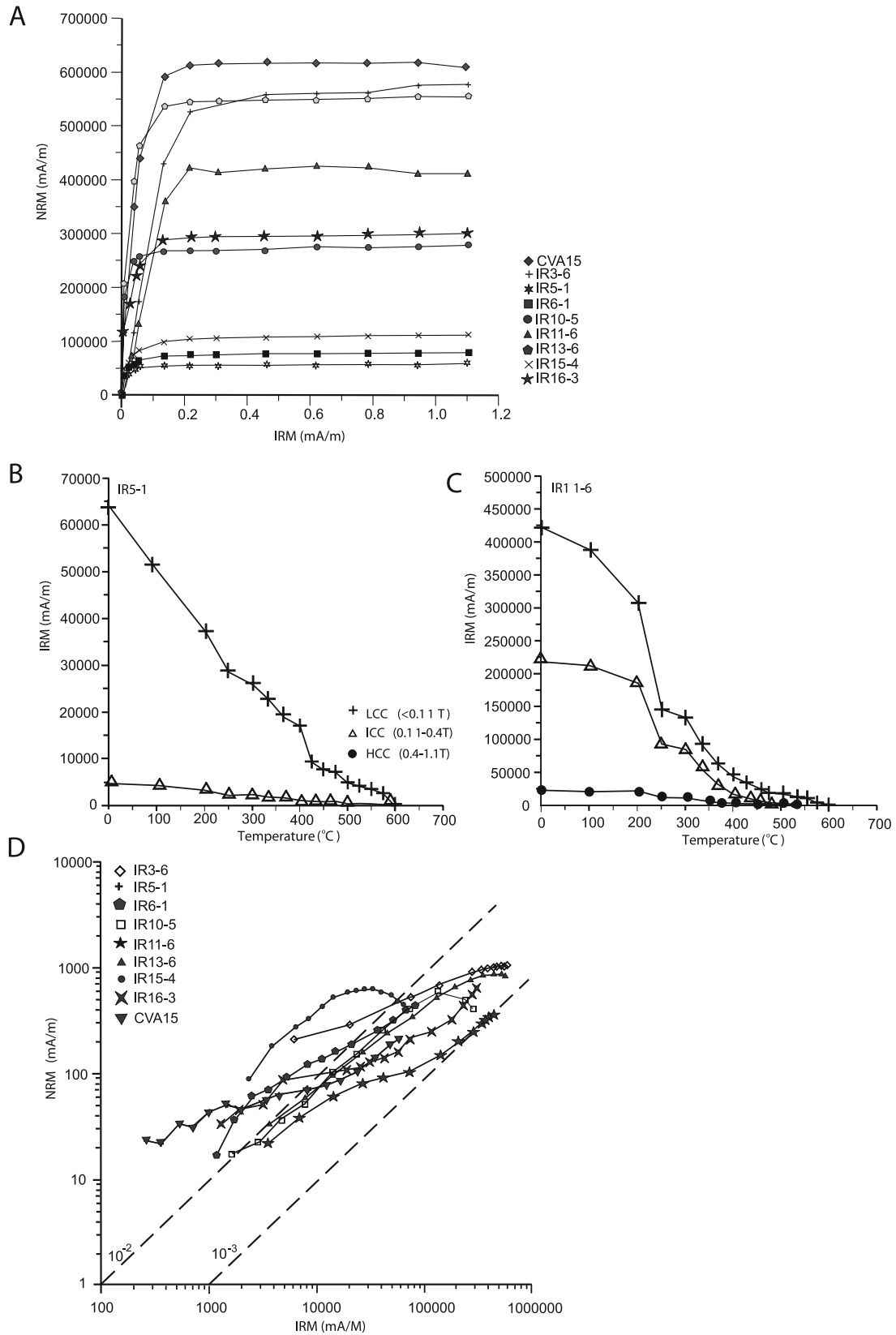
Figure 22. (a) IRM acquisition, (b–c) thermal demagnetization and (d) NRM/IRM demagnetization curves for representative specimens from the intrusives of northern Central Cordillera.
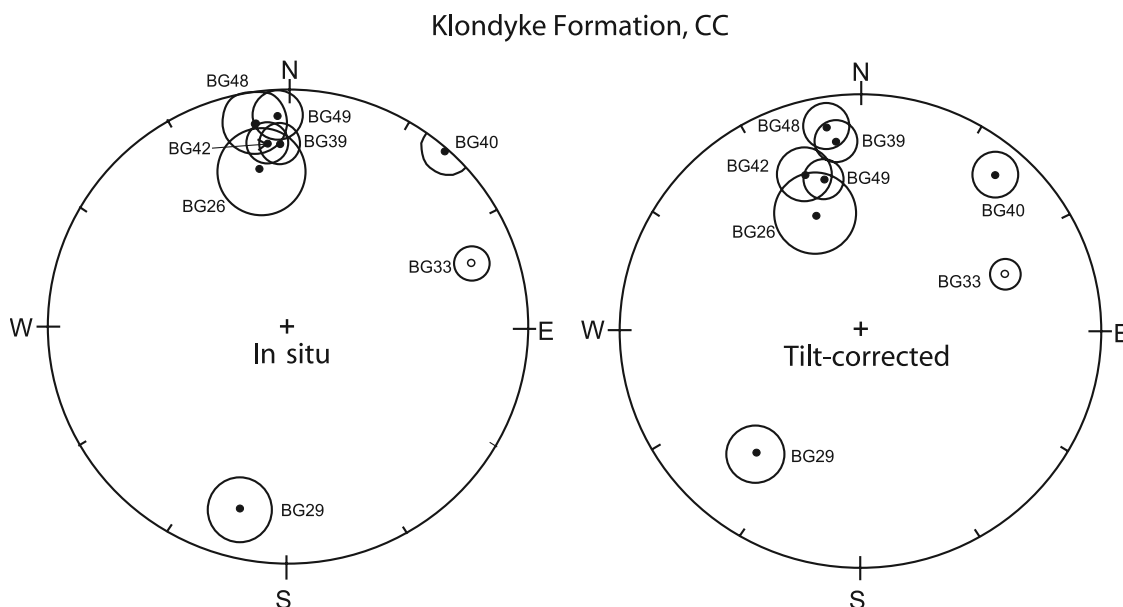
Figure 23. Summary of ChRM directional data from the Klondyke Formation sites in southern Central Cordillera in in situ and tilt-corrected coordinates. Symbols are as in Figure 8.

($\alpha_{95} = 8.8°$, $k = 37.3$). This result equates to a formation latitude of $10.5°N \pm 4.8°$.

4.3.3. Middle to Upper Miocene Klondyke Formation

[61] Twenty nine sites were collected from the sandstones and siltstones of the Klondyke Formation exposed along three major thoroughfares (Marcos Highway, Kennon Road and Asin Road) leading to Baguio City (Figure 3). Of these, only eight sites from seven localities yielded useful paleomagnetic data (Figure 23). Specimens from the rejected sites have unstable magnetizations or have quite scattered paleomagnetic directions at site level ($\alpha_{95} > 15°$) (e.g., BG31 and 34).

[62] IRM experiments on representative specimens consistently yield IRM ratios of 0.99 indicating magnetite as the principal remanence carrier (Figure 24). This result is also supported by thermal demagnetization experiment on a specimen from site BG48 which shows a simple decay of remanence, with complete unblocking at 600°C (Figure 24). However, for site BG42, the magnetism of the specimen appears to be carried by maghemite identified by low-IRM saturation field and unblocking temperatures ~650°C.

[63] AF demagnetization of specimens from sites with reliable paleomagnetic result mostly yielded two components of magnetization: a randomly oriented LCC (likely a laboratory storage), usually removed at 10 mT and a higher stability ChRM isolated starting ≥13 mT (Figure 6k). NRM/IRM experiments show that most specimens have values plotting between 10^{-2} and 10^{-3} (BG29, 33, 40, 49) or roughly approximating 10^{-3} (BG 39, 42 and 48) (Figure 24). This suggests a primary remanence for the specimens. Specimen from BG26 has values that plot way above 10^{-2}; its remanence is also likely primary as the site includes both normal and reverse polarity directions.

[64] Although the general clustering of the sites appears to be NNW directed, the stereoplot also suggests that the individual outcrops record local rotations (a number of faults that could bring such movements were observed in

several areas in Baguio City). Taking into consideration the directions from eight sites (BG26, 29, 33, 39, 40, 42, 48 and 49; BG26, 29 and 33 inverted to normal polarity) and using the *McFadden and Reid* [1982] inclination-only statistics give an in situ mean inclination of 11.7° where $\alpha_{95} = 5.8°$ and k = 69.1, and a tilt-corrected mean is 23.7° where $\alpha_{95} = 8.9°$ and k = 46.6. Although the in situ directions are slightly more clustered than the tilt-corrected vectors (suggesting that the remanence postdates deformation), magnetization of the Klondyke Formation is still considered to be primary as suggested by the aforementioned AF and NRM/IRM demagnetization results. The mean inclination translates to a formation latitude of $12.4°N \pm 5.0°$.

5. Discussion

5.1. North Luzon and Philippine Sea Plate Connection

[65] Although several papers have been published dealing with the evolution of Luzon [e.g., *Mitchell et al.*, 1986; *Billedo*, 1994; *Florendo*, 1994; *Encarnacion*, 2004] (and the rest of the Philippine archipelago), they do not go as far as to reconstructing the arc's position with respect to the other tectonic elements of SE Asia This may be due partly to the scarcity of paleomagnetic and other geological data as well as the enormously complex nature of the region. To date, the most comprehensive work detailing the Cenozoic evolution of SE Asia is that of *Hall* [2002]. His reconstruction dates back 55 Ma, when Luzon is placed in an ~45° clockwise orientation relative to its present position and forming part of the Eurasian margin alongside Borneo. Successive paleogeographic reconstructions highlight Luzon as (1) rotating counterclockwise and with minor northward translation and (2) evolving as a unit (alongside Negros and western Mindanao) independent of the islands comprising the central and southern parts of the Philippine Archipelago. Corollaries to these are that Luzon remained in the Northern Hemisphere throughout its evolution and that
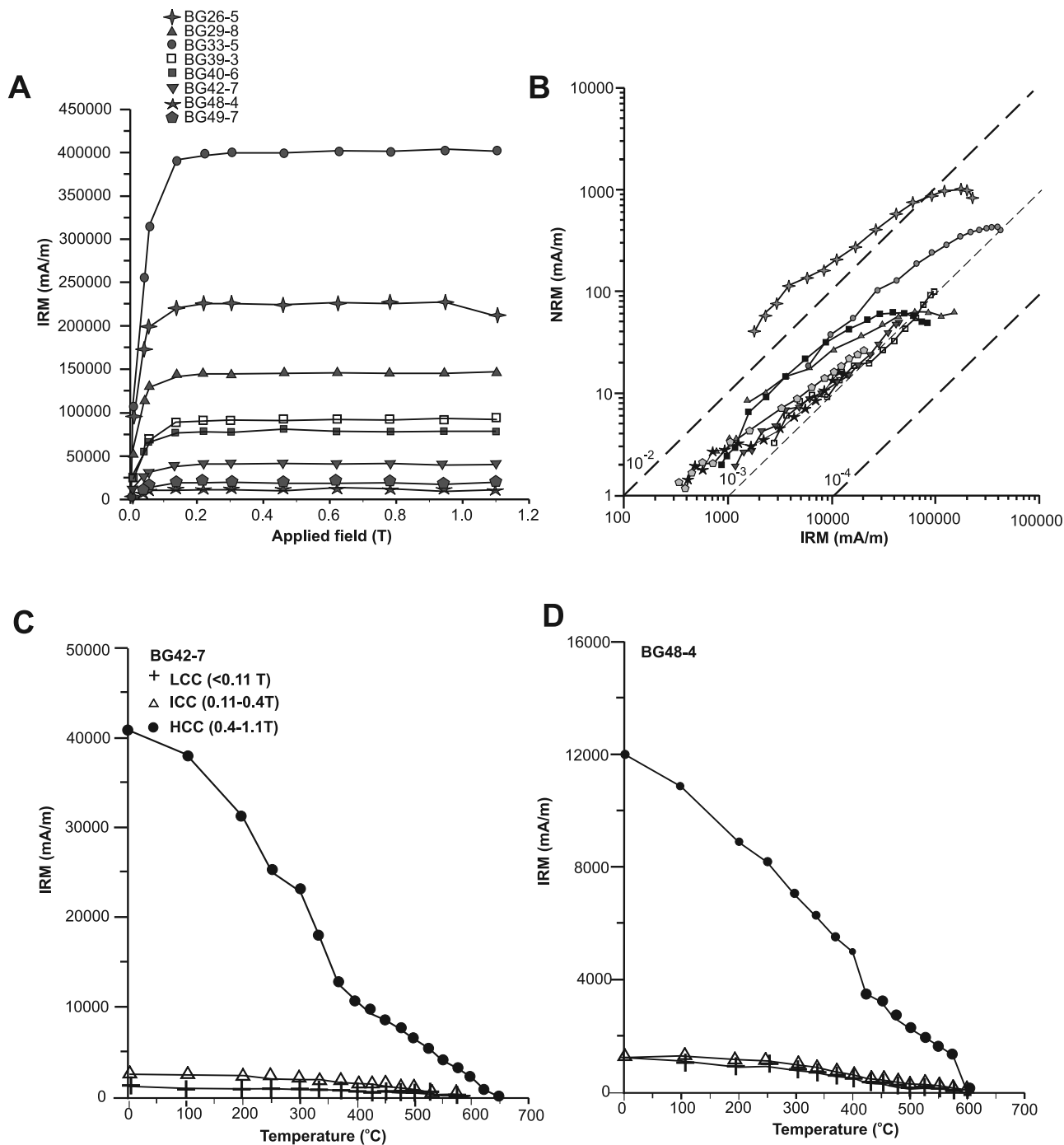
Figure 24. (a) IRM acquisition, (b) NRM/IRM demagnetization and (c–d) thermal demagnetization curves for representative specimens from the Klondyke Formation sites.

its stratigraphy records events and timings different from most of the southern Philippine islands. *Hall*'s [2002] reconstructions of Luzon drew heavily upon on the earlier paleomagnetic work conducted by the University of California Santa Barbara Group [*Fuller et al.*, 1983; *McCabe et al.*, 1987].

[66] For this study, a substantial geologic and paleomagnetic data set was collected from northern Luzon. Together with existing geologic data from the region, this provides key information for reevaluating the paleogeographic position (and hence evolution) of Luzon during the Cenozoic.

[67] Geological studies [e.g., *Billedo*, 1994; *Florendo*, 1994; this work] indicate that arc volcanism in northern Luzon started during the Eocene, possibly extending back to the Late Cretaceous based on studies on southeastern Luzon [e.g., *David et al.*, 1997]. This event, which is recorded mostly in rocks of the southern and northern Sierra Madre range, lasted until the early Miocene. The rocks of the Central Cordillera (e.g., Eocene Bangui Formation, Oligo-
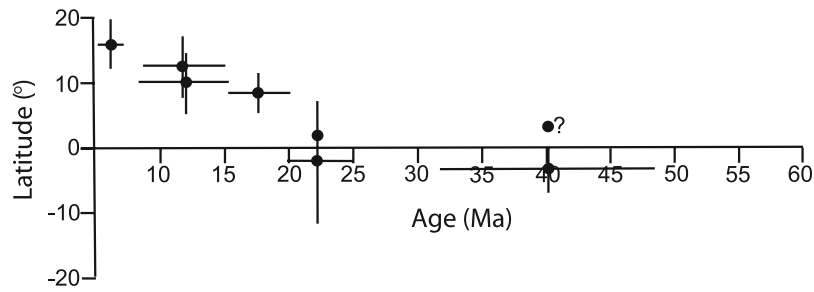
Figure 25. Paleolatitudes derived from northern Luzon inclination data. Note that because of the shallow inclination and associated confidence limits, there is a degree of ambiguity in determining whether the early Cenozoic latitudes are in Northern or Southern Hemisphere.

cene Central Batholith) also record early Cenozoic magmatic activity and represent traces of a remnant arc which rifted from the northern Sierra Madre following the formation of the Cagayan Valley Basin [*Florendo*, 1994; *Encarnacion*, 2004]. Interestingly, early Cenozoic magmatic activity in Luzon is almost synchronous with the observed onset of arc development in the Visayan region, eastern Mindanao, and even further south in Halmahera [*Rangin and Pubellier*, 1990; *JICA-MMAJ-MGB*, 1990; *Hall et al.*, 1995b]. This observation suggests that these

regions were likely situated within the same geological province during their early stage of evolution.

[68] Reliable ($\alpha_{95} \leq 15°$) paleomagnetic results from units of northern Luzon were obtained from seven out of the 13 groups of rocks (Tables 1a–1c). The observed inclinations of primary magnetization from Eocene (or earlier) to early Miocene formations suggest that northern Luzon mainly occupied low, subequatorial latitudes (Figure 25). Because of the shallow inclinations and their associated confidence limits, however, it is difficult to determine if this early Cenozoic paleolatitude is in the
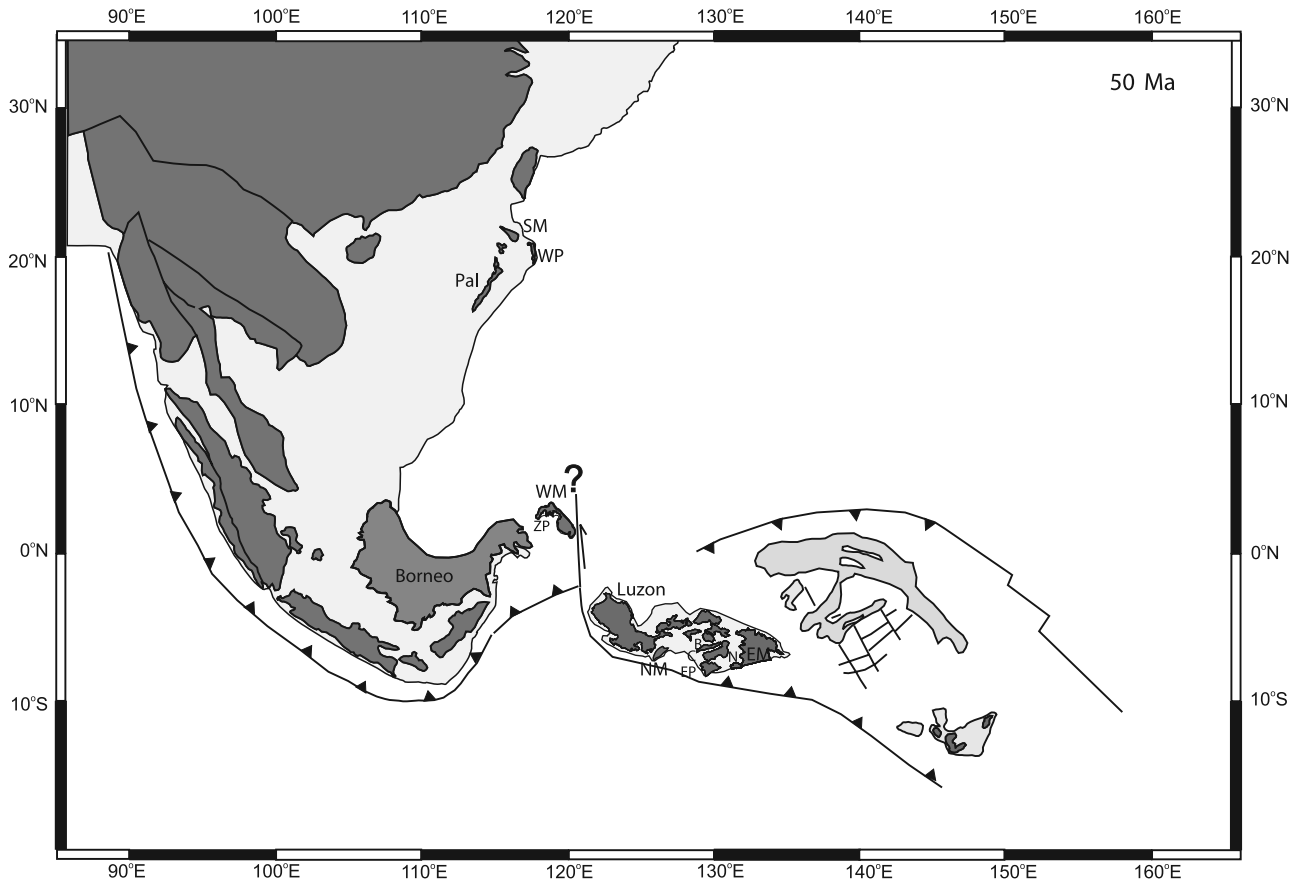
Figure 26. Tectonic reconstruction at 50 Ma modified after *Hall* [2002]. NM, northeastern Mindoro; SM, southwestern Mindoro; Pal, Palawan; WP, western Panay; EP, eastern Panay; C, Cebu; B, Bohol; N, Negros; ZP, Zamboanga Peninsula; WM, western Mindanao; EM, eastern Mindanao. Also see Figure 2.
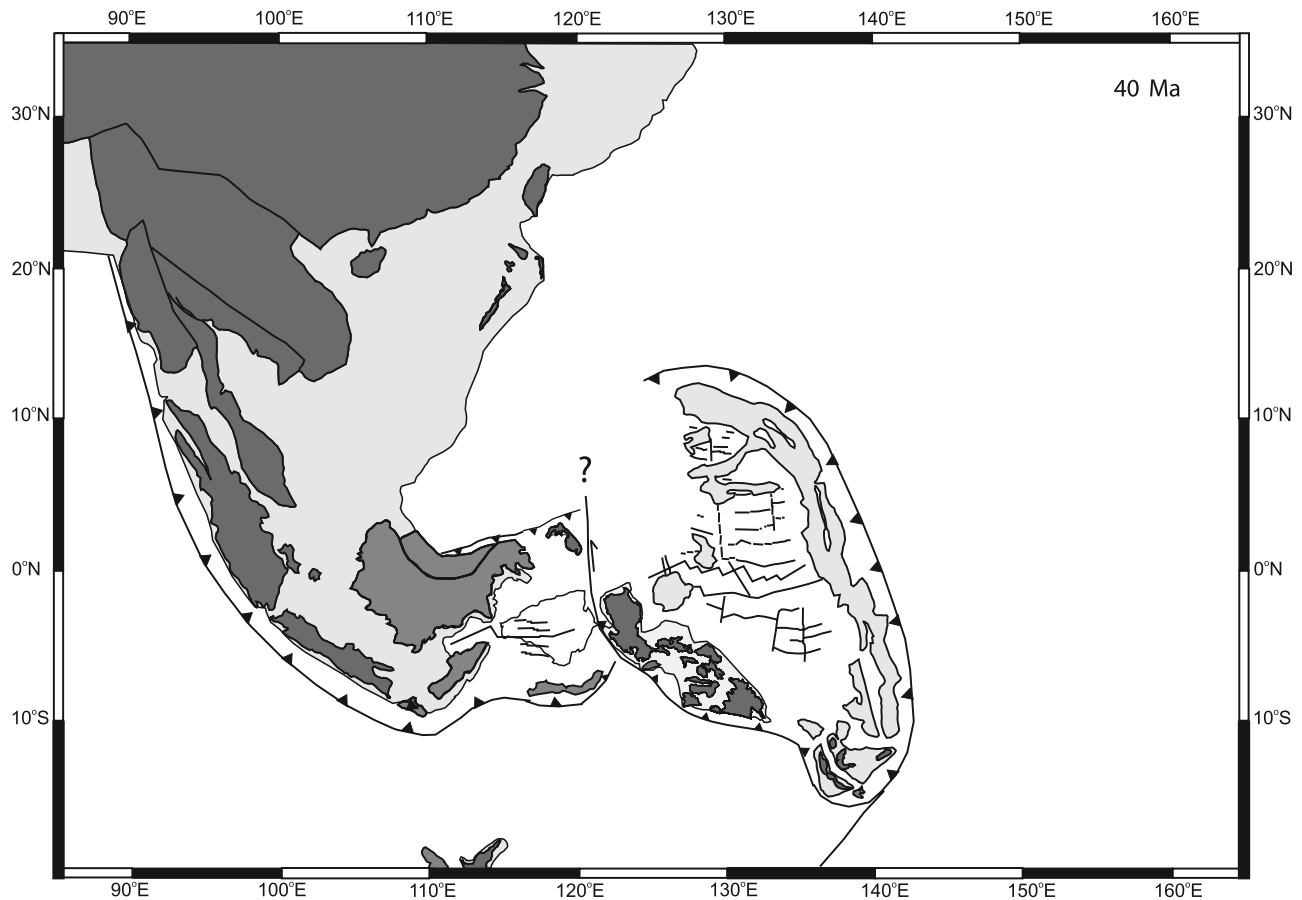
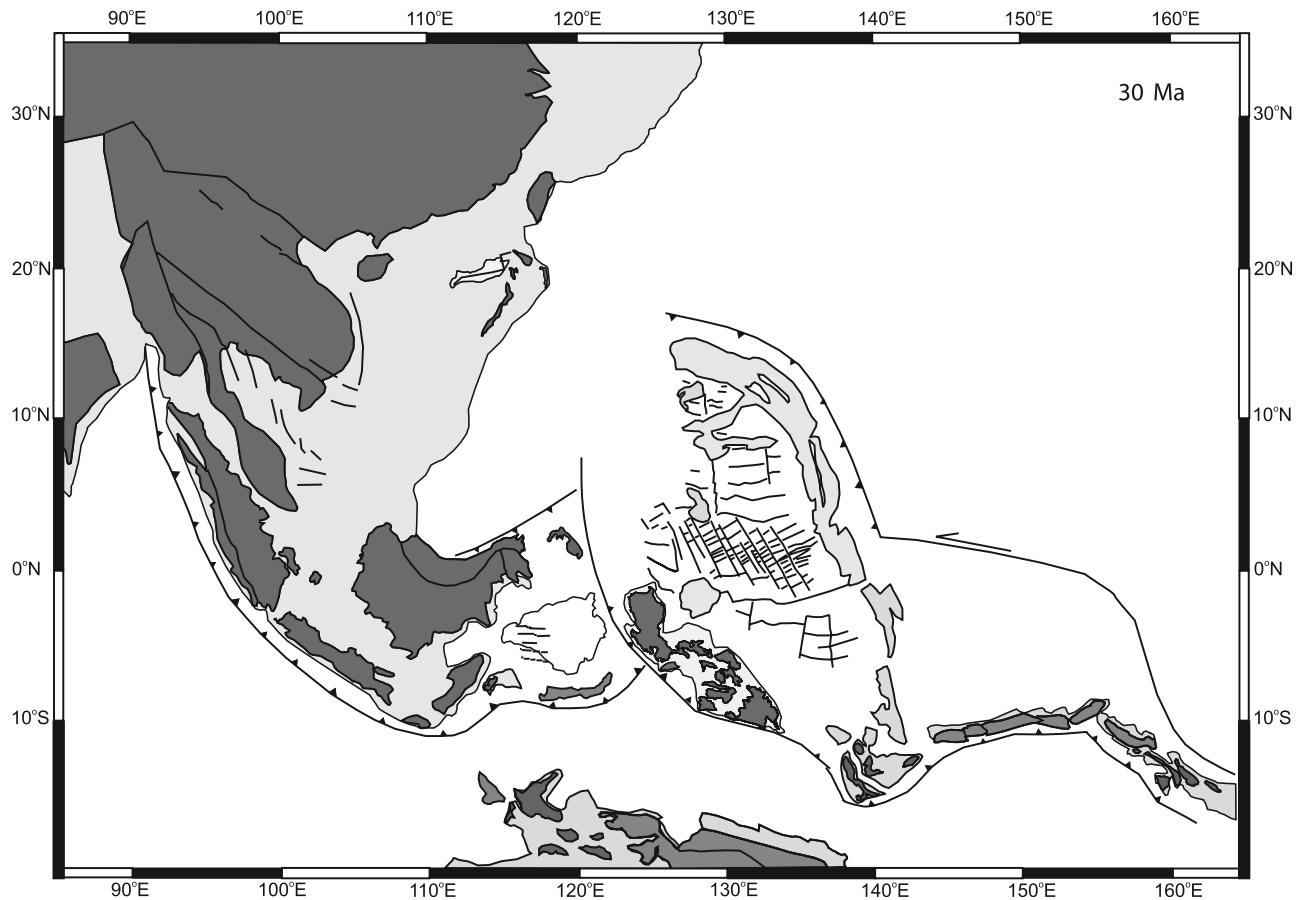**Figure 27.** Tectonic reconstruction at 40 Ma modified after *Hall* [2002].

Northern or Southern Hemisphere. In Figure 25, the mean inclination for the Eocene (Abuan River section) to early Miocene (Lubuagan Formation) is tentatively placed south of the equator. Within this time frame, no significant latitudinal movement can be observed. In contrast, starting from approximately the late Oligocene to early Miocene, the mean inclinations from northern Luzon suggest northward motion by as much as 10–15°. The region appears to have possibly attained its present position by the end of Miocene.

[69] The inclination results gathered in this study contrast sharply with the earlier findings [e.g., *Fuller et al.*, 1983], which suggest no important early Miocene to present northward motion (implying that Luzon already attained its present position by this time). A review of the data set of *Fuller et al.* [1983] explains the discrepancy in the results. The bulk of the data used by the latter in interpreting the early to middle Miocene paleomagnetic results for Luzon comes from the Zigzag and Klondyke formations exposed in Baguio City. Apparently, in this study, these formations are treated as separate entities based on geologic mapping [e.g., *UNDP*, 1987; *Malettere*, 1989; this work] and paleontological study on these units [*Malettere*, 1989; *De Leon*, 1995]. Such an undertaking places the Zigzag Formation in the upper Oligocene to lower Miocene and the Klondyke Formation in the middle to lower upper Miocene. Clearly, the recent relative age assignment given to these formations has serious implications for the paleomagnetic interpretations made by *Fuller et al.* [1983]. One is that the mean

paleomagnetic direction they obtained from Baguio City represents that for the middle to upper Miocene rather than that for the lower to middle Miocene. Another is that the paleomagnetic directions from the Zigzag Formation could represent secondary overprints acquired during the deposition of the Klondyke Formation. Calculating the mean direction (from five sites) for the Klondyke Formation obtained by *Fuller et al.* [1983] gives a D = 348.9°, I = 30.9°, α_{95} = 6.2° and k = 150.1. The mean inclination translates to a paleolatitude of 16.7°N ± 3.8. This result resembles that obtained from the present study, taking into consideration the associated confidence limits.

[70] *Fuller et al.* [1983] and *McCabe et al.* [1987] reported inclinations from Plio-Pleistocene rocks that are shallower than predicted by the geocentric axial dipole field model. Although limited, paleomagnetic directions gathered from this study do not seem to reflect such an anomaly. It is also worth noting that *McCabe et al.* [1987] suggested a northward drift for the Philippine arc based on limited data collected from eastern Mindanao, the Visayas and west central Luzon. Some reservations, however, are held regarding their paleomagnetic interpretations, as they acknowledge a lack of detailed geological information for many sampled units.

[71] The latitudinal shifts interpreted from the mean inclination data from northern Luzon resemble those gathered by *Hall et al.* [1995a] in eastern Indonesia to model the Cenozoic history of the Philippine Sea Plate. Their data
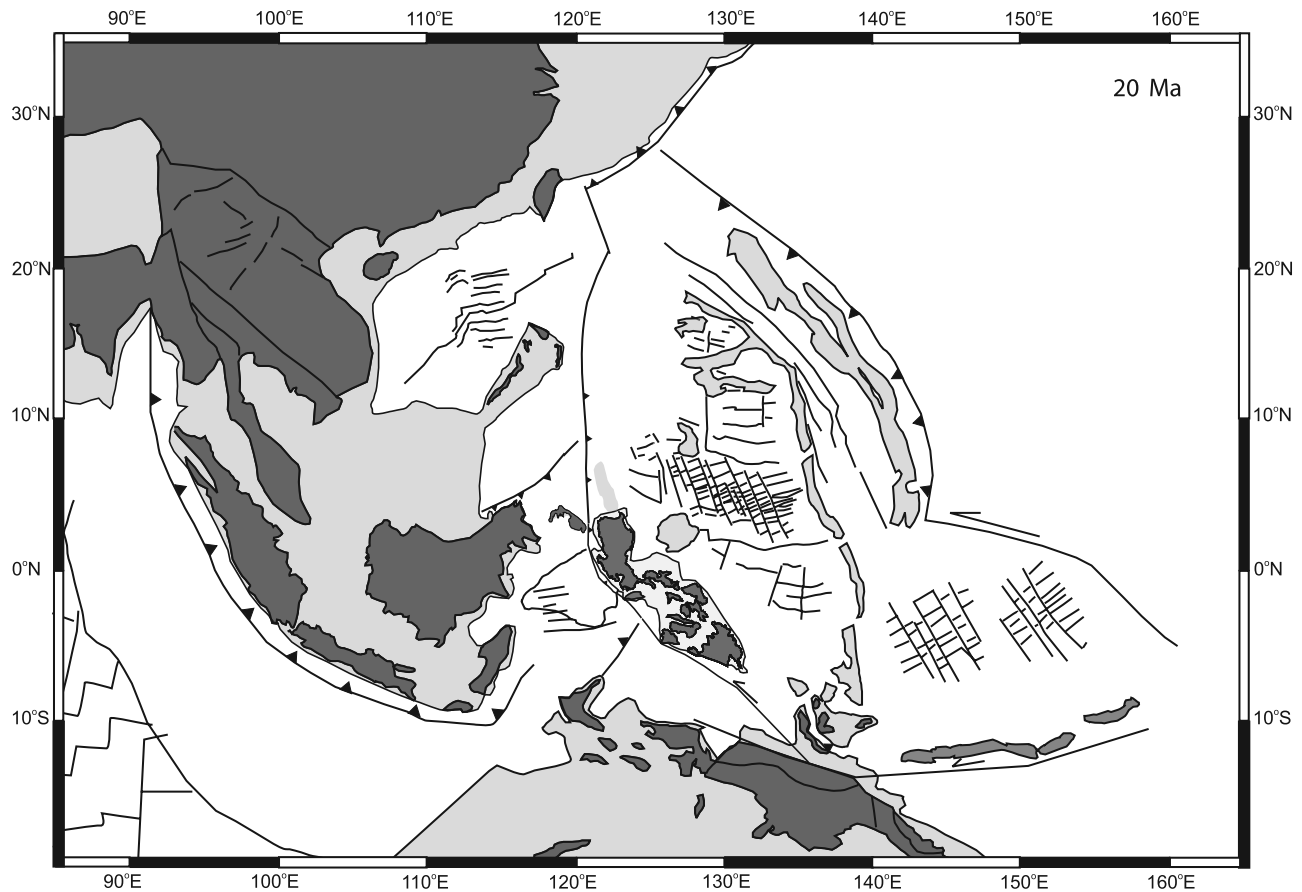
Figure 28. Tectonic reconstruction at 30 Ma modified after *Hall* [2002].

records little or no latitudinal shift between the late Eocene and the early Miocene, and a 10–15° northward motion since the early Miocene. Such similarities provide evidence that Luzon and possibly the eastern and southern regions of the Philippine arc (based on the data of *McCabe et al.* [1987]) have indeed been part of the Philippine Sea Plate during most of Cenozoic. This also provides additional support to the earlier suggestion by *Hall et al.* [1995a] that the plate has behaved coherently as a single entity since the early Cenozoic. Given that volcanism has been active in Luzon and adjacent southern islands of the Philippine archipelago since the early Cenozoic, these regions must have occupied positions near the edges of the plate.

[72] On the basis of the paleomagnetic data from eastern Indonesia, *Hall et al.* [1995a] reported a discontinuous clockwise rotation for the Philippine Sea Plate. Rotation amounts and Euler poles are (1) 50° clockwise about 10°N, 150°E between 40 and 50 Ma, (2) no rotation between 25 and 40 Ma, and (3) 35° clockwise about 15°N, 160°E between 5 and 25 Ma [*Hall et al.*, 1995a]. *Ali and Hall* [1995] used this information to explain the Cenozoic evolution of the boundary between the PSP and Australia and the presence of arc fragments in the New Guinea orogenic belt. Their results indicate that the PSP-Australian plate boundary changed from subduction to strike-slip fault (the Sorong Fault system) as the PSP began its Neogene rotation. The paleomagnetic studies of *Hall et al.* [1995a, 1995b] and *Ali and Hall* [1995] also proved useful for

Deschamps and Lallemand [2002] in their reconstructions of the Cenozoic history of the West Philippine Basin.

[73] *Hall et al.* [1995b] acknowledged the need to collect further data from Eocene and early Neogene rocks to define more precisely the intervals of rapid rotation. Assuming a Philippine Sea Plate origin for Luzon, declination data from this region could provide crucial information for refining the plate's motion history. Unfortunately, interpreting such data is extremely difficult. As it is, the present data set is insufficient to permit discrimination of components due to local tectonic deformation from those associated with rotation of the main plate. Deformation affecting Luzon since the early Cenozoic makes block rotations about a vertical axis a likely occurrence. Given the current tectonic setting of the Luzon (in which it is sandwiched between two opposing subduction zones and transected by several faults), subduction- or collision-related events could also provide a potential explanation for any observed rotations. Of particular significance is the early to middle Miocene collision of the Palawan microcontinental block with the Philippine Mobile Belt [*Sarewitz and Karig*, 1986; *Marchadier and Rangin*, 1990]. *Fuller et al.* [1983] cited the former event as having caused the counterclockwise rotation of Luzon, predominantly since the mid-Miocene. (Note, however, that the data which showed a convincing ~15° counterclockwise rotation of Luzon are from the lower to middle Miocene units. The age assignment given

Figure 29. Tectonic reconstruction at 20 Ma modified after *Hall* [2002].

to latter units is questioned in the present study as earlier discussed.)

[74] Because of these deformational events, it is not surprising that previous authors [e.g., *Fuller et al.*, 1983; *McCabe et al.*, 1987] reported inconsistency in the declination in some of their Luzon data set and gave conflicting interpretations with regards to the rotational history of Luzon. For instance, *McCabe et al.* [1987] reported that the central and northern portions of Luzon rotated clockwise sometime in the late Miocene. This is in contrast with the findings of *Fuller et al.* [1983], who argued for a counterclockwise rotation based on data from rocks of lower to middle Miocene (but herein treated as middle to upper Miocene). The present data also show a counterclockwise rotation during the middle to upper Miocene (Klondyke Formation data). These paleomagnetic studies, however, yielded similar results for the Plio-Pleistocene, noting an absence of paleomagnetically detectable rotations for Luzon.

5.2. Reconstructions and Implications

[75] The newly gathered geological and paleomagnetic data from northern Luzon place important constraints on reconstructions of its paleogeographic position in the context of SE Asia evolution (Figures 26 to 32). The reconstruction was made with the aid of paleomagnetic and geologic data from surrounding regions. *Hall* [2002] already synthesized these data covering periods extending from early to late Cenozoic. As such, the present study used

Hall's [2002] paleogeographic maps as template to show a simple model for Luzon's paleogeographic position in the context of SE Asia tectonic evolution. This study also takes into consideration the results of the recent gravity survey in northern Luzon showing an abrupt termination of northern Luzon [*Milsom et al.*, 2006].

[76] In utilizing *Hall*'s [2002] data, the present study necessarily required some modifications to his paleogeographic maps. Negros island and northeastern Mindoro form part of the Philippine Sea Plate based on earlier suggestions [e.g., *Rangin*, 1990; *Pubellier et al.*, 1996]. It also takes note that the western portion of Panay and the southwestern part of Mindoro are not of PSP affinity, but rather a fragment forming part of the Palawan microcontinental block rifted from China [*Rangin*, 1990; *Yumul et al.*, 2003]. While maintaining the position of the Zamboanga Peninsula, the present study has also included the southwestern portion of Mindanao as being of Eurasian affinity [*Rangin*, 1990; *Pubellier et al.*, 1991]. Last, in consideration of the findings of *McCabe et al.* [1987] and modeling of *Yumul et al.* [2000] for central Visayas, this study considered rotating the islands of Panay, Negros, Cebu and Bohol by ~45° counterclockwise from their present position. Being at the deformational front, central Visayas is thought to have moved clockwise to its present position following the completion of the Palawan microcontinental block-PMB collision in the central Philippines (see later discussions).
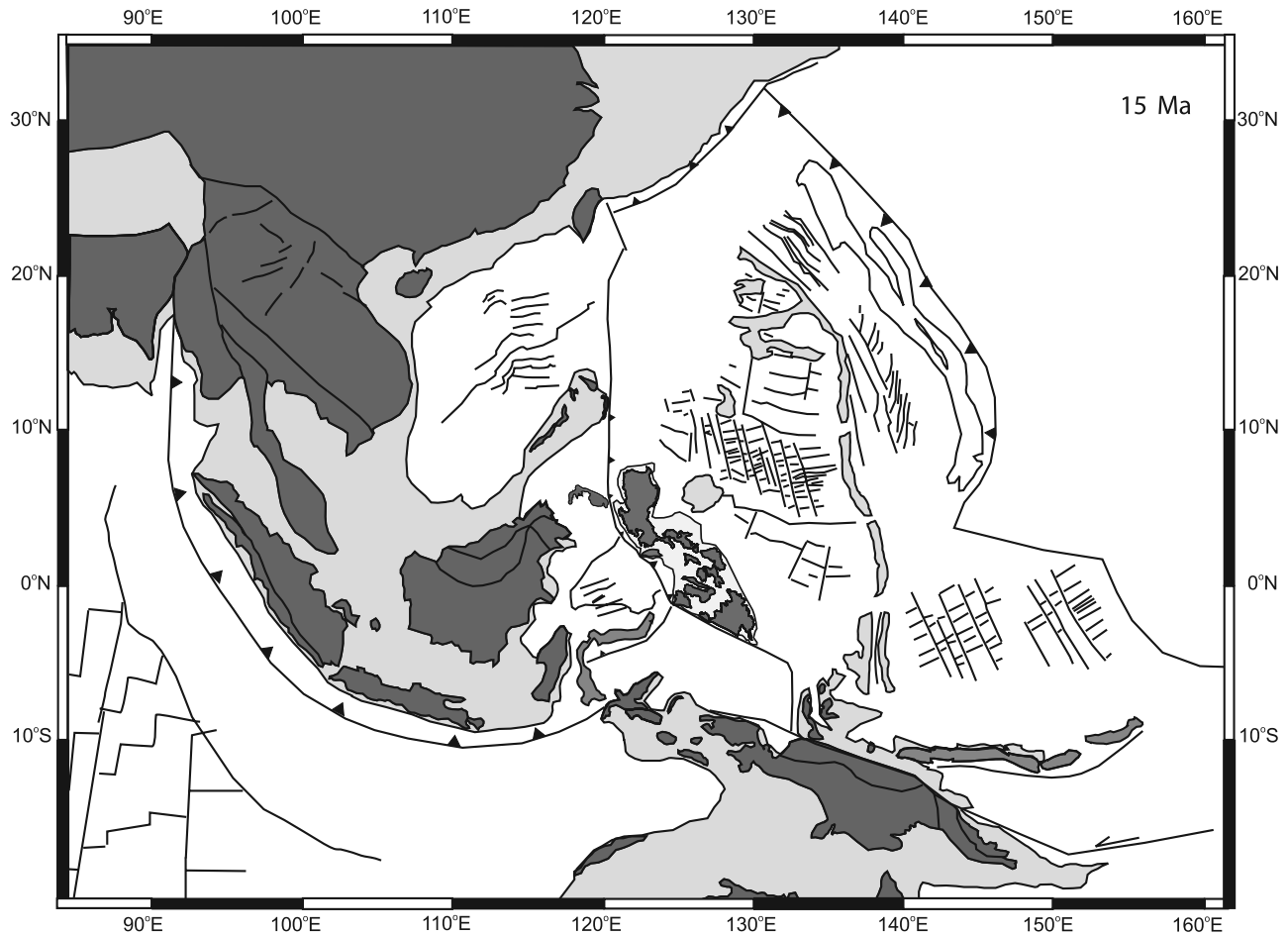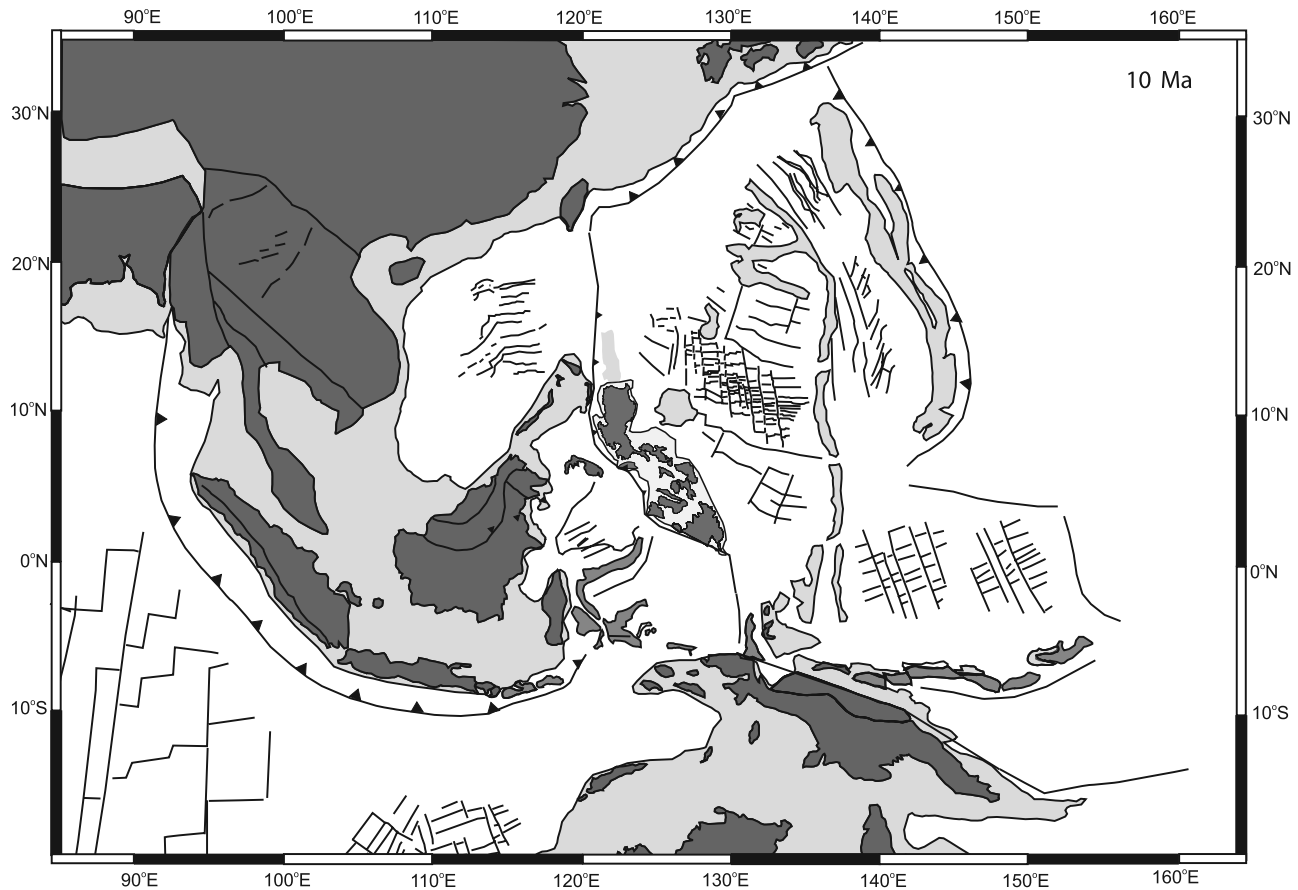
Figure 30. Tectonic reconstruction at 15 Ma modified after *Hall* [2002].

[77] The Benham Plateau was used as a reference location to position Luzon starting in the early Cenozoic, essentially maintaining a fixed distance between the plateau and the northeastern part of the island. This is based on the aforementioned PSP origin inferred for Luzon (and other islands of the PMB) and previous studies [e.g., *Louvenbruck*, 2003; *Pubellier et al.*, 2003b] which suggest northeast Luzon as being essentially fixed to the PSP (North Luzon had only recently decoupled from the plate due to the formation of the East Luzon Trough subduction system). *Deschamps and Lallemand* [2002] put the formation of the major part of the Benham Plateau at ~40 Ma. The present study used this time period as a starting point to estimate the paleogeographic position Luzon and other PSP-related islands of the PMB back at 50 Ma and at later periods (up to 5 Ma). In its earliest Cenozoic evolution, the reconstruction puts Luzon in a NW-SE orientation, with arc volcanism in this island being attributed to the Indo-Australian plate subduction. Such orientation contrasts significantly from those proposed by *Hall* [2002] and *Deschamps and Lallemand* [2002], which place Luzon in a NE-SW and N-S trend, respectively. It is suggested that the minimal amount of arc volcanism in Luzon between ~40 and ~33 Ma may be related to an earlier opening of the Celebes Sea and subsequent conversion of a convergent zone separating PSP from Eurasia to a fault boundary. The

presence of a fault boundary during the early Cenozoic (especially at ~50 Ma) could also account for the abrupt termination of northern Luzon as reported by *Milsom et al.* [2006].

[78] A striking aspect of the reconstruction adopting the aforementioned method is that Luzon's position ties well with the paleomagnetic data obtained during this study. The reconstruction clearly shows Luzon (and southern islands) as showing insignificant or minimal rotation from ~45–25 Ma and significant clockwise rotation and northward translation after 25 Ma. However, the present study acknowledges some problems in the reconstructions. In modifying *Hall*'s [2002] model, Luzon's position would overlap that of north Sulawesi (situated ~5°S) at 40 Ma and the eastern boundaries of the Celebes Sea (although only slightly) at 20–15 Ma. The reconstruction also encountered a problem in positioning eastern Mindanao as this island would also overlap Luzon at 15 Ma (Note that adjustments were made on the position of Mindanao in the 15–5 Ma reconstructions; also no paleomagnetic data exist for this island). This implies incorrect positioning either of Luzon or the concerned tectonic elements (or both) during these time periods. The new paleomagnetic data set from Luzon and the relatively well determined Cenozoic motion history of the Philippine Sea Plate make the former unlikely. *Hall* [2002] also noted that reconstructing the area of eastern

Figure 31.   Tectonic reconstruction at 10 Ma modified after *Hall* [2002].

Indonesia between the Bird's Head and SE Asia revolves strongly around the interpretation of Sulawesi's geology. Unfortunately, making such interpretation is not easy. The arms of Sulawesi are separated by deep basins, the origins and evolution of which are still relatively unknown [*Hall*, 2002].

[79]   The *Pubellier et al.* [2003b] geographic information system (GIS)-based reconstruction of SE Asia starting at 20 Ma shows Sulawesi, Borneo, Celebes Sea and eastern Mindanao occupying latitudes similar to their current positions. This contrasts with the study by *Hall* [2002] for this time period, which locates Sulawesi south of the equator and has Borneo and the Celebes Sea orientated ~45° clockwise from their current position. Both reconstructions, however, seem to agree with regards to the position of the other tectonic elements of Eurasian affinity (e.g., Palawan microcontinental block) and rotation history of the PSP. Given the orientation of Borneo, the Celebes Sea and eastern Mindanao at 20 Ma, *Pubellier et al.*'s [2003b] reconstruction shows a more easterly position for the boundary between the PSP (including Luzon) and Eurasia. Interestingly, they also regard Luzon as part of the PSP and place it at a latitude similar to that obtained in this study.

[80]   Clearly, the differing views on how to position Borneo, Celebes Sea and eastern Mindanao would require reinterpretation and/or gathering of paleomagnetic and geologic data from these regions. *Hall* [2002] took note of *Fuller et al.*'s [1999] paleomagnetic data for Borneo and

Ocean Drilling Program Leg 124 results [*Shibuya et al.*, 1991] for the Celebes Sea. The latter showed declinations suggesting a gradual counterclockwise rotation for the Celebes Sea by about 30° ± 10° between 42 and 20 Ma. Despite this, *Hall* [2002] opted to rotate the Celebes Sea counterclockwise at a later time, starting from ~20 Ma.

[81]   The reconstruction presented in this study has some other important geological implications. With a Philippine Sea Plate origin for Luzon (as well as the southern Philippine islands), the model considers arc development for this region as being attributed to NE-E directed subduction, an idea supported by some workers [*Stephan et al.*, 1986; *McCabe et al.*, 1987]. This contrasts with the more popular view [e.g., *Wolfe*, 1981; *Malettere*, 1989; *Florendo*, 1994; *Yumul et al.*, 2000, 2003] of an "arc polarity reversal" origin for Luzon. The latter considers the oldest magmatism in Luzon (recorded in the rocks of northern Sierra Madre) as resulting from westward subduction along the proto-East Luzon Trough possibly until the late Oligocene. Following arc rifting along the protonorthern Sierra Madre and formation of the Cagayan Valley Basin (between 26 and 22 Ma), eastward subduction along the Manila Trench ensued [*Florendo*, 1994]. This phase of activity started in the late Oligocene to early Miocene and is recorded in the rocks of the Central Cordillera.

[82]   The "arc polarity" origin was proposed to explain the temporal and spatial relationships of rocks in Luzon. A problem with this model is that no convincing argument
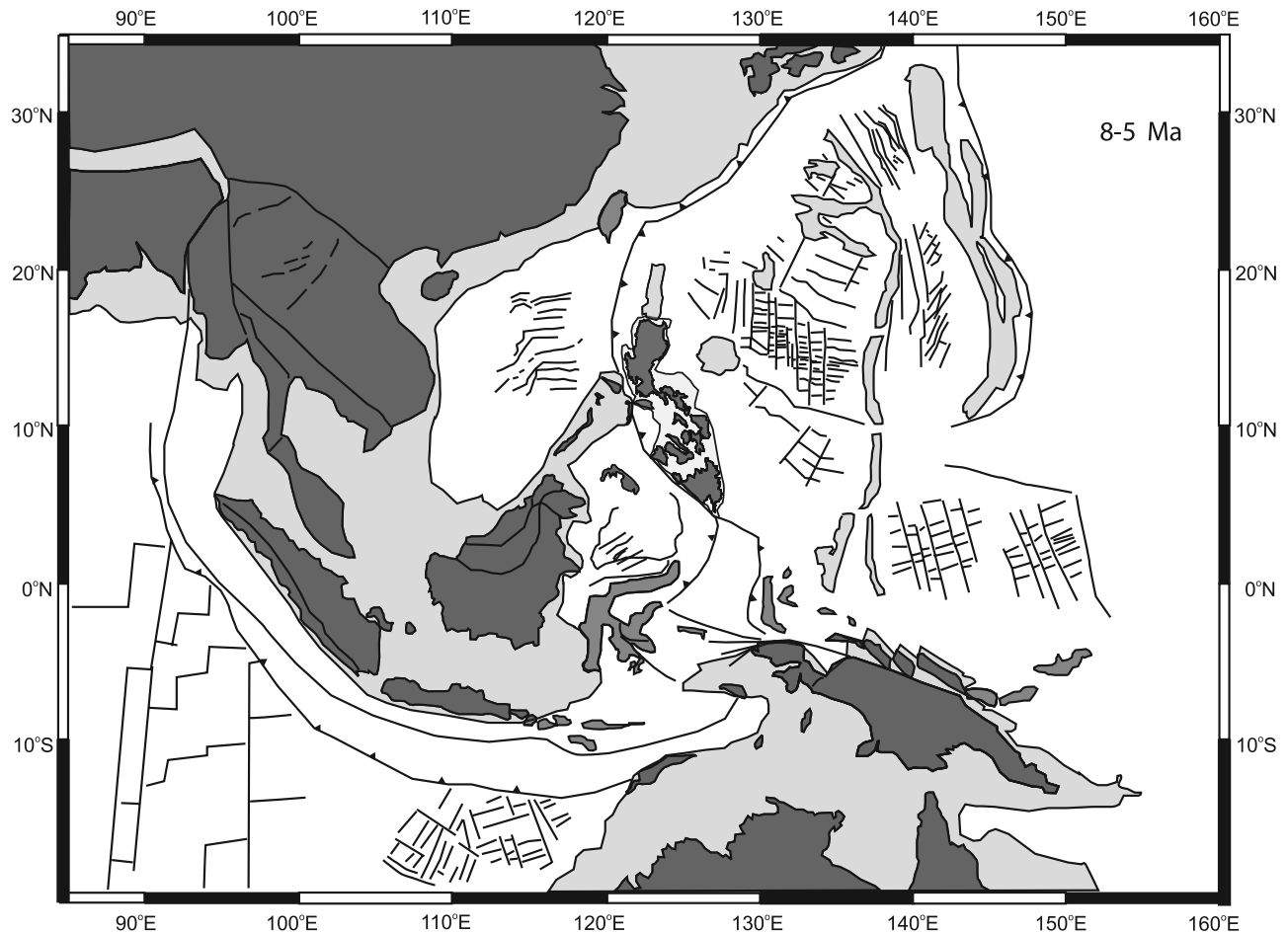
Figure 32. Tectonic reconstruction at 8−5 Ma modified after *Hall* [2002].

exists to explain the change of subduction polarity from east to west. *Lewis and Hayes* [1983] floated the idea of an earlier subduction (along the proto-East Luzon Trough) occurring east of Luzon, using seismic reflection data (from which they noted the possible occurrence of an ancient accretionary prism offshore of NE Luzon) as evidence. They, however, acknowledged that they could not suggest a cause for a flip of subduction polarity, putting into doubt the arc polarity reversal happening in Luzon. Unfortunately, no follow-up studies were made to confirm the existence of such tectonic feature east of Luzon.

[83] *Florendo* [1994] argued that the arrival of the Benham Plateau at the proto-East Luzon Trough resulted in a shift in subduction. This idea, however, has been refuted by *Bautista et al.* [2001], who noted that focal mechanism data indicate that the plateau has not yet begun to subduct along the present-day East Luzon Trough. *Yumul et al.* [2003] provided an alternative explanation, relating the arc polarity reversal to the collision of Palawan microcontinental block with the PMB in the early Miocene. They envisage the collision to have caused the counterclockwise rotation of Luzon and conversion of a strike-slip system bounding the western side of Luzon into a subduction zone (the Manila Trench). The paleomagnetic data obtained in this study do not support this argument. As shown in the reconstruction, the Palawan microcontinental block is still far from Luzon

during the early Miocene and that the collision with the PMB occurred, most likely during the late Miocene. The present study proposes a simple scenario whereby a "permanent" and relatively persistent subduction beneath western Luzon is enough to cause rifting between the Central Cordillera and the Sierra Madre.

[84] Volcanic and volcaniclastic rocks of Eocene age (e.g., those of the Bangui Formation) in the Central Cordillera provide evidence for an early subduction west of Luzon. Unlike those of the northern Sierra Madre, these Eocene units are rare in the Central Cordillera. This, however, is not surprising. As the Central Cordillera has always been the active arc, later volcanic events in the region likely overprinted the signature or "masked" the rocks produced by the early subduction west of Luzon.

[85] *Deschamps and Lallemand* [2002] suggested that subduction of a "young" West Philippine Basin beneath eastern Luzon might have occurred between 33 and 27 Ma, accounting for the presence of adakites reported by *David* [1994] in Catanduanes. This idea is not being discounted in the present study. Being a short-lived subduction event, Luzon would essentially still be part of the PSP during most of the Cenozoic. This event is unlikely to have caused the aforementioned arc rifting in Luzon given the timing of subduction.

[86] The reconstruction at 10–5 Ma shows the Palawan microcontinental block as located immediately west of Luzon (Figures 31 and 32). This scenario supports the suggestion by *Pubellier et al.* [2003b] that the Central Cordillera underwent significant uplift and shortening starting the late Miocene possibly due to "partial subduction" of the Palawan microcontinental block. Evidence for this tectonic event is the thick pile (over 5 km) of middle to early late Miocene submarine fan marine deposits (the Klondyke Formation) outcropping along the ~1,500 m high, southern part of the range. Indeed, a "sweeping off" of a buoyant microcontinental block by the Central Cordillera makes such a relatively rapid uplift of the Central Cordillera a possibility.

[87] *Louvenbruck* [2003] related the shortening and present topography of the Central Cordillera to the Plio-Quaternary southeastward subduction of the Scarborough seamount chain along the Manila Trench. The present study does not disregard the latter's contribution to the deformation of the range, as similar tectonic events have been documented elsewhere [e.g., *Bouysse and Westercamp*, 1990; *Pubellier et al.*, 1999]. This study, however, doubts the capability of the seamount of causing significant uplift of the region for a short period of time given its lesser buoyancy when compared to the Palawan block.

6. Conclusions

[88] A major investigation has been carried out on rocks from northern Luzon to provide information that might be used to constrain models for the tectonic development of SE Asia–western Pacific, in particular the Cenozoic motion history of the Philippine Sea Plate. About one quarter of the >240 paleomagnetic sites yielded reliable data. The declination data are of limited use, with many outcrops recording both local- and regional-scale movements. In contrast, the observed inclinations of primary magnetization provide crucial information, suggesting that Luzon occupied low, subequatorial latitudes for a reasonable portion of the early Cenozoic. Starting from the late Oligocene–early Miocene, Luzon moved northward by 10–15°. The new paleomagnetic data are incompatible with models that predict little or no latitudinal shift for the region. Instead, Luzon's motion history closely resembles that of the Philippine Sea Plate. This, along with geological data, suggests northern Luzon and neighboring regions of the Philippine archipelago as evolving with the plate during most of Cenozoic.

[89] With a Philippine Sea Plate origin, this study considers arc development for Luzon as being attributed to a "permanent" east directed subduction. This contrasts with the long-held view of an "arc polarity reversal" origin for Luzon. In addition, the reconstructions show that the Palawan microcontinental block-Philippine Mobile Belt collision occurred in the late Miocene, somewhat later than is commonly envisaged. Partial subduction of the Palawan block beneath Central Cordillera likely caused significant uplift of the Central Cordillera starting in the late Miocene.

[90] In light of the revised tectonic model proposed in this study, there is a need to review existing data from the region. The present study also acknowledges some problems in the reconstructions, particularly in the positions of the tectonic elements (Luzon, north Sulawesi, Celebes Sea and eastern Mindanao) at 20–15 Ma. Further geologic and paleomagnetic studies of these regions may be needed in refining models for SE tectonic evolution.

[91] There is also a controversy regarding the origin and spatial relationships of the ophiolites of Eocene (e.g., Zambales Ophiolite forming the Zambales Range in west Central Luzon; Angat Ophiolite in the SSM) and the Cretaceous (e.g., Casiguran Ophiolite in eastern NSM; Lagonoy Ophiolite in southeastern Luzon) age in the Philippine archipelago. One view [e.g., *Florendo*, 1994; *Encarnacion*, 2004] holds an "autochthonous model" for the ophiolites. Other workers [e.g., *Karig*, 1983; *Geary et al.*, 1988; *Yumul*, 2004] advocate for an "allochthonous" origin for these crust-mantle sequences. Paleomagnetic work on these ophiolites could shed light on the origin of these ophiolites.

[92] It is also worth noting that previous workers [e.g., *David*, 1994; *Yumul et al.*, 2003] suggested the existence of a "proto-Philippine Sea Plate" during the Mesozoic. They assumed the Cretaceous ophiolites in the central and eastern Philippines as part of this plate. However, the question remains as to whether there was indeed a proto-PSP. Unfortunately, reconstructing SE Asia during the Cretaceous is very difficult as many pieces of evidence have either been destroyed or dispersed due to the various tectonic processes operating in the region [*Hall et al.*, 1995a, 1995b; *Ali and Hall*, 1995].

[93] Additional paleomagnetic work in the Central Visayas and Mindanao could further refine tectonic model of the region. As it is, the data from the Central Visayas region is scarce. In Mindanao, no attempt has been made to collect paleomagnetic data from the terranes (eastern Mindanao vs. central and western Mindanao) of the island. Obtaining paleomagnetic data from these regions would enable the tectonic model presented in this study to be tested and refined. Already, there is a large set of information [e.g., *Pubellier et al.*, 1991; *Quebral et al.*, 1996; *Yumul et al.*, 2000] available on the geology of these regions that can be used to support the paleomagnetic studies.

References

Albrecht, A., and U. Knittel (1990), The petrology of the K-rich alkaline rocks in the Palali Mountains (northern Luzon Philippine island arc), *Neues Jahrb. Mineral.*, *161*, 255–286.

Ali, J. R. (1989), Magnetostratigraphy of early Paleogene sediments from NW Europe, Ph.D. thesis, 277 pp., Univ. Southampton, Southampton, U. K.

Ali, J. R., and R. Hall (1995), Evolution of the boundary between the Philippine Sea Plate and Australia, *Tectonophysics*, *251*, 251–275.

Ali, J. R., R. Hall, and S. J. Baker (2001), Paleomagnetic data from a Mesozoic Philippine Sea Plate ophiolite on Obi Island, eastern Indonesia, *J. Asian Earth Sci.*, *19*, 537–548.

Aurelio, M. A. (2000), Shear partitioning in the Philippines: Constraints from Philippine Fault and global positioning system data, *Island Arc*, *9*, 584–597.

Aurelio, M. A., and E. B. Billedo (1987), Tectonic implications of the geology and mineral resources of northern Sierra Madre, internal report, Bur. of Mines and Geosci., Manila.

Aurelio, M. A., E. Barrier, C. Rangin, and C. Müller (1991), The Philippine Fault in the late Cenozoic evolution of the Bondoc-Masbate-N. Leyte area, central Philippines, *J. Southeast Asian Earth Sci.*, *6*, 221–238.

Balce, G. R., R. Y. Encina, A. Momongan, and E. Lara (1980), Geology of the Baguio District and its implications on the tectonic development of the Luzon Central Cordillera, *Geol. Paleontol. Southeast Asia*, *21*, 265–288.

Barrier, E., P. Huchon, and M. A. Aurelio (1991), Philippine Fault: A key to Philippine kinematics, *Geology*, *19*, 32–35.

Bautista, C. B., M. L. P. Bautista, K. Oike, F. T. Wu, and R. S. Punongbayan (2001), A new insight on the geometry of subducting slabs in northern Luzon, Philippines, *Tectonophysics*, *339*, 279–310.

Becker, G. F. (1899), Brief memorandum on the geology of the Philippine islands, 20th Annual Report, U.S. Geol. Surv., Reston, Va.

Bellon, H., and G. P. Yumul Jr. (2000), Mio-Pliocene magmatism in the Baguio Mining District (Luzon, Philippines): Age clues to its geodynamic setting, *C. R. Acad. Sci.*, *331*, 295–302.

Billedo, E. B. (1994), Geologie de la Sierra Madre Septentrionnale et de l'Archipel de Polillo (Ceinture Mobile Est Pacifique), Ph.D. thesis, 215 pp, Univ. de Nice-Sophia, Antipolis, France.

Bouysse, P., and D. Westercamp (1990), Subduction of Atlantic aseismic ridges and Late Cenozoic evolution of the Lesser Antilles island arc, *Tectonophysics*, *175*, 349–355.

Briais, A., P. Patriat, and P. Tapponnier (1993), Updated interpretation of magnetic anomalies and seafloor spreading stages in the South China Sea: Implication for the Tertiary tectonics of Southeast Asia, *J. Geophys. Res.*, *98*, 6299–6328.

Caagusan, N. L. (1977), Source material, compaction history and hydrocarbon occurrence in the Cagayan Valley Basin, Luzon, Philippines, Offshore Southeast Asia Conference, Southeast Asia Pet. Explor. Soc., Singapore, 21–24 Feb.

Caagusan, N. L. (1981), Late Tertiary stratigraphy, paleogeography, and paleostructures of the Cagayan Valley Basin, Philippines, in *Geology and Tectonics of the Luzon-Marianas Region*, pp. 119–131, Philippine SEATAR Comm., Manila.

Cardwell, R. K., B. L. Isack, and D. E. Karig (1980), The spatial distribution of earthquakes, focal mechanism solutions, and subducted lithosphere in the Philippine and northeastern Indonesian islands, in *The Tectonic and Geological Evolution of SE Asian Seas and Islands*, *Geophys. Monogr., Ser.*, vol. 23, edited by D. E. Hayes, pp. 1–35, AGU, Washington, D. C.

Christian, L. B. (1964), Post-Oligocene tectonic history of the Cagayan Valley Basin, Philippines, *Philippine Geol.*, *18*, 114–147.

Cisowski, S. M., J. R. Dunn, M. Fuller, and P. J. Wasilewski (1990), NRM:IRM (s) demagnetization plots of intrusive rocks and the origin of their NRM, *Tectonophysics*, *184*, 35–54.

Corby, G. W., et al. (1951), Geology and oil possibilities of the Philippines, *Dep. Agric. Nat. Res. Tech. Bull.*, *21*, 363 pp.

David, S. (1994), Geologie du Sud-Est de Luzon-Contributions a l'etude geodynamique ante-Neogene de la Ceinture Mobile Est Philippine, Ph.D. thesis, Univ. de Nice-Sophia, Antipolis, France.

David, S., Jr., J. F. Stephan, J. Delteil, C. Müller, J. Butterlin, H. Bellon, and E. B. Billedo (1997), Geology and tectonic history of southeastern Luzon, Philippines, *J. Asian Earth Sci.*, *15*, 435–452.

Defant, J., R. C. Maury, J. De Boer, and J. L. Joron (1989), Geochemistry and tectonic setting of the Luzon arc, Philippines, *Geol. Soc. Am. Bull.*, *101*, 663–672.

De Leon, M. M. (1995), Calcareous nannofossil biostratigraphy of the submarine fan sequence of the Klondyke and Amlang formations in Benguet and La Union provinces, Philippines, Ph.D. thesis, 198 pp., Natl. Inst. of Geol. Sci., Univ. of the Philippines, Quezon City.

Deschamps, A., and S. Lallemand (2002), The West Philippine Basin: An Eocene to early Oligocene back arc basin opened between two opposed subduction zones, *J. Geophys. Res.*, *107*(B12), 2322, doi:10.1029/2001JB001706.

Deschamps, A., P. Monie, S. Lallemand, K. Hsu, and K. Y. Yeh (2000), Evidence for Early Cretaceous oceanic crust trapped in the Philippine Sea Plate, *Earth Planet. Sci. Lett.*, *179*, 503–516.

Dunlop, D. J., and O. Ozdemir (1997), *Rock Magnetism: Fundamentals and Frontiers*, 573 pp., Cambridge Univ. Press, New York.

Durkee, E. F., and S. L. Pederson (1961), Geology of northern Luzon, Philippines, *Am. Assoc. Pet. Geol. Bull.*, *45*, 137–168.

Encarnacion, J. (2004), Multiple ophiolite generation preserved in the northern Philippines and the growth of an island arc complex, *Tectonophysics*, *292*, 103–130.

Encarnacion, J., S. B. Mukasa, and E. J. Obille (1993), Zircon U-Pb geochronology of the Zambales and Angat ophiolites, Luzon, Philippines: Evidence for an Eocene arc-back-arc pair, *J. Geophys. Res.*, *98*, 19,991–20,004.

Fisher, R. A. (1953), Dispersion on a sphere, *Proc. R. Soc. London, Ser. A*, *217*, 295–305.

Fitch, T. J. (1972), Plate convergence, transcurrent faults, and internal deformation adjacent to Southeast Asia and the western Pacific, *J. Geophys. Res.*, *77*, 4432–4460.

Florendo, F. F. (1994), Tertiary arc rifting in northern Luzon, Philippines, *Tectonics*, *13*, 623–640.

Fuller, M., R. McCabe, S. Williams, J. Almasco, R. Y. Encina, and A. S. Zanoria (1983), Paleomagnetism of Luzon, in *The Tectonic and Geologic Evolution of SE Asian Seas and Islands: Part II*, *Geophys. Monogr. Ser.*, vol. 27, edited by D. E. Hayes, pp. 79–94, AGU, Washington, D. C.

Fuller, M., S. Cisowski, M. Hart, R. Haston, E. Schmidtke, and R. Jarrard (1988), NRM:IRM (s) demagnetization plots—An aid to the interpretation of natural remanent magnetization, *Geophys. Res. Lett.*, *15*, 518–521.

Fuller, M., J. R. Ali, S. J. Moss, G. M. Frost, B. Richter, and A. Mahfi (1999), Paleomagnetism of Borneo, *J. Asian Earth Sci.*, *17*, 3–24.

Garcia, J. S., and M. B. Bongolan (1990), Developments on enargite ore search at Lepanto, Mankayan, Benguet, Philippine, internal report, Lepanto Consolidated Min. Co., Mankayan, Philippines.

Geary, E. E., T. M. Harrison, and M. Heizler (1988), Diverse ages and origins of basement complexes, Luzon, Philippines, *Geology*, *16*, 341–344.

Gervasio, F. C. (1966), Age and nature of orogenesis of the Philippines, *Tectonophysics*, *4*, 379–402.

Haeck, G. D. (1987), The geological and tectonic history of the central portion of the southern Sierra Madre, Luzon, Philippines, Ph.D. thesis, 294 pp., Cornell Univ., Ithaca, N. Y.

Hall, R. (2002), Cenozoic geological and plate tectonic evolution of SE Asia and the SW Pacific: Computer-based reconstructions, model and animations, *J. Asian Earth Sci.*, *20*, 353–431.

Hall, R., J. R. Ali, and C. D. Anderson (1995a), Cenozoic motion of the Philippine Sea Plate: Paleomagnetic evidence from eastern Indonesia, *Tectonics*, *14*, 1117–1132.

Hall, R., J. R. Ali, C. D. Anderson, and S. J. Baker (1995b), Origin and motion history of the Philippine Sea Plate, *Tectonophysics*, *251*, 229–250.

Hamburger, M., R. Cardwell, and B. L. Isacks (1983), Seismotectonics of the northern Philippine island arc, in *The Tectonic and Geologic Evolution of SE Asian Seas and Islands: Part II*, *Geophys. Monogr. Ser.*, vol. 27, edited by D. E. Hayes, pp. 1–22, AGU, Washington, D. C.

Japan International Cooperation Agency-Metal Mining Agency of Japan (JICA-MMAJ) (1975), Report on the geological survey of northeastern Luzon, part 2, Tokyo.

Japan International Cooperation Agency-Metal Mining Agency of Japan (JICA-MMAJ) (1977), Report on the geological survey of northeastern Luzon, Tokyo.

Japan International Cooperation Agency-Metal Mining Agency of Japan-Mines and Geosciences Bureau (JICA-MMAJ-MGB) (1990), Report on the mineral exploration, mineral deposits and tectonics of two contrasting geologic environments in the Republic of the Philippines, terminal report, Tokyo.

Jolivet, L., P. Huchon, and C. Rangin (1989), Tectonic setting of western Pacific marginal basins, *Tectonophysics*, *160*, 23–47.

Karig, D. E. (1975), Basin genesis in the Philippine Sea, *Initial Rep. Deep Sea Drill. Proj.*, *31*, 857–879.

Karig, D. E. (1983), Accreted terranes in the northern part of the Philippine archipelago, *Tectonics*, *2*, 211–236.

Knittel, U. (1983), Age of the Cordon Syenite Complex and its implication on the mid-Tertiary history of North Luzon, *Philippine Geol.*, *37*, 22–31.

Knittel, U., and A. Cundari (1990), Mineralogical evidence for the derivation of metaluminous, potassic rocks from peralkaline precursors: The Cordon Syenite Complex (Philippines), *Mineral. Petrol.*, *41*, 163–183, doi:10.1007/BF01168493.

Lee, T. Y., and L. A. Lawver (1995), Cenozoic plate reconstruction of Southeast Asia, *Tectonophysics*, *251*, 85–138.

Lewis, S. D., and D. E. Hayes (1983), The tectonics of northward propagating subduction along eastern Luzon, Philippines islands, in *The Tectonic and Geologic Evolution of SE Asian Seas and Islands: Part II*, *Geophys. Monogr. Ser.*, vol. 27, edited by D. E. Hayes, pp. 57–78, AGU, Washington, D. C.

Lewis, S. D., and D. E. Hayes (1984), A geophysical study of the Manila Trench, Luzon, Philippines, *J. Geophys. Res.*, *89*, 9196–9214.

Li, Q., Z. Jian, and X. Zu (2005), Late Oligocene rapid transformations in the South China Sea, *Mar. Micropaleontol.*, *45*, 5–25.

Louvenbruck, A. (2003), Deformation active du domain nord Luzon, Philippines et de Taiwan, these de doctorat, 278 pp., Univ. Paris XI Orsay, France.

Lowrie, W. (1990), Identification of ferromagnetic minerals in a rock by coercivity and unblocking temperature properties, *Geophys. Res. Lett.*, *17*, 159–162.

Malettere, P. (1989), Histoire sedimentaire, magmatique, tectonique, metallogenique d'un arc cenozoique deforme en regime de transpression, Cordillere centrale de Luzon, a l'extremite de la faille philippine sur les transects de Baguio et de Cervantes-Bontoc. Contexte structural et geodynamique mineralisations epithermales auriferes, Ph.D. thesis, 304 pp., Univ. de Bretagne Occidentale, Brest, France.

Marchadier, Y., and C. Rangin (1990), Polyphase tectonics at the southern tip of Manila trench, Mindoro-Tablas islands, Philippines, *Tectonophysics*, *183*, 273–287.

Mathisen, M. E., and C. F. Vondra (1983), The fluvial and pyroclastic deposits of the Cagayan basin, northern Luzon, Philippines: An example of none marine volcaniclastic sedimentation in an interarc basin, *Sedimentology*, *30*, 369–392.

McCabe, R. J., E. Kikawa, J. T. Cole, A. J. Malicse, A. J. Baldauf, G. P. Yumul Jr., and J. Almasco (1987), Paleomagnetic results from Luzon and the central Philippines, *J. Geophys. Res.*, *92*, 555–580.

McElhinny, M. W., and P. L. McFadden (2000), *Paleomagnetism: Continents and Oceans*, 386 pp., Elsevier, New York.

McFadden, P. L., and A. B. Reid (1982), Analysis of paleomagnetic inclination data, *Geophys. J. R. Astron. Soc.*, *69*, 307–319.

Milsom, J., J. R. Ali, and K. L. Queano (2006), Peculiar geometry of northern Luzon, Philippines: Implications for regional tectonics of new gravity and paleomagnetic data, *Tectonics*, *25*, TC4017, doi:10.1029/2005TC001930.

Mitchell, A. G., F. Hernandez, and A. P. Dela Cruz (1986), Cenozoic evolution of the Philippine Archipelago, *J. Southeast Asian Earth Sci.*, *1*, 3–22.

Okino, K., Y. Shimikawa, and S. Nagaoka (1994), Evolution of the Shikoku basin, *J. Geomagn. Geoelectr.*, *46*, 463–479.

Ozawa, A., T. Tagami, E. L. Listanco, C. B. Arpa, and M. Sudo (2004), Initiation and propagation of subduction along the Philippine Trench: Evidence from the temporal and spatial distribution of volcanoes, *J. Asian Earth Sci.*, *23*, 105–111.

Pena, R. (1992), A review of the stratigraphy of Baguio District, *J. Geol. Soc. Philippines*, *47*, 151–166.

Pinet, N. (1990a) Un exemple de grand decrochement actif en contexte de subduction oblique: La faille Philippine dans sa partie septentrionale. Etudes regionale, thematique et modelisation analogique, Ph.D. thesis, 390 pp. Inst. de Geodyn., Univ. de Nice-Sophia, Antipolis, France.

Pinet, N., and J. F. Stephan (1990b) The Philippine wrench fault system in the Ilocos foothills, northwestern Luzon, Philippines, *Tectonophysics*, *183*, 207–224.

Pubellier, M., R. Quebral, C. Rangin, B. Deffontaines, C. C. Müller, and J. Butterlin (1991), The Mindanao collision zone: A soft collision event within a continuous Neogene strike-slip setting, *J. Southeast Asian Earth Sci.*, *6*, 239–248.

Pubellier, M., Q. Quebral, M. Aurelio, and C. Rangin (1996), Docking and post-docking escape tectonics in the southern Philippines, in *Tectonic Evolution of Southeast Asia*, edited by R. Hall and D. Bundell, *Spec. Publ. Geol. Soc.*, *106*, 511–523.

Pubellier, M., A. G. Bader, B. Deffontaines, C. Rangin, and R. Quebral (1999), Upper plate deformation induced by subduction of a volcanic arc: The Snellius Plateau (Molucca Sea Indonesia and Mindanao, Philippines), *Tectonophysics*, *304*, 345–368.

Pubellier, M., J. Ali, and C. Monnier (2003a), Cenozoic plate interaction of the Australia and Philippine Sea Plates: "hit and run" tectonics, *Tectonophysics*, *363*, 181–199.

Pubellier, M., F. Ego, N. Chamot-Rooke, and C. Rangin (2003b), The building of pericratonic mountain ranges: Structural and kinematic constraints applied to GIS-based reconstructions of SE Asia, *Bull. Soc. Geol. Fr.*, *174*(6), 561–584, doi:10.2113/174.6.561.

Queano, K. L. (2006), Tectonic modeling of northern Luzon and regional implications, Ph.D. thesis, 500 pp. Univ. of Hong Kong, Hong Kong.

Quebral, R., M. Pubellier, and C. Rangin (1996), The onset of movement on the Philippine fault in eastern Mindanao: A transition from a collision to a strike slip environment, *Tectonics*, *15*, 713–726.

Rangin, C. (1989), The Sulu Sea, a back-arc setting within a Neogene collision zone, *Tectonophysics*, *161*, 119–141.

Rangin, C. (1990), The Philippine Mobile Belt: A complex plate boundary, *J. Southeast Asian Earth Sci.*, *6*, 209–220.

Rangin, C., and M. Pubellier (1990), Subduction and accretion of Philippine Sea Plate fragments along the Eurasian margin, in *Tectonics of Circum-Pacific Continental Margins*, edited by J. Bourgois, P. Huchon and G. Pautot, pp. 139–164, E.J., Brill, Boston, Mass.

Rangin, C., and E. A. Silver (1991), Development of the Celebes Basin in the context of western Pacific marginal basin history, *Proc. Ocean Drill. Program Sci. Results*, *124*, 39–49.

Rangin, C., L. Jolivet, and M. Pubellier (1990), A simple model for the tectonic evolution of Southeast Asia and Indonesia regions for the past 43 Ma, *Bull. Soc. Geol. Fr.*, *6*, 887–905.

Rangin, C., W. Spakman, M. Pubellier, and H. Bijwaard (1999), Tomographic and geological constraints on subduction along the eastern Sundaland continental margin (South-East Asia), *Bull. Soc. Geol. Fr.*, *170*, 775–788.

Revilla, G. P., and E. R. Malaca (1987), Geology of southern Sierra Madre, internal report, 62 pp., Bur. of Mines and Geosci., Manila.

Ringenbach, J. C. (1992), La Faille Philippine et les chaines en decrochement associees (center et nord de Luzon): Evolution Cenozoique et cinematique des deformations quaternaries, Ph.D. thesis, 336 pp., Institute de Geodynamique, Univ. de Nice-Sophia, Antipolis, France.

Ringenbach, J. C., N. Pinet, J. F. Stephan, and J. Delteil (1993), Structural variety and tectonic evolution of strike-slip basins related to the Philippine Fault System, northern Luzon, Philippines, *Tectonics*, *12*, 187–203.

Sajona, F. G., R. C. Maury, H. Bellon, J. Cotton, M. J. Defant, and M. Pubellier (1993), Initiation of subduction and generation of slab melts in western and eastern Mindanao, Philippines, *Geology*, *21*, 1007–1010.

Sarewitz, D. R., and D. E. Karig (1986), Geologic evolution of western Mindoro Island and the Mindoro suture zone, Philippines, *J. Southeast Asian Earth Sci.*, *1*, 117–141.

Sdrolias, M., W. R. Roest, and R. D. Müller (2004), An expression of Philippine Sea plate rotation: The Parece Vela and Shikoku Basins, *Tectonophysics*, *394*, 69–86.

Seno, T., S. Stein, and A. Gripp (1993), A model for the motion of the Philippine Sea Plate consistent with NUVEL-1 and geological data, *J. Geophys. Res.*, *98*, 17,941–17,948.

Shibuya, H., D. L. Merrill, V. Hsu, and ODP Leg 124 Shipboard Scientific Party (1991), Paleogene counterclockwise rotation of the Celebes Sea: Orientation of ODP cores utilizing the secondary magnetization, *Proc. Ocean Drill. Program Sci. Results*, *124*, 519–523.

Sibuet, J. C., S. K. Hsu, X. Le Pichon, J. P. Le Formal, D. Reed, G. Moore, and C. S. Liu (2002), East Asia plate tectonics since 15 Ma: Constraints from the Taiwan region, *Tectonophysics*, *344*, 103–134.

Silver, E. A., and C. Rangin (1991), Leg 124 of the Ocean Drilling Program, *Geophys. Res. Lett.*, *17*, 2059–2060.

Stephan, J. F., R. Blanchet, C. Rangin, B. Pelletier, J. Letouzey, and C. Müller (1986), Geodynamic evolution of the Taiwan-Luzon-Mindoro belt since the late Eocene, *Tectonophysics*, *125*, 245–268.

Tamesis, E. V., R. A. Lorentz Jr., R. V. Pascual, and E. M. Dizon (1982), Stratigraphy and geologic structures of the Central Valley Basin, Luzon, Philippines, in *Geology and Tectonics of the Luzon-Marianas Region* (*Proceedings CCOP-IOC-SEATAR Workshop, Philippines, November 1981*), pp. 83–118, Philippine SEATAR Comm., Manila.

United Nations Development Program (UNDP) (1987), Geology and mineralization in the Baguio area, Northern Luzon, *UNDP Tech. Rep. 5*, 82 pp.

Van der Voo, R. (1990), The reliability of paleomagnetic data, *Tectonophysics*, *184*, 1–9.

Weissel, J. K. (1980), Evidence for Eocene oceanic crust in the Celebes Basin, in *The Tectonic and Geological Evolution of SE Asian Seas and Islands*, *Geophys. Monogr., Ser.*, vol. 23, edited by D. E. Hayes, pp. 37–47, AGU, Washington, D. C.

Wolfe, J. A. (1981), Philippine geochronology, *J. Geol. Soc. Philippines*, *35*, 1–30.

Yang, T., T. Lee, C. Chen, S. Cheng, U. Knittel, R. Punongbayan, and A. Rasdas (1996), A double island arc between Taiwan and Luzon: Consequence of ridge subduction, *Tectonophysics*, *258*, 85–101.

Yumul, G. P., Jr. (2004), Zambales Ophiolite (Philippines) transition zone dunites: Restite, cumulate or replacive products?, *Int. Geol. Rev.*, *46*, 259–272.

Yumul, G. P., Jr., M. T. Samson, R. J. T. Claveria, L. P. de Silva Jr., E. O. Diomampo, and J. P. Rafols (1992), Preliminary geochemical evidences for a marginal basin basement complex for the Baguio Mining District, Luzon, Philippines, *J. Geol. Soc. Philippines*, *47*, 5–17.

Yumul, G. P., Jr., C. Dimalanta, R. A. Tamayo, and J. A. Barretto (2000), Contrasting morphological trends of islands in central Philippines: Speculation on their origin, *Island Arc*, *9*, 627–637.

Yumul, G. P., Jr., C. Dimalanta, R. A. Tamayo, and R. C. Maury (2003), Collision, subduction and accretion events in the Philippines: A synthesis, *Island Arc*, *12*, 77–91.

Zijderveld, J. D. A. (1967), A. C. demagnetization of rocks, in *Methods in Paleomagnetism*, edited by D. W. Collinson, K. M. Creer, and S. K. Runcorn, pp. 256–286, Elsevier, New York.

_____

J. C. Aitchison, J. R. Ali, and J. Milsom, Department of Earth Sciences, University of Hong Kong, James Lee Science Building, University of Hong Kong, Pokfulam Road, Hong Kong SAR, China.

M. Pubellier, Laboratoire de Géologie, Ecole Normale Supérieure URA 1316 du CNRS UMR 8538, 24 Rue Lhomond, F-75231 Paris, France.

K. L. Queano, Lands Geological Survey Division, Mines and Geosciences Bureau, North Avenue, Diliman, Quezon City, 1104, Philippines. (kqueano@gmail.com)